The Behaviour of Reactive Powder Geopolymer Concrete at Elevated Temperature

Thesis submitted in fulfilment of the requirements for the degree of

Master of Engineering by research

A. M. U Thathsarani Kannangara

BSc (Hons) Civil and Structural Engineering

College of Engineering and Science
Civil & Building Engineering
March 2018

ABSTRACT

Concrete is one of the most widely used materials within the construction industry due to its versatility, durability, superior mechanical properties and excellent resistance to fire. In addition to this, the rapid growth in population and urbanisation has accelerated the demand for high strength concretes. However, high strength concretes suffer a condition called spalling when exposed to elevated temperature levels which is associated with the breaking away or exploding of concrete layers due to the internal stresses. Additionally, concrete is a material having a very high carbon footprint mainly due to its binding material, cement, which is reported to be the second largest emitter of carbon dioxide.

These issues have driven researchers to experiment alternative materials which can better benefit the economy and the environment. Studies show that blended concretes, which use supplementary cementitious materials such as slag, fly ash, silica fumes in partial replacement to cement and Geopolymer (GP) concretes, which eliminate cement usage altogether, display a high degree of resistance to fire. Additionally, these materials are further deemed worthy due the reduction or elimination of cement making it a more sustainable material.

This study focuses on the fire performance of GP pastes, reactive powder concretes (RPC) and a newly developed GP paste based reactive powder concrete called reactive powder GP concrete (RPGC). RPGC was produced using class F fly ash and sodium-based activators in relation with silica fumes and micrometre aggregate. The study investigates properties such as workability, setting times, density, compressive strength, residual strength, thermal cracking and mass loss under controlled laboratory conditions. The study further investigates the performance of GP paste specimens of varied sizes subjected to different curing conditions. A comparison on the properties of two fly ash materials, namely Gladstone fly ash and Gladstone/Callide fly ash are also presented.

Both types of fly ash displayed high early strengths and exceptional fire performance with a maximum strength gain of approximately 45% after an exposure to 400°C. RPC on the other hand exhibited high levels of explosive spalling at a temperature of around 360°C despite initial compressive strengths reaching a maximum of 140.7 MPa at 7-day testing. RPGC displayed good workability conditions with a maximum of 252 mm and a minimum of 187.5 mm, whilst achieving an initial compressive strength of 76.3 MPA at 24-hour testing. Furthermore, RPGC resulted in the lowest degree of thermal cracking with majority of the specimens having no visible cracking even after an exposure of 800°C. Moreover, RPGC recorded the lowest percentage mass loss amongst all experimented specimens.

DECLARATION

"I, A. M. U. Thathsarani Kannangara declare that the Master by Research thesis entitled 'The Behaviour of Reactive Powder Geopolymer Concrete at Elevated Temperature' is no more than 60,000 words in length including quotes and exclusive of tables, figures, appendices, bibliography, references and footnotes. This thesis contains no material that has been submitted previously, in whole or in part, for the award of any other academic degree or diploma. Except where otherwise indicated, this thesis is my own work".
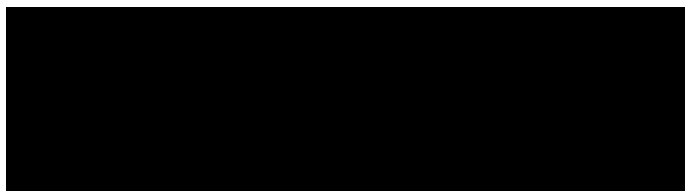
A. M. U. Thathsarani Kannangara   27 March 2018

ACKNOWLEDGEMENTS

This thesis has become a reality with the help and support of several notable people and I would like to offer my heartfelt gratitude to them.

First and foremost, I would like to express my sincerest gratitude to my supervisors, Professor Sam Fragomeni and Dr. Maurice Guerrieri for their genuine support, guidance and continuous encouragement. Their expertise, vast knowledge and constant supervision enabled me to complete this endeavour to the best of my abilities. They went above and beyond their way time after time to open up opportunities for me for which I am forever grateful.

My genuine appreciation and very special thanks goes to Professor Paul Joseph for his positive motivation, vital advice, unwavering guidance in helping me achieve this milestone.

I would like to sincerely thank to Mr. Joe Angelone, Mr Lyndon Macindoe, Mr. Philip Dunn, Mr. Laurence Martin, Mr. Donald Ermel and Mr. Miroslav Radev, for all their technical knowledge and assistance throughout my laboratory works.

I would also like to offer my appreciation to Mr. Michael Culton, Senior Technical Officer at Swinburne University of Technology for all the support given to me on some of the experimental programs during my testing stages.

Last, but not the least, I would like to thank my parents who have always stood by me through thick n' thin with encouraging words and unconditional love. Thank you for all the sacrifices you made in giving me the opportunity to pursue my dreams. I am also very grateful to my sister and my brother-in-law who, not only sheltered and financially supported me throughout the years, but also protected me, advised me and encouraged me during my time in Australia. Finally, I would like to thank my uncle, Mr. Wimal Lokuliyana, Landscape Architect and Lecturer at University of Moratuwa, Sri Lanka, for all the knowledge, advice and ideas he gave me before and during my post graduate studies. I am certain that I would not be who I am or where I am without the support of my family.

TABLE OF CONTENTS

LIST OF FIGURES

LIST OF TABLES

LIST OF TERMS AND ABBREVIATIONS

Al – Aluminium

CaO – Calcium oxide

CCP – Coal combustion productions

CO_2 – Carbon dioxide

FA – Fly Ash

GHG – Greenhouse gases

GP – Geopolymer

MPa – Mega Pascal

Na_2SiO_3 – Sodium Silicate

NaOH – Sodium Hydroxide

OPC – Ordinary Portland cement

RPC – Reactive Powder Concrete

RPGC – Reactive Powder Geopolymer Concrete

RPM – Revolutions per minute

SF – Slump Flow

Si – Silicon

SSD – Saturate Surface Dry

TGA – Thermogravimetric analysis

W/C Ratio – Water to Cement ratio

CHAPTER 01

INTRODUCTION

1.1. Background

The growth in population and economy has greatly increased the demand for high performance infrastructures capable of satisfying client and consumer requirements. To meet this growing demand, researchers are determined in developing new and innovative materials which can provide high performance infrastructures whilst reducing the carbon footprint. In other words, a high performance sustainable construction material is needed.

Concrete, which is a basic mixture of cement, fine aggregate, coarse aggregate and water, can be identified as one of the oldest, most versatile and most prominent building materials within the construction industry. Additionally, the inclusion of chemical and/or mineral admixtures in the mix design can enhance the properties of concrete to producing high performing concretes that are less vulnerable to susceptibility which can be used for large scale infrastructures (Poon et al., 2004). However, concrete is a material having a high carbon footprint throughout its lifecycle and the over extraction of raw materials required to manufacture concrete have caused irreversible damages on the Earth's natural resources. Furthermore, despite concrete having high resistance to fire in comparison to alternative materials such as steel or timber, it is vulnerable to a phenomenon known as concrete spalling which can create disastrous consequences, especially in high strength concrete structures.

Cement, which is the binding ingredient in concrete, is manufactured using naturally occurring minerals (calcium, silicon, aluminium and iron) and heated to over 1500°C to produce cement clinker. Edwards (2015) gives information showing the rapid increase in cement production globally, from 133 million

tonnes in 1950 to 1 billion tonnes in 1983. Edwards (2015) further showed that this increment continued up to 4.2 billion tonnes in 2014. Similar research shows that a global production of 3.5 billion tonnes of Ordinary Portland Cement (OPC) in the year 2005 is predicted to increase by three times its demand by the year 2050 (Wardhono, 2014) and this would in turn lead to extreme Carbon dioxide (CO_2) emissions along with severe depletions of natural quarries (due to limestone extraction required in cement production).

The production of cement is found to be the second largest source of Green House Gas (GHG) emission, where, for every 1000kg of OPC produced, 900kg – 1100kg of CO_2 is emitted roughly (NRMCA 2012).

In response to this dangerously accumulated problem, researchers are determined in finding alternatives for the basic constituents of concrete. Several supplementary cementitious materials or pozzolans such as fly ash (FA), slag, rice husk ash, volcanic ash, etc are now being used in concrete production that can be used to fully or partially replace cement in concrete.

In the 1970s, Prof. Dr. Joseph Davidovits first developed Geopolymer (GP) Concrete which is free from traditional cement (Davidovits, 2002). Davidovits (2002) stated that GP cements are manufactured through the process of geopolymerisation involving the chemical reaction of alumino-silicate oxide with alkali and calcium poly-silicates which yield Si-O-Al bonds. FA is a material most commonly utilized in the production of GPs and it has been reported that FA based GPs possess low thermal shrinkage and high strengths when exposed to elevated temperature conditions (Li and Wu, 2005). Swanepoel and Strydom (2002), Hardjito et al. (2004) and Rovnaník (2010) stated that pozzolanic materials that are rich in silicon-dioxide and aluminium oxide such as fly ash, blast furnace slag or metakaolin are often used as the source materials in GP concrete. The key advantage in GP concrete is that it uses zero cement content, thus reducing its carbon footprint and achieving high early strength (within 24 hours), which can be developed using optimal temperatures (Lloyd and Rangan, 2010, Ryu et al., 2013).

Reactive Powder Concrete (RPC), first developed in early 1990s by a French Corporation BOUYGUES (Team, 2007), is a widely used ultra-high

performance concrete which displays high compressive strength, high flexural strength, high ductility and low permeability properties due to the improvements in gradation, porosity and microstructure. These enhanced properties are obtained by using very fine particles hence achieving high density and reduced porosity (Chan and Chu, 2004, Lee et al., 2007). According to Washer et al. (2003) ultra-high performance concrete should display compressive strengths greater than 150 MPa. The basic constituents of RPC are cement, ultra-fine quartz sand, silica fumes and steel fibres. The exclusion of course aggregate, reduction in w/c ratio and lowering of calcium oxide to silicon dioxide ratio and the addition of steel fibre reinforcement are given as the key reasons for the enhancement of mechanical properties (Chan and Chu, 2004).

Though RPC is a highly valuable type of concrete which can reach ultra-high strengths, it behaves poorly in the case of a fire undergoing explosive spalling conditions (Peng et al., 2012, Zheng et al., 2013, Ju et al., 2013, So et al., 2014, Tian et al., 2012). Additionally, RPC has adverse effects on the environment, increasing the carbon footprint, mainly due to the use of cement in the mix matrix. GPs, on the other hand, have excellent resistance to fire but produce comparatively lower strengths. Despite the fact that extensive studies have been conducted on GP and RPC separately, research regarding the behaviour of a combination of RPC and GP is limited.

This research is focused on an extensive experimental program on FA based GP pastes, RPC and a combined FA based RPC activated using sodium based alkaline solutions called Reactive Powder Geopolymer Concrete (RPGC). Ng et al. (2012) conducted a sustainability study on a combination of RPC and GP concrete and concluded that this combined material will contribute significantly to sustainable development while lowering environmental impact and providing efficient structural performance. Therefore, further studies on a combination of RPC and GP factors can be regarded as a highly valuable area of study and this research investigated factors such as characteristic strength, workability, curing regime, production methods along with the residual strength, thermal cracking and weight loss

parameters at elevated temperatures of RPGC through a series of controlled laboratory tests.

1.2. Aim and Objectives of Research

The main aim of this research is to develop an environmentally friendly high–performance concrete with excellent fire resistance that can be used for high fire risk infrastructures. To achieve this aim, the following objectivities are targeted:

➢ Review past literature on the properties, applications, fire resistance and benefits of GP concrete and RPC within the construction industry.

➢ Prepare GP and RPC mixes separately based on existing literature and develop RPGC mixes based on optimised combinations of existing GP and RPC mixes.

➢ Determine the effect of two different FA source materials on the properties of GPs, i.e. Gladstone FA vs Callide/Gladstone FA.

➢ Carry out experiments and analyse the density, workability, curing regimes and compressive strength of reported GPs and RPCs mixes (used as controls) in literature and carry out similar tests for trial and error RPGC mixes.

➢ Examine the effect of temperature exposure, at $400^{o}C$ and $800^{o}C$, on the compressive strength and thermal capability of the mixes investigated in the study.

➢ Conduct Thermogravimetric analysis (TGA) to determine the percentage loss in mass after exposure to elevated temperatures.

1.3. Scope of Thesis

The scope of this study is to investigate the performance of a newly developed material called RPGC when exposed to elevated temperatures. Following the initial literature review, a series of sample experiments based on past research were carried out. GP paste samples and RPC samples were prepared and tested separately to establish optimum conditions in terms of material

compositions, chemical levels, curing techniques and mechanical properties. The material matrix, curing regime and mechanical properties of the samples which produced the best results were then used to develop the new material. Properties such as compressive strength, residual strength, density, workability and mass loss parameters were investigated in this study.

1.4.   Contribution to knowledge

The high strength and rapid hardening concrete market is at the peak of its demanding stages (Mehta and Burrows, 2001). The fast-moving schedules in the industry have driven out slow-hardening, average-strength concretes. Research estimates that the compound annual growth rate on the usage of high strength rapid hardening concrete will grow by 10.2% from 2015 to 2020. Hence, the impact on global climate change can only be expected to massively increase over time (Mehta, 2004). The main aim of this research is to develop RPGC that has high strength, excellent fire resistance and is environmentally friendly, which will contribute greatly to the field of Civil Engineering under areas of Sustainability and Innovation. These concretes will help to address Australia's National Research Priorities – i) *Reducing the Carbon Footprint*, in addition to ii) *Safeguarding Australia* as these concretes will provide security against acts of terrorism and hydrocarbon fuel accidents for high fire risk infrastructures.

Past literature shows extensive research and findings on RPC and GP concrete as two separate topics however, to date, there is limited reported literature regarding RPGC. The works conducted in this study aim to provide information on the performance of RPGC at elevated temperatures.

1.5.   Statement of significance

RPC is a valuable type of concrete as high strength infrastructure is a growing necessity. However, because of the utilization of high amounts of cement in the mix, it imposes a high carbon footprint on the environment. On the other hand, GP concrete is an eco-friendly material with a comparatively low carbon

footprint on the environment. However, GPs cannot achieve the high strengths that RPCs display. This creates a research gap in this study which aims to combine these two concrete types into developing a sustainable high-performance concrete. The research further proves to be beneficial as it taps into the behaviour of RPGC at elevated temperatures. Though the longevity and durability of RPGC has not been vastly explored, this project provides the foundation into further works and deep investigations in long-term studies.

1.6. Outline

This thesis is organized into five chapters in accordance to the stages of testing which were conducted. An outline of each chapter is given below.

Chapter 01 introduces the research project and gives a justification for conducting a study of this magnitude. It further emphasizes the significance of the study and the contribution it has on existing knowledge. In addition to this, the aims, objectives and the scope of the study are identified.

Chapter 02 presents information from existing literature which gives an in-depth insight to areas such as environmental issues of concrete, behaviour of concrete in fires, GP concrete and RPC. Areas such as history, fundamental chemistry, material properties, curing techniques, compressive strength, workability and performance in fire will be covered in relation to both GP and RPC.

Chapter 03 presents the materials used and experimental procedures carried out on a series of GP and RPC mixtures. Figure 1.1 provides an overview of the experimental program which was conducted in the study. Detailed descriptions on the materials used, mix designations, sample preparation, curing regime and test methods and specifications will be provided.

Chapter 04 presents the testing and analysis carried out on a series of GP and RPC mixtures. Results on the density, workability and compressive strength for GP paste, RPC and RPGC specimens are presented. Residual strength properties and mass loss information on GP paste and RPGC samples using cube samples and thermogravimetric analysis (TGA) are also

presented. Differences in performance using two types of FA and varied curing methods will be analysed. Discussion and conclusion of the overall results and major findings will be discussed and compared to that of past researchers.

Chapter 05 will summarize all the findings and conclusions made throughout the course of the research. Recommendations for future work on improving and enhancing the study further, will also be provided.

```
┌─────────────────────────────────────────────────────────────────────────────┐
│                                                                               │
│   ┌──────────────────┐                        ┌──────────────────┐           │
│   │  Performance of GP│                        │ Performance of RPC│          │
│   │     in fire        │                        │     in fire       │          │
│   └──────────────────┘                        └──────────────────┘           │
│            │                                            │                      │
│            ▼                                            ▼                      │
│   ┌──────────────────────────────┐     ┌──────────────────────────┐          │
│   │ Conduct workability and      │     │ Conduct workability and  │          │
│   │ density testing on a series  │     │ density testing on a     │          │
│   │ of Gladstone FA GP and       │     │ series of RPC mixes      │          │
│   │ Callide/Gladstone FA GP mixes│     │                          │          │
│   └──────────────────────────────┘     └──────────────────────────┘          │
│            │                                            │                      │
│       ┌────┴────┐                                       ▼                      │
│       ▼         ▼                              ┌──────────────────┐           │
│  ┌─────────┐ ┌─────────────┐                   │ Conduct          │          │
│  │ Conduct │ │ Conduct     │                   │ workability,     │          │
│  │compress.│ │ compressive │                   │ density and      │          │
│  │strength,│ │ strength,   │                   │ compressive      │          │
│  │residual │ │ residual    │                   │ strength testing │          │
│  │strength │ │ strength    │                   │ on 25mm cube     │          │
│  │testing  │ │ testing and │                   │ samples          │          │
│  │and mass │ │ mass loss   │                   └──────────────────┘           │
│  │loss     │ │ testing on  │                            │                     │
│  │testing  │ │ 50mm cube   │                            │                     │
│  │on 25mm  │ │ samples to  │                            │                     │
│  │cube     │ │ test the    │                            │                     │
│  │samples  │ │ effects of  │                            │                     │
│  └─────────┘ │ size on the │                            │                     │
│              │ final       │                            │                     │
│              │ strength.   │                            │                     │
│              └─────────────┘                            │                     │
│       │            │                                    │                     │
│       └────────────┴──────────────┬─────────────────────┘                    │
│                                    ▼                                          │
│   ┌──────────────────────────────────────────────┐                          │
│   │        Performance of RPGC in fire            │                          │
│   └──────────────────────────────────────────────┘                          │
│                        │                                                      │
│                        ▼                                                      │
│   ┌──────────────────────────────────────────────┐                          │
│   │ Based on the best properties, conduct         │                          │
│   │ workability, density, compressive strength,   │                          │
│   │ residual strength testing and mass loss       │                          │
│   │ testing on a series of trial and error mixes  │                          │
│   │ for RPGC                                       │                          │
│   └──────────────────────────────────────────────┘                          │
│                                                                               │
└─────────────────────────────────────────────────────────────────────────────┘
```

Figure 1.1 – Overview of experimental program

CHAPTER 02

LITERATURE REVIEW

2.1. Chapter overview

This chapter presents an in-depth literature review in areas of concrete, GPs and RPCs. The chapter starts with an insight to the issues related with increasing consumptions of cements and concretes in relation to the environment followed by the effects of fire exposure on normal and high strength concretes. The chapter then moves on to GP pastes, mortars and concretes covering areas such as chemical compositions, material properties, curing techniques and GPs in fire. The latter part of the chapter discusses similar sub topics under RPC technologies and the current studies using GP based high strength concretes.

2.2. Cement and the environment

2.2.1. Related issues

Concrete has been claimed to be the second most utilized material in the construction industry next to water. It is a key building material in the field of construction due to its strength, resistance to fire, durability, workability and several other factors (Gan, 1997). Though conventional concretes behave poorly under tensile loading, it has good compressive properties (Neville, 1995), therefore, concrete is a highly advantage construction material within the industry. However, the production of concrete comes at the cost on the environment.

Cement is the binding ingredient in concrete, without it, concrete cannot be produced. Three principal sources of CO_2 emission during cement production were identified as the emissions associated with the de-carbonation of

limestone, the combustion of fuels and the power required for the mixing and production of cement (cement finishing) (Cook, 2009). It has been reported that for every ton of OPC produced, one and a quarter tonnes of CO_2 is emitted into the environment of which 60% is due to the energy inputs required for cement production and 40% is due calcination (Watson et al., 1996, Griffin, 1987).

A research project conducted by Flower and Sanjayan (2007) revealed that about 74%–81% of the total CO_2 emission in concrete was due to the production of Portland cement from the combustion of fossil fuels in the kiln, calcination process of limestone, mixing and transportation, whilst 11%–20% of the total CO_2 emission in concrete was due to coarse aggregate. Mehta (2001) described the manufacturing of Portland cement as an energy intensive process which emits extreme amounts of GHG into the environment.

According to Gregg et al. (2008), the manufacturing of cement and fossil fuel combustion are the two primary sources of CO_2 emissions. USA, which held the position of being the country with the largest CO_2 emissions was overrun by China in the year 2006. By 2015, China was accountable for approximately 30% of the worlds' CO_2 emissions. Studies conducted revealed China being responsible for 56% of global cement consumption which has more than doubled (Gregg et al., 2008). In 2008, the cement production in Australia accounted for roughly 1.3% of GHG emissions (McLellan et al., 2011). Edwards (2015) showed that the global production of cement increased to 4.2 billion tonnes in 2014 (Figure 2.1) whilst Crow (2008) after reviewing the effects of concrete on the current environment, stated that by the year 2050 the use of concrete globally is predicated to reach four times the usage level in 1990.
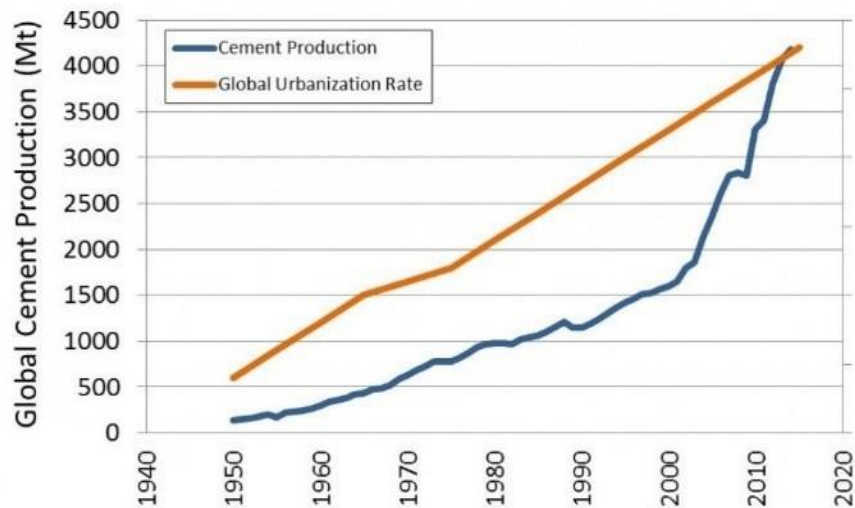
Figure 2.1 – Global cement production since 1950 (Edwards, 2015)

Over the years, several researchers have suggested many solutions to mitigate this growing crisis. As recognised by Mehta (2001), the conservation of cement is a key solution in reducing the GHG emissions globally. The use of alternative materials containing cementitious or pozzolanic by-products, such as FA, ground granulated blast-furnace slag, silica fumes, recycled concrete, etc., are of vital importance. Meyer (2009) concluded a research by giving five suggestions to the issues, of which the most effective one was identified as replacing as much of the Portland cement with other cementitious materials. Cook (2009) also stated that the principal option to reducing the CO_2 emissions is by partially or fully replacing cement in the concrete matrix. Blending cement with pozzolans or cementitious materials vary from country to country depending on material availability, however, the current blending ratio around the world is approximately 22%. Figure 2.2 gives information of the CO_2 emission reduction potentials achieved in the year 2006. Furthermore, Anand et al. (2006) stated that the reduction of the amount of CO_2 emitted by cement industries can be achieved by decreasing the amount of cement in concrete and by decreasing in the number of infrastructures using concrete.
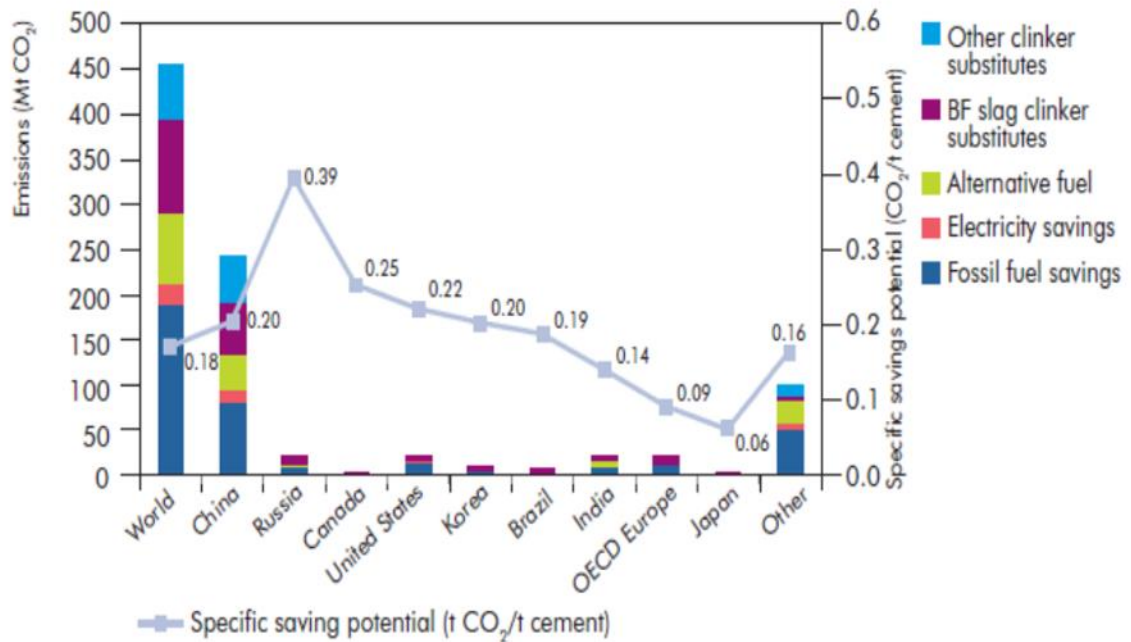
Figure 2.2 – CO$_2$ emission reduction potentials in 2006, based on best available technology (Cook, 2009)

2.2.2. Concrete in fire

Concrete is a heterogeneous material which undergoes complex changes chemically, physically and mechanically when exposed to elevated temperatures. The difference in behaviour of the shrinking paste and the expanding aggregate at elevated temperature induces thermal incompatibility between the two. This gives rise to thermal stresses within the concrete which entertain breakage of concrete members. Additionally, the microstructural changes which occur during temperature rise can greatly influence the strength, stiffness and the durability of the concrete. Figure 2.3 presents the microstructural changes which occur at high temperatures (Khoury, 2000).
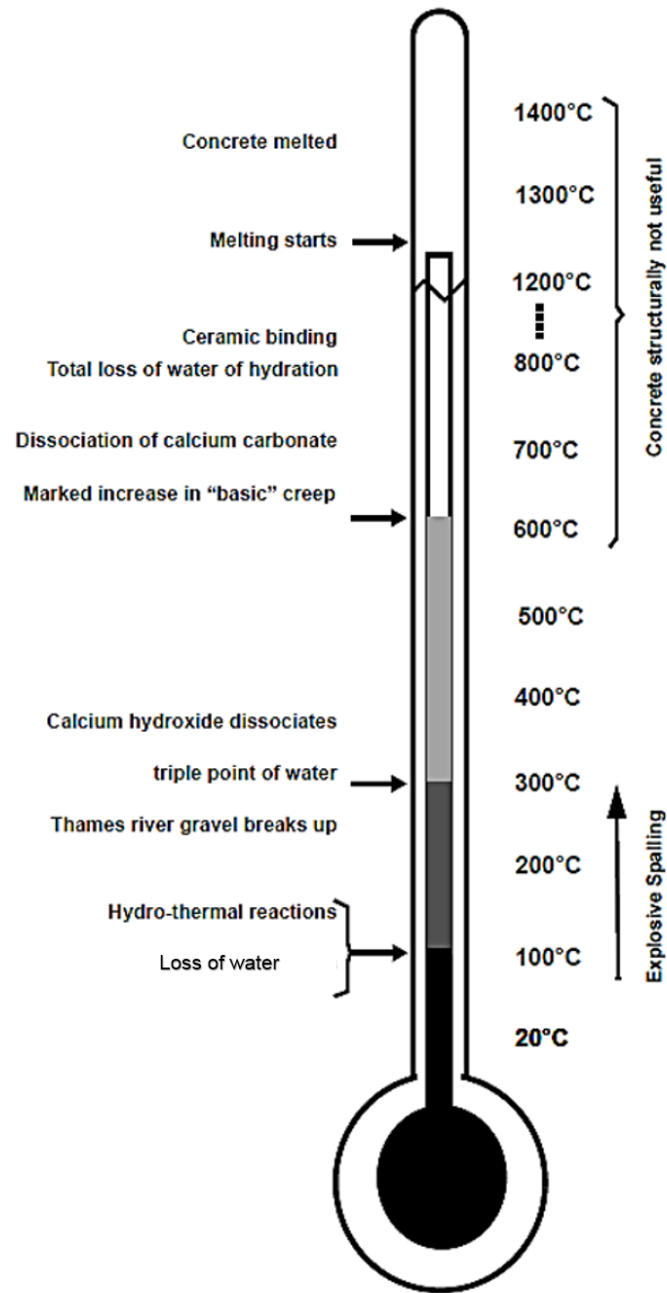
Figure 2.3 – Microstructural changes of OPC concrete at high temperatures (Khoury, 2000).

The density of concrete which is generally around 2400 kg/m^3 is reported to decrease by about 100 kg/m^3 as the temperature increses to 100°C (Buchanan and Abu, 2017). Kodur (2014) stated that this condition occurs due to the evaporation of moisture upon reaching 100 ^{o}C. However, apart from the loss of moisture, elevated temperture levels does not create much changes to the density of concrete (Hsu and Lin, 2008). Zhang (2011) reported that when

concrete is exposed to elevated temperatures, large changes in volume can be observed due to thermal shrinkage and creep which is associated with water loss. Water is known to evaporate at temperature of 100°C (Anderberg, 1997), however, there are three types of water in concrete which behave very differently to one another. Capillary water, which is found in the capillary pores in the concrete paste, the aggregate and interface, is easily evaporable. Gel water which exist in the gel pore of the cement paste and considered as physically bound water is not as easily evaporated however, it is found to evaporate at an ambient temperature of 200°C. Chemically combined water, often referred to as non-evaporable water, is the part of cement hydrate compounds and is found to expel the concrete when chemical decomposition of the cement paste and aggregate occur at temperatures of about 500°C.

Studies also report that the behaviour of concrete structures during elevated temperatures is mainly dependent on the mix design, material type and its thermal conductivity which induces significant changes in factors such as compressive strength, diffusivity, mass, density, and porosity (Hsu and Lin, 2008, Fu and Li, 2011). Conventional concretes are known to have excellent fire resistance properties and high load bearing capacities whereas high strength concretes are reported to behave poorly with lower resistance and poorer bearing capacities. The extent of this resistance and capacity, as stated by Kodur (2014), is dependent on the mechanical and deformation properties which come in to play when concrete is exposed to high levels of heat.

The mechanical properties are defined as the compresssive strength, tensile strength, stress-strain properties and the modulus of elasticity and the deformation properties are identified as creep and thermal expansion/shrinkage (Kodur, 2014). The compressive strength is mainly dependent on the mix design which includes the aggregate type and size, water to cement ratio, cement type and admixtures, the interfacial transition zone, curing regime, heating rate and loading factor (Mehta, 1986). When considering the tensile strength, many studies focus less on the calculation of the tensile properties as it is found to be only 10% of the compressive strength. However, the tensile strength is an important factor when analysing the

mechanical properties because cracking generally occurs due to the concrete failing in tension (Li, 2011, Khaliq and Kodur, 2012). Figure 2.4 and 2.5 illustrates the stress-strain relationship of concrete and a comparison of different strength concretes when exposed to elevated temeratures showing clearly significant decreaments in the residual strength as the temperature increases (Beeby and Narayanan, 2005). Similar graphs have been provided by Fu et al. (2005) where a study of normal strength concretes and high strength concretes have been conduted (Figure 2.6). The modulus of elasticity which is also known to decrease with increasing temperture levels is dependent on the loss of moisture, creep and type of aggregate (Kodur, 2014).
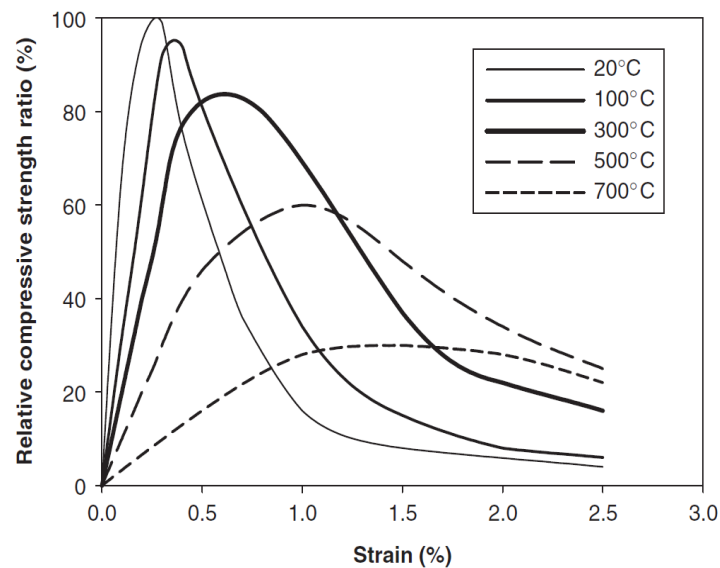
Figure 2.4 – Stress-strain relationship of concrete when exposed to high temperature levels (Beeby and Narayanan, 2005)
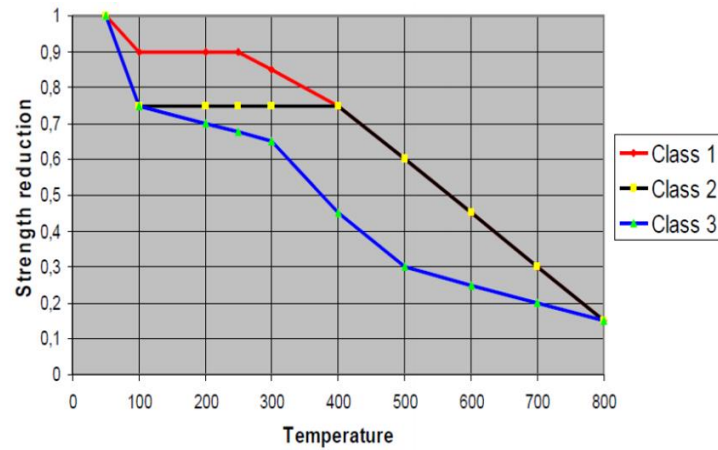
Concrete C 55/67 and C 60/75 is Class 1, concrete C 70/85 and C80/95 is Class 2 and concrete C90/105 is Class 3.

Figure 2.5 – Reduction of strength (%) at elevated temperatures (℃)(Beeby and Narayanan, 2005)
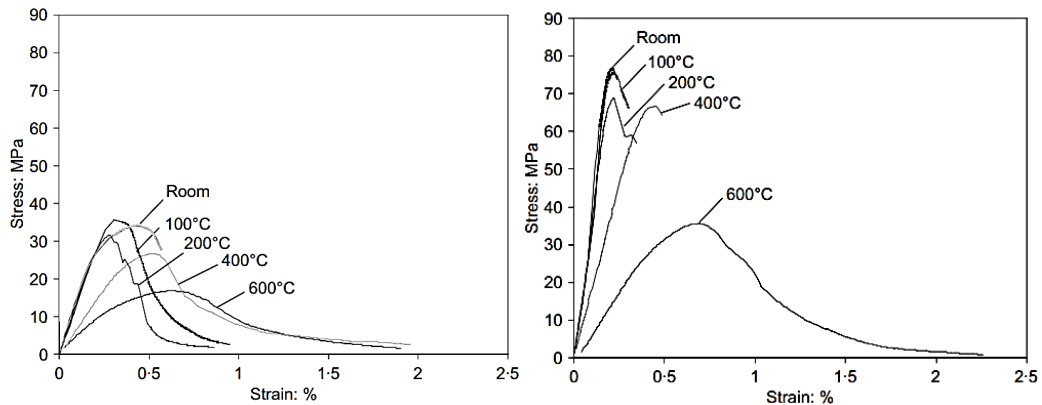
Figure 2.6 – Temperature-dependent stress–strain curves in unstressed test condition: Normal strength concretes (left) High strength concretes (right) (Fu et al., 2005)

The deformations which occur when concrete is exposed to elevated temperature levels are creep and thermal expansion/shrinkage. Creep occurs due to the existence of moisture within the microstructure of the concrete and depends on the stress levels and the temperature gradients within the concrete when exposed to high levels of temperature. Thermal expansion/shrinkage, which is generally determined through the dilatometric curve, is dependent on the age of concrete, type of cement, moisture content and type of aggregate (KIM et al., 2003, Bažant and Chern, 1987, Su et al., 2017). The strength of concrete which is a significant measurement when

16

concrete is exposed to fire, has been traditionally measured through the course of standard fire testing, however, numerical methods are gaining more recognition due to its cheap and less time consuming nature (Kodur and Raut, 2010, ASTM, 1999).

A study condcuted by Yu et al. (2012a) investigated the residual fracture properties of concrete when exposed to high tempreatures. They conducted testing on 50 conventional concrete specimens and found that the residual compressive strength decresed sharply from 31.41 MPa to 22.91 MPa upon reaching 100°C Afterwards the strength increased slightly to 26.34 MPa until 300°C and finally decreased contiuously until 16.74 MPa upon reaching a temperature of 600°C.

Hsu and Lin (2008) studied the residual bending moment, shear strength and effective elastic modulus of reinforced concrete beams when exposed to fire. It was reported that beams having positive bending moments resulted in a residual ratio of 30.82% at a fire exposure of 240 minutes whereas beams having negative bending moment failed after just 173 minutes of fire exposure.

Beams produce a negative bending moment when the tension tends to occur above the neutral axis and the compression below the neutral axis and vice versa. Furthermore, the shear strength had been seen to decrease smoothly to 64.76% after 240 minutes of fire exposure and the elastic modulus had also decresed significantly (Hsu and Lin, 2008). Zhang (2011) stated that in general, the compressive stength, tensile strenth and flexural strength of concrete does not decrease significantly up to about 200°C, after which considerable decrements can be witnessed. A study conducted by Yu et al. (2012b) investigated the residual fracture toughness on concrete specimens when exposed to a maximum temperature of 600°C and deduced that the residual fracture toughness decreased after 500°C of heating. Additionally, during a temperature of 200°C–500°C considerable reductions in the brittleness of the concrete was observed (Yu et al., 2012b).

In the report by Phan and Carino (2001) the effects of elevated temperatures on the mechanical properties of high strength concrete were investigated where testing was conducted in accordance to steady state temperature test conditions. A steady state temperature test is when the specimens are exposed to a constant rising rate until the target temperature is reach and then held constant for a period of time after which they are allowed to cool down naturally until room temperature. Results showed an increase in strength loss for high strength concretes compared to normal strength concretes when exposed to high temperatures.

Another factor which is of significant importance when the concrete is exposed to fire, is concrete spalling. Ali et al. (1997) defined spalling as "*The process of disintegration of a concrete surface on exposure to heat*". When concrete is exposed to fire, or when the concrete is heated to above the boiling point of water (100°C), a vapour pressure is built up within the concrete forcing the moisture to evaporate via the concrete pores. The rate of this evaporation depends on the permeability of the concrete and because new developments require higher strengths, concrete is made to be denser which in turn limit the number of pathways for water evaporation. This increases the pore pressure within the concrete which result in violent spalling conditions. Pore pressure depends on the permeability, heating rate, moisture content and the size of the member. Simultaneously, thermal stresses also built up within the concrete as a result of thermal gradients arising between the surface and the core of the concrete. Once these stresses exceed the maximum allowable tensile stress, thermal cracks and breakage of the external layers of the concrete occurs. This breakage is identified as concrete spalling which can be either violent or non-violent and occur in the form of surface spalling, corner spalling, aggregate spalling or explosive spalling (Sanjayan and Stocks, 1993, Kalifa et al., 2000, Khoury, 2000, Ali et al., 1997, Boström et al., 2007, Guerrieri, 2009, Willam et al., 2005, Consolazio et al., 1998).

Surface spalling, which is classified as a violent type of spalling, is basically the degradation of the surface layers of the concrete and can occur as a progressive form of spalling, starting within the first 20 minutes of a fire. The

main concern in surface spalling is that it exposes the reinforcement within the concrete thus making it vulnerable to high levels of temperature and as the yield strength of steel reduces significantly at elevated temperatures, the load bearing capacity of the structure can be reduce drastically.

Corner spalling, which occurs after 30 minutes of exposure to fire, is the breaking off of corner sections due to the difference in thermal gradient on either side of the structural element. As corner spalling occurs at a latter stage where the structure integrity has already been affected, this type of spalling is comparatively of lesser importance and is considered a less violent form of spalling.

Aggregate spalling is the splitting off or bursting away of the aggregate within the concrete due to the difference in thermal expansions or contractions. This type of spalling is recorded to occur within the first 20 minutes of a fire.

Explosive spalling, considered as a violent form of spalling, is identified as a particularly dangerous type which can lead to catastrophic consequences. It is recorded to be mainly dependent on high heating rates (>30°C/min) and occur during the first 30 minutes of a fire. It can be fast, loud and occur in a random, unplanned pattern (Connolly, 1995, Shah and Sharma, 2017, Guerrieri, 2009, Phan, 2008, Hertz, 2003).

Hertz (2003) stated that concrete spalling is less likely to occur if the concrete is dry. The thermal gradient and stresses which form within the concrete when heated can only entertain concrete spalling where there is the presence of moisture. This makes moisture a governing factor behind concrete spalling (Shorter and Harmathy, 1961, Zhukov, 1976, Phan and Carino, 1998). Hertz (2003), deduced that concretes having <3 wt.% moisture with not cause concrete spalling.

A study conducted by Sideris (2007) tested the residual strength and spalling properties of cubical and cylindrical specimens when exposed to elevated

tempertures of up to 700ºC. Results reveled that specimens which displayed low strength readings (29.5–39.6 MPa at 28 days) did not spall at all during its rise to 700ºC, whereas specimens which displayed higher strengths of 45.2 MPa–67 MPa suffered explosive spalling at temperatures between 500ºC–580ºC and 380ºC–480ºC. This further confirmed the conclusions made by Sanjayan and Stocks (1993) of high strength concretes being more vulnerable to explosive spalling when compared to normal strength concretes.

The theory of high strength concretes being prone to explosive spalling has been studied by several other researchers and it has been deduced that high strength alone is insufficient to cause explosive spalling. Further unfavourable factors such as loading factor, heating rate, moisture content, permeability or the strength of the pore structure can be probable causes of explosive spalling conditions (Ali et al., 1997, Williamson and Rashed, 1984, Phan and Carino, 1998, Boström et al., 2007).

Hertz (2003) stated that when considering traditional concrete, the effect of explosive spalling can mostly be witnessed in the first 20 minutes of exposure. It was reported that the increase in the volume of quartz crystals at 570ºC can create microcracking to occur around the stones which can deteriorate the concrete but not cause explosive spalling conditions. Furthermore, Hertz stated that the heating rate is a key factor in concrete spalling, where rapid heating causes large temperature and moisture gradients to form which causes explosive spalling conditions to occur. Zhang (2011) stated that in general, the compressive stength, tensile strenth and flexural strength of concrete does not decrease significantly up to about 200ºC, after which considerable decrements can be witnessed. Boström et al. (2007) conducted testing at different loading rates on several concrete specimens of varied dimensions when exposure to fire and deduced that the loading rate is a key factor which affect the amount and probability of spalling.

2.3. Geopolymers

In 1978, a French scientist by the name of Joseph Davidovits brought into light a new technology where alkaline solutions could be coupled with silicon and aluminium rich materials to produce binders called Geopolymers (GPs). Since then, this has been an emerging development due to its high performance and zero utilisation of cement thus making it a 'greener' concrete (Davidovits, 2002). Geopolymeric binders is basically a mixture of a source material(s), rich in silica and alumina and alkaline liquid, which is most commonly a combination of sodium hydroxide or potassium hydroxide and sodium silicate or potassium silicate manufactured through the process of geopolymerisation under hydrothermal conditions (Lloyd and Rangan, 2010). Several studies prove that GP materials have excellent resistance to fire and chemical attacks, achieves high early strength, has low permeability, has a good freezing–thawing cycles and is environmental friendly when compared to conventional concretes (Li et al., 2004, Wallah and Rangan, 2006, Davidovts, 2013, Duxson et al., 2007).

When considering the basic material in GP cement, several reports, Bondar et al. (2010), Aldred and Day (2012b), Davidovts (2013) show that a material rich in aluminium and silicon such as FA, slag, rice husk ash, silica fumes, etc. is considered as the source material. Swanepoel and Strydom (2002), Hardjito et al. (2004), Rovnaník (2010) all utilized pozzolanic materials such as FA, blast furnace slag or metakaolin as the source material in their studies. The choice of the type of source material depends mainly on the cost of material, availability and type of application. Li et al. (2004) gives information that the abundance of raw material resources together with properties such as fast setting conditions, reduced carbon dioxide emission, high early strength and excellent fire resistance properties (up to $1200^{\circ}C$ resistance) are the key advantage behind making GPs the most responsible and smartest choice for a sustainable future.

There have been many studies (Kong and Sanjayan, 2010, Mane and Jadhav, 2012, Brahammaji and Muthyalu, 2015, Bakharev, 2006, Hardjito et al., 2005a) which utilise low-calcium FA as opposed to high-calcium FA as the source material in GP. It has been reported that high levels of calcium affect the polymerisation process which alter the microstructure pf GPs (Gourley and Johnson, 2005). Davidovits (1999) stated that even though calcined source materials such as FA, slag, metakaolin, produce higher compressive strengths compared to non-calcined source materials such as kaolinite, kaolin clays or naturally occurring minerals, a combination of the two types show significant improvements in the mechanical properties. It was further suggested a silicon to aluminium molar ratio of around 2.0 for the source material produce ideal results.

The utilisation of slag as a source material has been conducted several times however, the complexity of the chemistry of slags create a pathway for FA based GPs to be more popular compared to slags. Additionally, FA based GPs are reported to be stronger, more durable and having a microstructure best described as a gel-bonded ash composite compared to slags (Duxson et al., 2007).

When comparing the microstructure of cement mortar to GP mortar, cement mortar consists of coarser grains unevenly fit together whereas the GP mix displays finer particles which are more closely packed (Cheng and Chiu, 2006). Higher compressive strengths of GPs can be achieved through the use of higher molecular masses in the sodium hydroxide and with the use of higher sodium silicate to sodium hydroxide solution ratios (Hardjito and Rangan, 2005). In comparison to conventional concrete, GP concretes have proved to have excellent resistance to chemical attacks which makes GP concretes more applicable to structures built in harsh and aggressive environmental conditions, such as marine structures and sewer pipe manufacturing, (Wallah et al., 2005, Brahammaji and Muthyalu, 2015).

After an extensive investigation, Brahammaji and Muthyalu (2015) stated that the resistance to acid attacks is higher for GP concretes with a considerably

low loss of compressive strength and low percentage of weight loss in comparison to conventional concretes. However, when exposed to magnesium sulphate, it had been observed that the drop in compressive strength for GP concretes were much higher compared to conventional concretes which was proof that GP concrete are highly sensitive to magnesium sulphate acids. A study which investigated the acid and alkaline resistance of GP pastes using class F FA with sodium-based solutions (D-grade silicate, 14M hydroxide) deduced that the resistance can be increased in considerably by calcination at 600°C due to partial surface crystallisation of the amorphous elements (Temuujin et al., 2011).

When considering the economic benefits of GP concretes, studies show that the use of FA based GPs is estimated to be 10-30% cheaper than the use of conventional concretes (Lloyd and Rangan, 2010). In addition, due to its high levels of resistance to chemical attacks and low shrinkage and creep properties, GP concretes further prove to be beneficial and economical (Lloyd and Rangan, 2010). The carbon dioxide emission is reported to reduce by 80–90% when using GP materials in comparison to OPC concretes (Davidovits, 1999).

2.3.1. The Chemistry behind GPs

The term 'Geopolymers' was first introduced by Davidovits (1999) which involved a process called polymerisation, a fast chemical reaction occurring under highly alkaline conditions of silicon and aluminium minerals which yield polymeric Si-O-Al-O bonds in amorphous form. Brahammaji and Muthyalu (2015) stated that chemical composition of GPs are very much similar to natural zeolite materials having high amounts of silicon, aluminium and oxygen. However, zeolites have a crystalline microstructure whereas GPs are amorphous. GPs based on silicon and aluminate are referred to as 'Polysialates', which are chain and ring polymers with Si^{4+} and Al^{3+} in IV-fold coordination with O_2. The structure of the Polysialates is shown in Figure 2.7 (Davidovits, 1994).
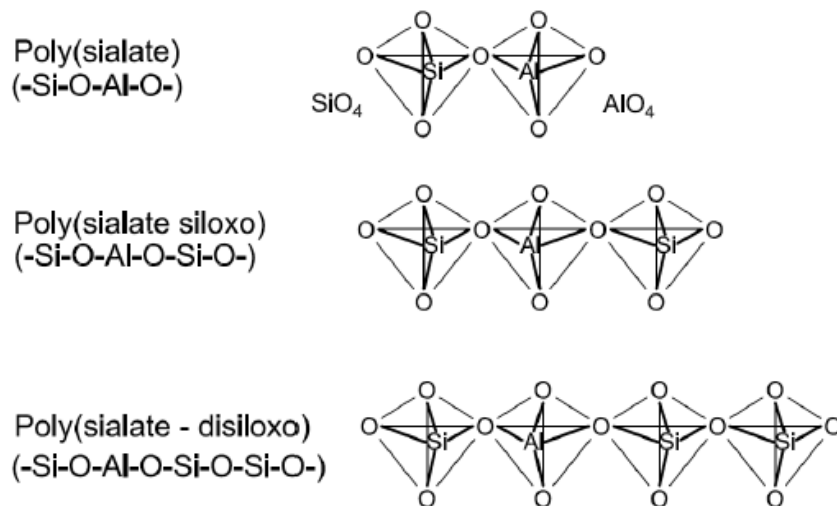
Figure 2.7 – Chemical structure of Polysialates (Davidovits, 1994)

The stages of the polymerisation process are divided mainly into three stages; the destruction-coagulation stage; the coagulation-condensation stage; and the condensation-crystallisation stage. The first stage occurs when the pH value of the alkaline solution is at a very high level which forces a breakdown in the covalent bonds Si-O-Si and Al-O-Al. The second stage form a coagulated structure by destroying and interacting the elements with each other. In the final stage a condensed structure is generated and crystallised (Li et al., 2010, Glukhovsky, 1959). Temuujin et al. (2011) describes the chemical structure of GPs as cross-linked aluminium silicate networks which links one polymer chain to another. A highly simplified version of the geopolymerisation process is given in Figure 2.8 Duxson et al. (2007).
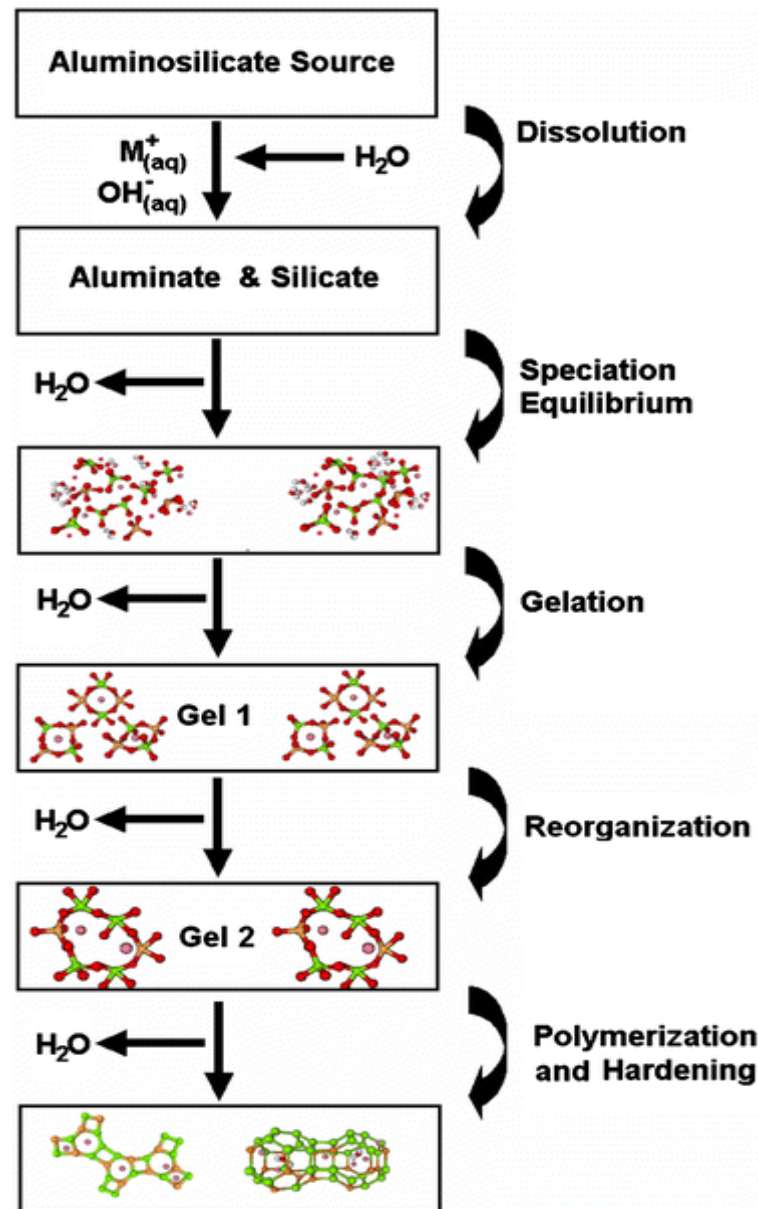
Figure 2.8 – Conceptual model for geopolymerisation (Duxson et al., 2007).

2.3.2 An insight to FA

Over time, researchers have discovered materials (cementitious materials) which can partially replace cement and can achieve similar and/or higher compressive strengths whilst reducing the carbon emissions (Barbour, 1991). Amongst these cementitious materials FA, which can be defined as a fine powdered residue generated in coal fired power stations, have been proven to be a fine cement-replacement material in concrete (Ahmaruzzaman, 2010). Originally, FA was used as a cement-replacement material to improve the rheological characters, reduce the alkali-aggregate reactions and most

importantly to reduce the carbon footprint by reducing the amount of cement in concrete. However, over time FA has been rapidly attracting attention to being used as a source material in the production of GPs due to high compositions of silicon and aluminium (Davidovits, 2008).

During the combustion process of coal three main products are formed, namely FA, bottom ash and gas/vapour. FA is identified as the fine part of ash and the bottom ash is identified as the heavier residue having coarser particles. The gas/vapour is partly condensed onto the surface of the FA particles and the remainder is discharged into the atmosphere (Joshi and Lohtia, 1993). FA is considered as fine, mostly spherical, hollow glassy particles having a diameter ranging from 1μm–150μm, which is finer than Portland cement and lime particles (Brahammaji and Muthyalu, 2015, Siddique, 2008). Figure 2.9 shows the collection of FA from coal fired electrical generating station.
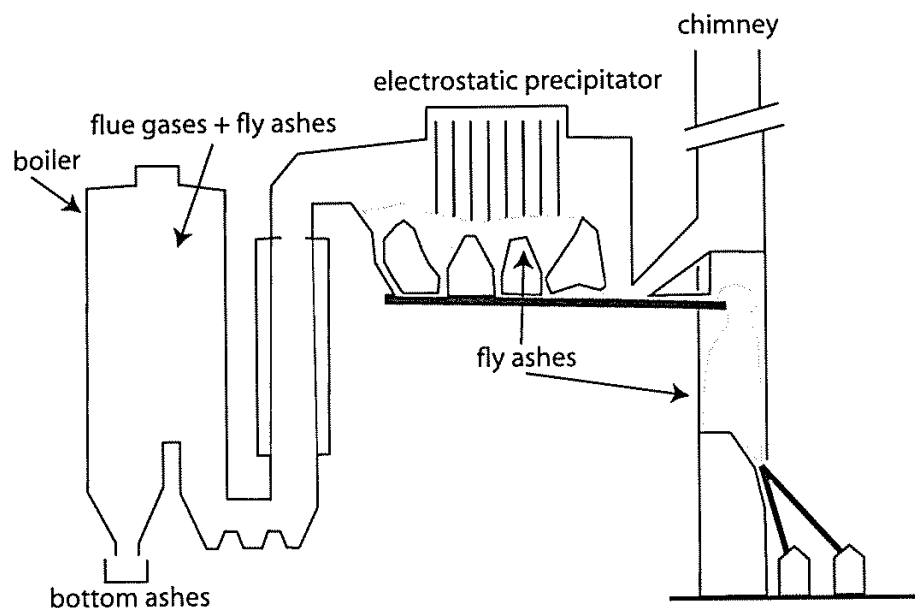
Figure 2.9 – The collection of FA from flue gases (Davidovits, 2008)

When considering the chemical composition of FA, it is mainly comprised of silica, alumina and ferric oxide and other minor constituents such as calcium, sulphur, magnesium, phosphorus, titanium, alkaline and manganese (ASTM, 2003). However, the chemical and the physical compositions of FA vary and are dependent on the type of coal, the method of combustion and the particle

26

shape from which the FA is produced. Fly ash can be categorised mainly into high calcium class C FA or low calcium class F FA. Table 2.1 shows the main categories of FA as given by Davidovits (2008). Hardjito and Rangan (2005) states that more than 10% Calcium oxide (CaO) can be found in FA which is produced from burning sub-bituminous coals These types are identified as high calcium class C FA containing high levels of calcium and low levels of both silica and alumina which provides cementitious and pozzolanic properties. FA having less than 10% CaO is considered to be low calcium class F FA and is formed from the bituminous and anthracite coals. These are found to contain high levels of silica and alumina and low levels of calcium resulting in only pozzolanic properties (Ramachandran, 1996, Davidovits, 2008, ASTM, 2003).

Table 2.1 – Main categories of FA (Davidovits, 2008)

| Low-calcium fly ash Class F | CaO content less than 10% Usually produced from anthracite and bituminous coals Roughly corresponds to American (ASTM 618) class F. |
| High-calcium fly ash Class C | CaO content greater than 10% Usually produced from sub-bituminous and lignite coals Roughly corresponds to American (ASTM 618) class C. |

Sub bituminous coals are generally brown to black in colour and contain a carbon percentage of around 42-52%. Records show that an estimated 50% of the worlds' coal reserves are of sub bituminous or lignite coals, including deposits which can be found in Australia. Bituminous coals are found to have around 77-78% of a carbon percentage and elements such as water, sulphur, hydrogen and few other impurities. The production of bituminous coals is found to occur when sub bituminous coals undergo a more organic process of metamorphism. Anthracite coals on the other hand, have the highest carbon percentage and therefore lesser impurities. Anthracite coals do not ignite easily and produce blue smokeless flames upon ignition for a short time. These types of coals are recorded to be comparatively rare and hard to find. Heidrich (2002) stated that a majority of the FA found in Australia contains 80%–85% silica and alumina and can be categorised as Class F low calcium

FA. Table 2.2 gives the chemical composition for class C and class F FA (Davidovits, 2008).

Table 2.2 – Range of chemical compositions for low and high class FAs (Davidovits, 2008)

	Class F %	Class C Lignite based (%)
SiO_2	47.2 to 54	18 to 24.8
Al_2O_3	27.7 to 34.9	12.1 to 14.9
Fe_2O_3	3.6 to 11.5	6.3 to 7.8
CaO	1.3 to 4.1	13.9 to 49
Free lime content	0.1	18 to 25
MgO	1.4 to 2.5	1.9 to 2.8
SO_3	0.1 to 0.9	5.5 to 9.1
Na_2O	0.2 to 1.6	0.5 to 2
K_2O	0.7 to 5.7	1 to 3

In 1998, the annual ash production was estimated to be more than 390 million tonnes and this value was estimated to massively increase to about 780 million tonnes annually by the year 2010 (Mehta, 2004). In the year 2000, FA production in Australia was calculated to be approximately 12 million tonnes out of which only 5.5 million tonnes had been utilised (Heidrich, 2002). FA production in the United Sates was about 68 million tonnes in the year 2001 of which only 32% had been utilised (Brahammaji and Muthyalu, 2015). A summary of the production of coal combustion products (CCPs) in the United States from 1991 to 2016 as given by the American Coal Ash Association is shown in Figure 2.10 (Association, 2017). The production of CCPs were seen to decrease in the years 2014, 2015 and 2016, however the usage remained somewhat constant. This report further gives information that out of the 107.4 million tonnes of CCPs produced in the year 2016 in the United States, 37.8 million tonnes was FA. Though the production of FA is seen to decrease from the year 2001 to 2016 in the United States, Harris (2017) stated that within the next 30 years, countries such as China, India and other South East Asian countries will experience an increase in the production of FA.
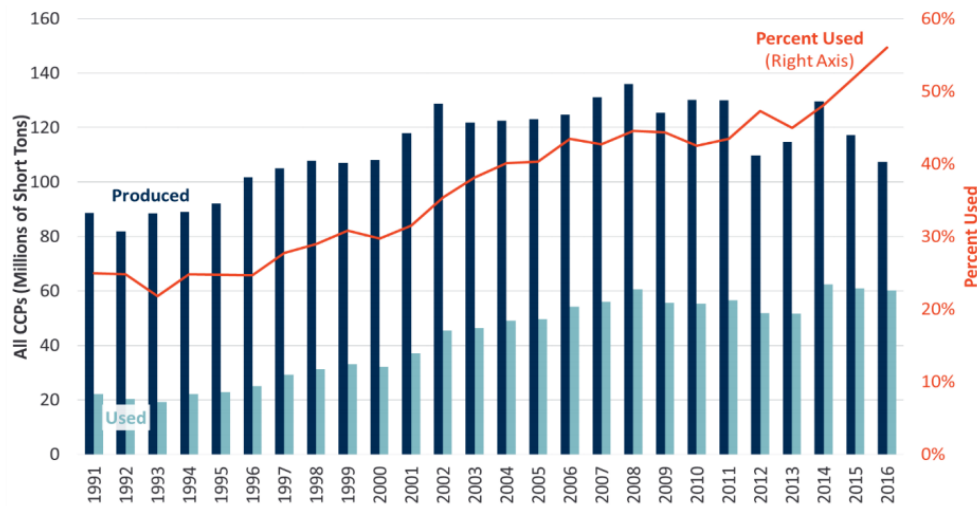
Figure 2.10 – Production and usage of all CCPs from 1991 to 2016 in the United States (Association, 2017).

After an extensive review, Izquierdo and Querol (2012) provides information that because FA is a heterogeneous material (diverse in character) and the elements are not equally distributed, it imposes a big threat on the environment in terms of land and water pollution whether it is used as recycled ash, sent off to landfills or disposed in surface impoundments.

Several advantages in both fresh and hardened concretes have been identified through the use of FA in concrete. These can be identified as improvements in workability, reduction of water consumption, reduction of bleeding and slower setting time in fresh concrete, together with higher strength readings, reduced permeability, increase durability in hardened concretes (Oner et al., 2005). Additionally, the use of FA contributes greatly into reducing the carbon footprint on the environment.

2.3.3. Alkali activated Solutions

In relation to the chemical composition, alkaline activators have been classified into 6 groups by Glukhovsky et al. (1980) as: (1) Caustic alkalis; (2) Non-silicate weak acid salts; (3) Silicates; (4) Aluminates; (5) Aluminosilicates; and (6) Non-silicate strong acid salts. Several researchers have studied the

effects of different alkali activated solutions on the performance of GPs (Xu and Van Deventer, 2000, Provis and Van Deventer, 2009, Lizcano et al., 2012, van Jaarsveld and Van Deventer, 1999, Palomo et al., 1999). However, sodium hydroxide and sodium silicate has been widely used as the alkali activating solutions. Sodium hydroxide due to low viscosity contributing to high workability, less expensive and highly available in nature and sodium silicate, manufactured through the process of mixing quartz sand and sodium carbonate at a temperature 1300℃, due to high viscosity contributing to high density, rapid hardening and high compressive strengths (Brough and Atkinson, 2002, Buchwald and Schulz, 2005, Jo et al., 2007).

Several studies prove the combination of sodium silicate and sodium hydroxide produce high quality results in terms of setting times, density, workability, durability and strength. However, the use of potassium-based activators (potassium silicates and potassium hydroxides) have also been widely utilised, but lacks publicity compared to sodium-based activators due to its expensive nature which makes potassium-based activators commercially unviable. (Pimraksa et al., 2008, Chindaprasirt et al., 2010, Su et al., 2016, Abdulkareem et al., 2014, Yunsheng et al., 2008b, Shrestha, 2014).

The mechanical properties of using different alkaline solutions on a FA based GP mortar had been studied by Fernández-Jiménez and Palomo (2005) where sodium silicate (a.k.a. waterglass solution), sodium hydroxide and sodium carbonate had been used. A mix of sodium hydroxide and sodium silicate solution was recorded to produce increased mechanical strengths whereas the carbonate ions had produced opposite results which lower mechanical strength results.

The difference between alkali activated binders and OPC binders is that alkali activated binders use strong alkali solutions to dissolve the elements where OPC cements use water to start the hydration reaction. As the hydration reaction occurring in the concrete progresses, several C-S-H bonds are formed which creates a highly alkaline condition. Therefore, an activator

having an initial neutral pH such as water, is required to activate the hydration reaction.

In contrast to this, when considering alkali activated binders, high pH values prevent the coagulation and polymerization of alkali silicates such as sodium silicates which are required to produce high end results in terms of physical and chemical properties. As the pH reduces, the main elements are dissolved, and condensation occurs at an elevated rate. Finally, a series of reactions and hardening processes occur to form alumina silicate particle in an amorphous aluminosilicate structure (Lee and Van Deventer, 2002a). Fernández-Jiménez and Puertas (2001) stated that though sodium carbonate is less expensive and can be used as an alkaline activator, it is relatively weak compared to hydroxide and silicate. Shrestha (2014) gives information that compared to potassium hydroxide, sodium hydroxide caused a higher dissolution of minerals which enhanced the reaction between the alkaline solution and the source material.

2.3.4. Curing techniques

Curing has been recorded to be an essential factor affecting the properties and performance of GPs. Heat curing using either steam curing or dry curing techniques, have been reported to be the best conditions for GP curing. Several studies have shown that maximum engineering properties in terms of strength, permeability, durability, etc. can be obtained when GPs are heat cured at high temperatures of $\geq 60^{\circ}C$ for a period of 24 hours (Shuaibu, 1950, Sindhunata et al., 2004, Duxson et al., 2007). Aldred and Day (2012a) showed statistical data proving that GP concrete achieved the required strength parameters by 7-14 days and temperature was found to play a key role in the strength development of GP concrete. It was found that adequate early strength was achieved in the samples subjected to curing at temperatures higher than $20^{\circ}C$. Vijai, Kumutha et al. tested the effects on strength by exposing the samples to ambient curing (placed at room temperature) and hot curing conditions (placed in an oven at $60^{\circ}C$ for 24 hours) and results showed the strength of hot cured samples to be much higher compared to ambient

curing (Vijai et al., 2010). Hardjito et al. (2004) and Rangan et al. (2006) also gives evidence that the optimum conditions in producing high properties for GP materials is heat curing in the form of dry curing at 60°C for a period of 24 hours.

When considering conventional concretes, the compressive strength depends greatly on the age of the concrete. Starting from about 65% at 7–day testing, the compressive strength would generally reach about 99% at 28 days. Furthermore, concrete must be cured, generally by water, until a standard of 7–days are complete. GPs on the other hand, are free from such conditions.

Studies show that after the initial curing process for 24 hours at a temperature of >60°C, the full strength of the material would have been reached, after which only moderate increments can be witnessed. Lloyd and Rangan (2010) gives information that heat curing assist in the geopolymerisation process and that both the curing time and temperature greatly affects the compressive strength of GPs. Hardjito (2005) deduced, after a series of tests, that GP specimens were found to have rapid increments in compressive strength up to 24 hours of heat curing in an oven at 60°C after which only slight increments in strength were recorded. It was stated that heat-curing for a period of 24 hours was sufficient for practical applications. Additionally, GP specimens which were dry-cured for a period of 24 hours were recorded to produce approximately 15% higher compressive strengths in comparison to stream-cured specimens. It was also reported that a delay in starting the heat-curing process after the casting process does not produce a drop in strength in GP specimens as conventional concretes display when the curing processes is delayed.

Low calcium FA specimens which have been heat-cured have proved to have high resistance to acid and sulphate attacks and shows signs of low drying shrinkage and creep (Lloyd and Rangan, 2010, Wallah, 2010). Hardjito et al. (2005a) conducted a study where the GP samples were prepared using low calcium class F FA as the source material and sodium silicate and sodium hydroxide as the alkaline solution. Curing of samples were conducted in two

methods, 60°C/90°C oven curing and 60°C/90°C steam curing. Results showed higher compressive strength readings for specimens which were cured at 60°C in the oven (dry) for a period of 24 hours. However, a key finding in this study was the effects of 'rest period', the time between the end of casting and the beginning of curing. Results showed a rest period of 60 minutes did not have any effects on the compressive strength of the specimens cured at 60°C oven (dry) for 24 hours. However, specimens which were subjected to a rest period of 24 hours or more had displayed significant increments in compressive strength (increments within the range of 20-50%). The study moves on to deducing that with increased mixing time, increments in the strength and density have been reported but at the cost of low workability conditions. Kong and Sanjayan (2010) conducted a series of heat elevated testing where the specimens were cured at a temperature of 80°C and a relative humidity of 93% for a period of 24 hours after being subjected to a rest period of 24 hours. It was found that the mean values for 3–day strengths of paste, mortar and concrete are 71.2 MPa, 72.3 MPa and 70.5 MPa, respectively.

2.3.5. GPs in Fire

GPs have proven to be a material having good fire resistance properties with numerous studies being conducted on its behaviour when subjected to elevated temperatures. The ceramic-like properties of GPs make it a material with superior resistance to fire when compared to other structural materials, including conventional concrete. However, unlike conventional concrete, GPs undergo both loses and gains in compressive strength when exposed to high heat. Strength loses, in comparison to OPC concretes, are found to be lesser for GP materials and recent studies have now reported that the strength gain or loss in some GP mix designations are closely associated with the ductility and thermal incompatibility within the mix matrix (Abdulkareem et al., 2014, Pan et al., 2009, Guerrieri and Sanjayan, 2010).

Mane and Jadhav (2012) studied the residual strength and mass loss properties of low-calcium FA GP mortars and concretes when exposed to elevated temperatures of up to 500°C. Results revealed that after an exposure of 500°C, GP concretes retained 84% more strength when compared to OPC concretes. Furthermore, the compressive strength of GP mortars increased upon reaching a temperature of 100°C after which it decreased until 500°C, whereas, OPC mortars displayed only strength losses as the temperature increased. Additionally, the expansion and shrinkage were also studied in this investigation. Results showed that GP specimens expanded up to 100°C, remained steady to 200°C, then displayed shrinkage until 300°C and then remained steady up to 500°C. This shrinkage was assumed to be associated with the loss in mass.

Kong and Sanjayan (2010) used class F Gladstone FA with sodium silicate and potassium hydroxide for the production of paste, mortar and concrete GP samples to test the effects of elevated temperatures (800°C). Results showed that for 100×200mm cylinders a 73.4% loss in strength for the paste samples, null results for the mortar samples (due to the specimens splitting into two halves) and a 58.4% loss for the concrete samples. However, cube paste samples which were of 25×25×25mm, were observed to undergo a strength gain of 6.4%. The authors went on to conclude that the size of the specimen did indeed have an effect on the strength when exposed to elevated temperature levels and this was due to the thermal incompatibility which occurs due to the thermal gradient.

Su et al. (2016) reported that the dynamic compressive strengths of GP concretes tested at 200°C exposures were higher (within a range of 84.9 MPa–104.8 MPa) than the strengths obtained at room temperature (within a range of 62.2 MPa–88.6 MPa). However, this strength was recorded to drop drastically to within a range of 15.4 MPa–36.7 MPa when tested after an exposure of 800°C. The mass loss was also recorded for the samples which resulted in a 4.6% loss at 200°C, due to the evaporation of water, and 8.4% loss at 800°C due to the decomposition of calcium carbonate.

The ductility of the material has been identified as a key factor which causes changes in the strength when GPs are exposed to elevated temperatures. Pan et al. (2009) found a correlation between the ductility and changes in strength of GP mortars. They found that samples having low initial strength showed increased residual strength whereas samples having high initial strength showed decreased residual strength after temperature exposure. Improvements in strength had been witnessed when the ductility of the samples were higher than a particular threshold value and losses in strength had been witnessed when the ductility of the samples were lower than the threshold value. The authors provided two main reasons for this phenomenon; (1) the increase in strength and ductility due to further geopolymerisation of the unreacted FA particles; and (2) the decrease in strength and ductility due to thermal incompatibility within the matrix. The final outcome of the material (strength gain/loss) would be a result of the more dominant process. Figure 2.11 shows a schematic demonstration of the two processes. The authors concluded the ductility or brittleness of the samples having a profound influence on the residual strength properties after temperature exposure regardless of the type of FA.
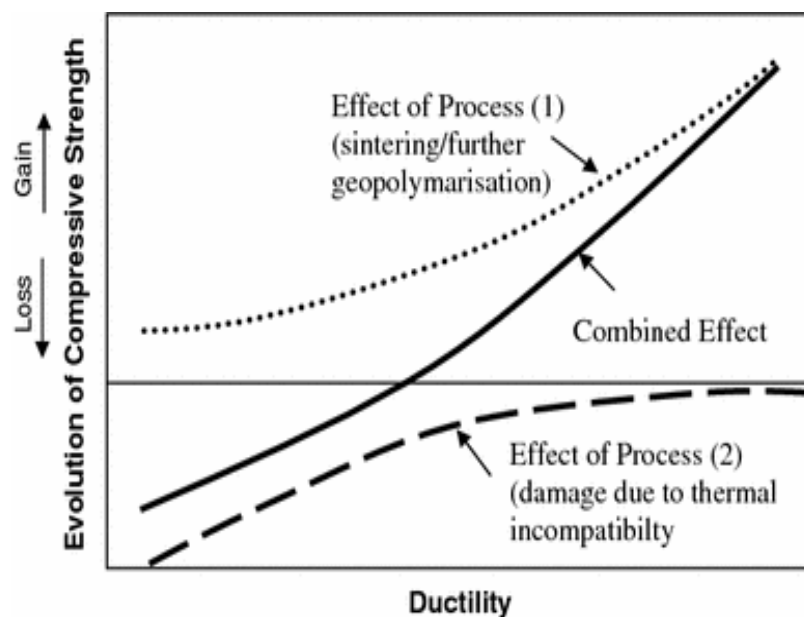
Figure 2.11 – A schematic diagram describing the two parallel processes in GP mortars at elevated temperatures (Pan et al., 2009).

Zhao and Sanjayan (2011) concluded that GP concretes display high resistance to spalling when compared to OPC concretes in a study where GP concretes and OPC concretes were exposed to elevated temperatures using the rapid surface temperature rise exposure test and the standard curve fire test. No spalling had been observed for the GP samples, while severe spalling was observed for the high strength OPC concrete samples. The results from the sorptivity test, which tests the materials ability to absorb and transmit liquid through the matrix via capillary suction, revealed that GP concretes are more porous and exposure to high temperature levels help facilitate the release of internal vapour thus reducing the internal stresses which enforce spalling.

A study conducted by Sakkas et al. (2015b) involved the fire testing on granulated slag based GP specimens. At a 28–day testing, where the samples were exposed to elevated temperatures, results were observed to be promising, with no mechanical damages or macroscopic deformations appearing. Sakkas et al. (2015b) conducted another study which involved the passive fire protection test on GP samples which were made primarily using granulated slag which was rich in oxides and alumina. At 28–day testing, the samples were exposed to 250ºC for the first test and 370ºC for the second test. Results were observed to be promising, with no mechanical damages or macroscopic deformations appearing. However, the authors stated that this is merely a small-scale test and large-scale testing must be conducted to fully understand the fire performance of these specimens.

Abdulkareem et al. (2014) studied the thermal and mechanical behaviour of GP pastes, mortars and lightweight concretes. The study used class C FA with a sodium based alkaline solution for the preparation of 100mm (l×b×h) cubic sample which were dry oven cured at 70ºC for 24 hours in wrapped moulds (sealed). The compressive strengths were observed to decrease for all paste, mortar and concrete samples when the temperatures rose from 70ºC–800ºC. This was due to the thermal shrinkage which occurs as the water evaporates from the structure and

the high thermal and vapour stress which form within the specimen resulting in intensive thermal cracking. Furthermore, the rate of weight loss was found to decrease steeply before 150°C, after which the rate stabilized up to 780℃ and then stopped. Additionally, the author noted changes in colour as the temperature rose which was stated to be due to the oxidation changes of the iron oxides in the FA.

Another investigation involving sodium-based GP samples proved to have somewhat similar results. The behaviour of the samples under thermal loading were observed and good mechanical and thermal properties had been obtained. Two types of fire tests were conducted, the least intensive standard ISO 834 fire load curve and the RWS fire load curve. Both tests showed very good results in terms of thermal resistance, however, at a temperature of 1300°C, creeping had been observed (Sakkas et al., 2015a). Testing on wall panels made by a fly ash based GP concrete has been conducted by Sarker and McBeath (2011) where 500mm×500mm panels which were 125mm, 150mm and 175mm thick, reinforced with a steel mesh (single layer), were subjected to fire (on one side) to a temperature of 960°C for two hours. Strengths were then calculated, and failure loads ranged between 61%-71% of the original values, in comparison to 50%-53% of the original values of the control (OPC panels). The author states that, in comparison to conventional concrete, GP concretes possess higher post fire strength characteristics.

Another study investigated the use of a FA based GP concrete subjected to temperature levels up to 750°C. Quartz aggregate or expanded clay aggregate were used in the mix design and results showed that at temperatures ≤300°C, cracking and loss of strength had been observed. However, in comparison to conventional concrete, good strengths had been recorded at higher temperature readings (Rickarda et al., 2016).

2.4. Reactive Powder Concretes

As the construction industry advances, high strength concretes which can achieve strengths of over 100 MPa is in great demand. Being first developed in the early 90s, RPC is an ultra-high strength concrete which can reach compressive strengths in the range of 150 MPa-800 MPa, flexural strengths in the range of 30 MPa-60 MPa, fracture energy in the range of 1200 J/m^2 – 40,000 J/m^2 and ductility which is around 250 times higher than that of conventional OPC concretes (Richard and Cheyrezy, 1995, Team, 2007, Richard and Cheyrezy, 1994). Some other studies (Ng et al., 2010, Lee et al., 2007) stated that RPC has been recorded to achieve strengths greater than 200 MPa up to 800 MPa, flexural strengths up to 60 MPa, tensile strengths between 6 MPa-13 MPa and very similar ductility recordings. These high performance properties are achieved through enhancement techniques in the microstructural matrix of the concrete which can improve the particle size homogeneity, reduce permeability and porosity and increase the compaction through granular optimisation thus, providing a denser microstructure and a more durable concrete. Ting and Patnaikuni (1992) classified the strengths of concrete as given in Table 2.3.

Table 2.3 – Classification of high strength concretes at 56 days testing

Classification	Concrete code	Strength (MPa)
Normal High Strength Concrete	HSC	50 – 100
Very High Strength Concrete	VHSC	100 – 150
Ultra-High Strength Concrete	UHSC	150 – 200
Super High Strength Concrete	SHSC	>200

Menefy (2007) stated that the performance of RPC is greatly dependent on the proper selection of raw materials. Changes to the mix design such as reducing the w/c ratio, incorporating steel fibres in to the matrix, eliminating the coarse aggregate particles, adding materials that are rich in silica, thus reducing the calcium oxide content are key factors contributing to the achievement of ultra-high strength of RPC (Chan and Chu, 2004).

Though various types of cement had been used in the production of RPC, OPC is the main type of cement utilised mainly due to its availability and low cost. Richard and Cheyrezy (Richard and Cheyrezy, 1995) stated that when considering the w/c ratio of RPC, it should generally lower than that of conventional concrete. Excess water will generally result in increased porosity and hence, low strength and durability. Menefy (2007) stated that while conventional concrete consists of a w/c ratio between 0.35–0.7, RPC generally utilise a w/c ratio between 0.1–0.25.

Lee et al. (2007) studied the properties of using RPC are a repair material by comparing the results of the freezing and thawing test on two cement based repair materials, namely, normal strength concrete repair material and high strength mortar repair material, and one RPC based repair material. Results revealed that the compressive and flexural strengths were about 150% and 200% higher in the RPCs, with an abrasion coefficient of about 8 and 4 times more compared to normal strength and high strength repair materials, respectively. Additionally, 1000 freeze-thaw tests had proved RPC to be a more durable repair material compared to both normal concrete and high strength mortar repair materials.

In reality, despite RPCs having a higher production cost due to its comparatively higher consumption of cement (generally over 800–1000 kg/m^3) it has been found to be a more economical option due to the reductions in reinforcing steel and concrete thickness, hence reducing the overall material costs (Yazıcı et al., 2008). Furthermore, several studies are experimenting the use of alternative replacement materials (cementitious materials) in RPCs which could further reduce the cost.

Yazıcı et al. (2009) conducted testing on RPCs containing mineral admixtures such as FA and slag which resulted in positive results where all specimens achieved compressive strengths of over 200 MPa. A similar study was conducted by Yazıcı et al. (2008) where the effects of using FA and slag as alternative materials in RPC production was investigated. At optimum proportions the compressive strength reached a maximum of 281 MPa which further increased to 324 MPa after applying external pressure during the

hardening process. Additionally, the use of these mineral admixtures was found to reduce the demand for superplasticisers thus reducing shrinkage. Wang et al. (2012) also studied the properties of replacing cement and silica fumes with slag and limestone powder where compressive strengths of about 175 MPa were achieved.

There are several applications of RPC of which the first major construction project was the Sherbrooke Pedestrian Bridge in Canada which was constructed in 1996 and having a single span of 60 meters (Altcin et al., 1998). Over the years several RPC projects had taken shape in some leading countries such as Japan, Malaysia, France, Germany, Australia and New Zealand. The 113 feet long single span Mars Hill Bridge in Iowa, USA whose construction was completed in 2006 had been constructed purely with RPC without any shear reinforcement and won excellence awards and honours. Another such noticeable project in South Korea was the Seonyu Footbridge which was constructed in the year 2002. A key point was that the concrete usage for the project was calculated to be around half the concrete required if it had been built with conventional concrete (Behloul and Lee, 2003, Resplendino and Toulemonde, 2013, Song and Liu, 2016). One of the very first RPC bridge construction project for normal highways took place in NSW, Australia over Shepherds Creek in the year 2005. The bridge has a span length of 15 meters and width of 21 meters (Cavill and Chirgwin, 2004). Several other non-structural applications such as anchor plates, acoustic sound panels, facades, precast pipes, etc. have been developed using RPC technology.

2.4.1. Material Properties

The material selection in RPC is a vital task in obtaining high quality results. The proper selection of ingredients and proportions such as the use of high cementitious material contents, ultra-fine pozzolans, higher amounts of good quantity superplasticisers, low water-cement ratios, very fine aggregates and the steel micro fibres play a key role in RPC production. The basic constituents of RPC can be identified as cement, silica fumes, silica sand, silica flour, water

and superplasticisers. Figure 2.12 shows the basic materials and proportions on a typical RPC mixture.
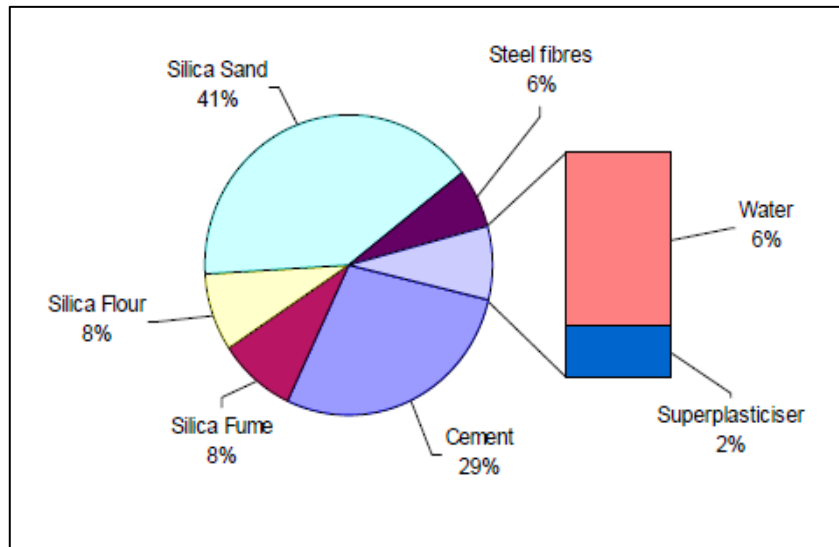
Figure 2.12 – Material proportion in a typical RPC mixture (Gowripalan et al., 2003)

Cement is considered the main binding material together with silica fumes. Cements such as sulphate resisting cement, low heat cement, high early strength cements have been utilised but the most commonly used type is general OPC due to its availability and low cost. Silica fumes are ultra-fine spherical shaped particles having an average diameter of about 0.15μm. Being a by-product produced during the manufacture process of zirconia, silicon and ferrosilicon alloys, silica fume is a popular pozzolanic material used specially in the development of high strength concretes. Additionally, its spherical shape contributes greatly into reducing the porosity in the concrete in two ways; firstly by filling up the voids in between the cement particles; and secondly by accelerating the rate of the hydration reaction, thus increasing the C-S-H bonds which also reduces the porosity (Menefy, 2007).

When considering the aggregate particles, conventional concretes incorporate course aggregate which has a particle size greater than 4.75mm. In RPC, however, the size of aggregate is reduced to less than 600μm. Particle homogeneity, increased density, early strength and lesser micro-cracking are the benefits achieved through the use of these fine sand/quartz particles (Richard and Cheyrezy, 1995, Menefy, 2007). Bonneau et al. (1996) used fine aggregate of 600μm and simple heat treatment methods to test the properties

of RPC. It was reported that the main negativity in RPC production is the high use of cement, recorded to vary between 800 kg/m³–1000 kg/m³, which increased the cost, imposed negative threats on the environment and had adverse effects on the heat of hydration, thus causing shrinkage cracks.

A well-known fact is that concrete behaves well under compression but poorly under tension. In RPC however, the tensile properties are enhanced through the incorporation of fibres which provide a more ductile medium. Steel fibres which display high tensile properties are generally used in RPC production. Dugat et al. (1996) studied the mechanical properties of RPCs and reported that the optimum fibre, which should be between 2–3% by volume, governs the fracture energy such as the toughness and the ductility.

The selection of a proper w/c ratio is crucial in RPC production as it governs a majority of the properties such as workability, strength, permeability, durability, etc. Conventional concretes would generally consist of a w/c ratio within the range of 0.35–0.7, whereas RPCs recommend lower ratios which are between 0.1–0.25. Upon selection of the w/c ratio, caution should be given to selecting one which provides just enough amounts for hydration. The workability conditions which are generally achieved through higher w/c ratios in conventional concretes are not considered in the same manner for RPCs. Generally, water reducers or superplasticisers would be used to enhance the workability and rheological characters of the mix without the utilising high levels of water.

The type of superplasticiser is also reported to play a major role in obtaining the proper mixture and also in the end results of RPC. (Coppola et al., 1997) tested the influence of naphthalene, melamine and acrylic polymer superplasticisers on the strength and w/c ratio of RPC. It was deduced that the incorporation of acrylic polymer superplasticiser required a low w/c ratio. Furthermore, the compressive strength of the acrylic polymer superplasticiser incorporated specimens were recorded to be comparatively higher compared to the other two at 3–day testing.

Originating from the works of Richard and Cheyrezy (1994), the properties of RPC is known to be enhanced mainly by the proper selection of ingredients

where large (coarse) aggregate particles were eliminated from the mix matrix. The size of aggregate was limited to between 0.4mm–0.6mm which provided a better reactive nature of the pozzolans and created a denser microstructure to produce strong durable concrete. However, a new version called modified RPC (MRPC) has been investigated which questions the original theory of material selection. Collepardi et al. (1997) studied the mechanical properties of original and modified RPC where the aggregate size was increased to a maximum of 8mm. At full replacement of the fine particles, no significant changes had been observed in compressive strength, however, reductions in flexural strength had been observed. Ting and Patnaikuni (1992) investigated the effects of aggregate size on the strength of concrete and suggested the addition of a strong course aggregate does not consequently reduced the strength. Strengths within the range of 150 MPa–185 MPa had been achieved by using basalt aggregate, sized 4mm–7mm. Rahman et al. (2005) stated that the use of a course aggregate which is stronger than the paste does not compromise the strength and can be advantageous by reducing the creep, shrinkage as well as the cost of production.

2.4.2. Curing and mixing regime

Apart from the selection of proper ingredients, the type of curing is considered to be a vital factor in the development of RPC. Enhanced mechanical properties can be achieved through the process of subjecting RPC to proper curing techniques. Numerous studies have been conducted to finalise a standard curing condition for RPC, however, no such standard has been developed. Researchers have investigated the effects of different curing regime and deduced various theories. Optimum curing techniques for RPC have been identified as thermal curing, which includes steam curing, hot water bath curing or hot air curing and autoclave curing, which is done by simultaneously applying pressure and heat on fresh RPC samples (Hiremath and Yaragal, 2017). Yunsheng et al. (2008a) studied the mechanical properties and the performance of RPC under different curing techniques where samples had been subjected to standard water curing, steam curing

and autoclave curing methods. Results displayed high performance in samples which were subjected to steam curing techniques. Compressive strengths of more than 200 MPa, flexural strengths of over 60 MPa and fracture energy of more than 30,000 J/m^2 were obtained.

A very recent study conducted by Hiremath and Yaragal (2017) tested the effects of four different curing regime, namely ambient air curing, hot air curing, hot water bath curing and accelerated curing. Samples had been prepared using cement, silica fumes, crushed quartz, silica sand and superplasticisers. Results had deduced that hot water bath curing for a period of 12-hours displayed strength results of 112 MPa and hot air curing at 200°C for 7-days had produced high results as well. However, a combined curing technique of 12-hours hot water bath curing followed by 7-day hot air curing had produced the highest strengths readings of up to 180 MPa. Under early strength development investigations, combined curing techniques had achieved higher strength readings within 36 hours compared to water curing strength readings achieved at 28 days.

Another study conducted by Yazıcı et al. (2009) tested the mechanical properties such as compressive strength, flexural strength and toughness of RPC made with class-C fly ash and slag at standard, autoclave and steam curing techniques. Results proved the compressive strength had increased considerably for steam and autoclave curing in comparison to standard curing, having a maximum strength of 255 MPa for steam curing done for 3 days at 100°C and 273 MPa for autoclave curing done with 2 MPa pressure for 8 hours at 210°C. Cwirzen et al. (2008) studied the basic mechanical properties of ultra-high strength and stated that the mixtures had a fluid-like nature and resulted in a 28-day compressive strength of between 170 MPa–202 MPa for specimens which were subjected to heat treatment methods. The authors reported that the microstructure of the RPC matrix densified after undergoing heat treatment methods. Non heat treatment methods resulted in strengths within the range of 130 MPa–150 MPa.

Early strength development has also been investigated where, the strength achieved at 28 days using standard water curing techniques can be achieved

within a shorter period using autoclaved curing techniques. Yang et al. (2009) stated that no significant developments in strength have been recorded after 7 days curing in high temperature conditions. Neville (1995) gives information that properties such increased porosity, decreased bond strength and higher levels of brittleness are factors which could occur through autoclave curing. However, the inclusion of silica fumes densifies the pore structure, thus reducing porosity and enhancing the mechanical properties even after autoclave curing techniques were used.

Massidda et al. (2001) stated that reactive powder mortar samples which were pre-cured for 3 days at ambient temperatures and subjected to high pressure steam curing techniques for 3 hours displayed compressive strengths of 200 MPa and flexural strengths of 30 MPa. The main reason for these high strength readings were stated to be a result of the modified microstructure which reduces the porosity. Zdeb (2017) analysed the effects of low pressure steam curing and autoclaving on the mechanical properties of RPC. It was concluded that both methods achieved 20% higher compressive strengths for steam curing and over 40% higher compressive strengths for autoclaving compared to normal water curing at 20°C. Additionally, the pre-set time, which the author recommends as 6 hours, had played an important role in steam curing but was insignificant for autoclaving processes.

Another study was conducted to understand the effects of autoclave pressure, temperature and duration of curing on the flexural and compressive strengths of RPC samples. Samples were initially kept in moulds for a period of 16 hours at about 20°C and high humidity levels after which some of the samples was cured in water at 20°C and the remaining samples were autoclaved at 1, 2 and 3 hours at 180, 210 and 235°C, respectively for time durations of 4, 6, 10, 12 and 24 hours. Results revealed that under autoclave curing conditions maximum flexural strengths were achieved which increased as the pressure level increased from 1 MPa to 2 MPa. Standard water curing had displayed a maximum compressive strength of 176 MPa and autoclave curing techniques produced maximum strength readings of over 260 MPa. Best results however, had been achieved using autoclaving with 2 MPa pressure at 210°C (Yazıcı et al., 2013). However, there are several limitations which have been identified

in using autoclave curing techniques. Studies have proven that autoclaving causes large expansions of the micro-cracks around the aggregate particles and releasing the applied pressure can in fact improve micro-cracking. Furthermore, when autoclave curing is conducted, the absence of silica fumes restricts the rapid formation of hydrated products which in turn can produce a more porous and hence a poorer concrete. A key disadvantage is the reduction in bond strength between concrete and reinforcement by around 50% causing the material to be more brittle in nature (Hiremath and Yaragal, 2017, İpek et al., 2012).

In the development of high quality RPCs, mixing techniques have been reported to play a vital role. Several studies report similar mixing procedures where the dry materials are first machine mixed for a period of 3-5 minutes at low speeds, after which the liquids are added, and machine mixed for about 5-10 minutes. Finally, steel fibres are incorporated and machine mixed for a period of 2-5 minutes (Yazıcı et al., 2009, Hiremath and Yaragal, 2017, Zdeb, 2017, Yazıcı et al., 2013, Helmi et al., 2016, Mostofinejad et al., 2016). However, the mixing times have been seen to vary from one study to another. Menefy (2007) stated that standard mixing procedures are not entirely sufficient and that the type and speed of the mixing equipment governs the quality of the RPC. Furthermore, he refers a typical staged mixing approach for RPCs that has been reported by Bonneau et al. (1997a) for his research work (Figure 2.13). Ma et al. (2004) reported that by using high energy machine mixers shorter mixing times can be achieved. Figure 2.14 illustrates the power consumption during the mixing process (Ma et al., 2004).
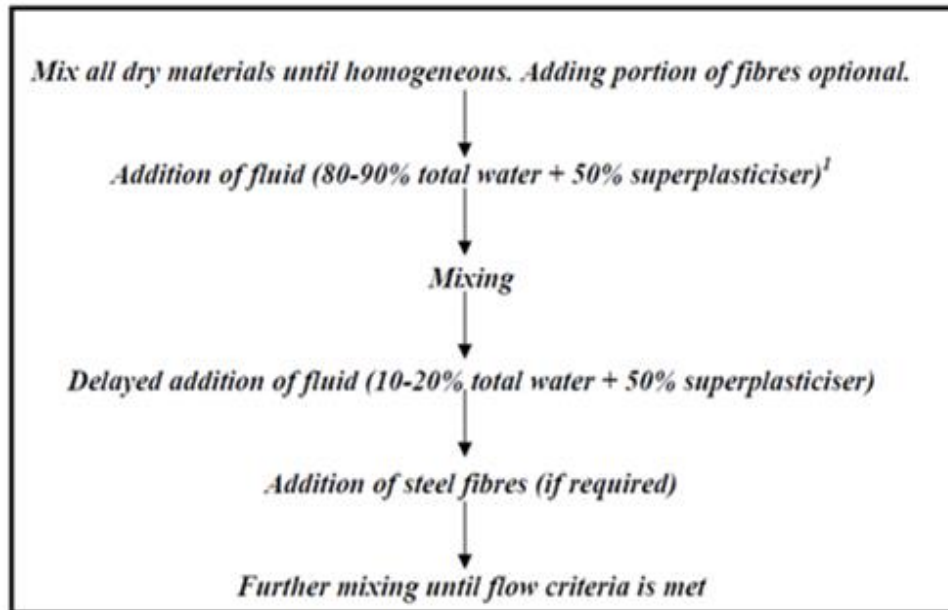
Figure 2.13 – Controlled mixing procedures as reported by Bonneau et al. (1997a).
(Menefy, 2007)
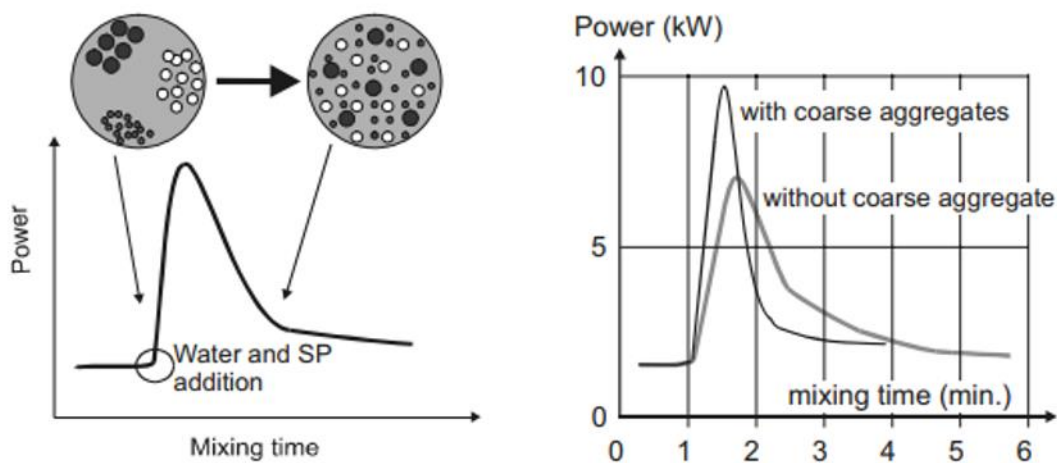
Figure 2.14 – Power consumption during mixing process (Ma et al., 2004)

2.4.3. RPC in Fire

In comparison to other structural building materials such as steel and timber, concretes behaves well under elevated temperature levels. However, concrete undergoes degradation and loss of mechanical properties during exposure. Compared to normal strength concretes, high strength concretes are more vulnerable to explosive spalling at high temperatures due to

limitations in openings/air voids, thus restricting the internal vapour from escaping causing vapour stresses from building up inside which results in explosive spalling.

Peng et al. (2012) studied the resistance of RPCs at temperatures up to 600°C in terms of compressive strength, tensile strength and fracture energy. Spalling was seen to occur considerably under elevated temperatures where samples having lower w/c ratios suffered higher spalling conditions. The compressive strength was observed to decrease significantly after 400°C exposure. Temperature range of 400°C-600°C was regarded as the critical temperature range for spalling. However, the resistance to high temperatures was seen to increase through the use of polypropylene and steel fibres (hybrid fibres).

Liu and Huang (2009) tested the fire performance of RPC and found that RPCs exhibit higher fire endurance compared to both normal strength concretes and high-performance concretes. During the fire tests, high performance concrete and normal strength concrete specimens were observed to spall at temperatures of 600°C and 690°C, respectively, whilst, RPC specimens had not experienced spalling until around 790°C. It must be noted here that no fibres had been incorporated into the RPC mix.

Zheng et al. (2013) tested similar properties with the incorporation of steel fibres. Cube strengths had seen to decrease up to 100°C, increased during 200°C-500°C and then decreased above temperatures of 600°C. Explosive spalling conditions had occurred during a range of 260°C-520°C, but with a 2% steel fibre incorporation this was seen to reduce below 300°C, where the compressive strength increased with steel fibres. Similar investigations of incorporating various fibres into RPC and testing the compressive strength relationships at elevated temperatures from 20°C-900°C had been conducted. Both investigations obtained similar results where initial increments followed by significant decrements in both the compressive strength and Young's modulus had been recorded with increasing temperatures (Zheng et al., 2012a, Zheng et al., 2012b).

2.5. Current studies on a combination of GP and RPC

Though several such studies are available in reporting the properties of RPC where mineral admixtures are used in replacement to cement, studies using alkaline activators and more importantly, studies related to the fire performance of alkaline activate RPC, is limited.

Yazıcı et al. (2008) studied the effects of replacing cement and silica fumes in RPC using slag and FA. The study resulted in a compressive strength of 281MPa from the RPC specimens which used mineral admixtures in replacement of cement and silica fumes. Another similar study conducted by Yazıcı et al. (2009) used FA and slag in replacement to cement and reported satisfactory mechanical properties with reductions in heat of hydration and shrinkage. Long et al. (2002) studied the mechanical properties of RPC using FA, slag and silica fumes in collaboration with cement, quartz sand, superplasticisers, and steel fibres which resulted in increased toughness and compressive strength.

As mentioned in Section 1.1, Ng et al. (2012) concluded that a combination of RPC and GP concrete will highly contribute to sustainable development. Jianfang and Wei (2003) conducted a GP based RPC where three curing systems had been studied, i.e. dry oven curing, steam curing and pressure-steam curing. Compressive strengths of up to 55.2 MPa and bending strengths of up to 22.4 MPa had been achieved with excellent durability properties. Another such study utilized slag and FA with sodium activators to produce high strength concretes. The study deduced that elevated temperature curing can indeed increase the compressive strength of GP based RPC. Additionally, by adding steel fibres, the material toughness can be enhanced (Chen et al., 2012). However, both studies investigated the initial mechanical properties of this GP based RPC and the fire performance of the material had not been evaluated.

2.6. Summary of Chapter Two

The literature review can be summarised as follows:

1. Studies generally show that about 74%–81% of the total CO_2 emission in concrete was due to the cement component. Furthermore, it was observed that the CO_2 fraction emitted by cement industries can be mitigated mainly by decreasing the cement proportion in concrete mixtures.

2. Normal strength concretes behave well in the case of a fire; however, high strength concretes undergo spalling conditions when exposed to elevated temperature levels.

3. FA could be used in complete replacement to cement for the production of GPs and sodium based alkaline solutions are more commonly used compared to potassium based alkaline solutions.

4. GPs are able to achieve high early strength (within 24 hours after casting) by curing at high temperature levels of >60°C.

5. Whilst all conventional concretes result in strength losses after exposure to fire, GPs experience strength gains as well as strength losses which is associated with the ductility of the material and further geopolymerisation.

6. RPC display high initial strengths which can be obtained by optimizing the mix design. However, RPCs have been reported to behave poorly under elevated temperature levels, undergoing explosive spalling conditions.

7. Partial replacement of cement in RPC using mineral admixtures such as FA or slag can produce ultra-high strengths and enhance the fire

performance of the material. However, the use of cement imposes negative effects on the environment.

8. Limited studies are available on the mechanical properties and more importantly, the fire performance of GP based RPC which use alkaline activators.

The literature presented in this chapter shows evidence that GPs can behave exceptionally well at elevated temperature levels. However, they cannot obtain high initial strength and are classified as normal strength concretes. In contrast to this, RPCs can obtain ultra-high initial strengths, but they behave very poorly in a fire. Specific studies on a combination of the two materials, thus producing a high initial strength concrete which can behave exceptionally well in elevated temperature, are limited. More detailed studies, based especially on the fire performance is required to fully understand the overall performance of this combined material that directly contributes to the sustainability attribute within the construction sector.

CHAPTER 03

MATERIALS AND EXPERIMENTAL PROCEDURES

3.1. Chapter overview

This chapter presents detailed descriptions of the materials and the experimental procedures which were undertaken in the project to find optimum conditions for the development of RPGCs. Raw material properties, specifications and mix design information of both GPs and RPCs are presented. Under experimental procedures test programs and parameters of density, workability, strength and mass loss are presented for GPs, RPCs and RPGCs. When considering GP and RPC, samples were prepared in reference to existing mix designs. Due to extremely limited literature found on the production of RPGC materials, trial and error processes were used in the production process.

3.2. Material Properties

3.2.1. Cementitious material properties

Type 1 Bastion General Purpose cement supplied by *DINGO Cement Pty Ltd* complying with AS 3972–2010-General purpose and blended cements (Standard, 2010) were used. Silica fume was supplied from *Master Builders Solutions by BASF Australia.* It is a mineral admixture comprising of very fine, spherical particles grey in colour and meets the requirements of AS/NZS 3582.3:2016–Supplementary cementitious materials. Part 3–Amorphous silica (Standard, 2016a). The X-Ray Fluorescence (XRF) analyser was used to determine the chemical compositions of silica fumes (Table 3.1).

Table 3.1 – Chemical composition of Silica Fumes

Silica Fumes	
Chemical	Component (Wt %)
Al_2O_3	0.7
SiO_2	95.5
CaO	0.4
Fe_2O_3	0.3
K_2O	1.0
MgO	0.5
Na_2O	0.4
Loss of Ignition	2.0

Namely two types of FA were used in this study, Gladstone FA and Gladstone/Callide FA supplied from *Cement Australia* which fully complies with the requirements of AS/NZS 3582.3:2002– Supplementary cementitious materials. Part 1–Fly Ash (Standard, 2016b). Both FAs were classified under class F (low calcium FA) having rather similar silicon dioxide and aluminium oxide contents and CaO content of 4.30% for Gladstone and 2.70% Gladstone/Callide. Gladstone FA was a darker grey in colour compared to Gladstone/Callide FA. The fineness percentage passing the 45µm sieve was recorded to be 86.13% for Gladstone FA and 80.48% for Gladstone/Callide FA. The fineness percentage requirements for special grade, grade 1 and grade 2 FA is given in Table 3.2 (Standard, 2016b). The particle size distribution curve is given in Figure 3.1.

In accordance with the standard, both Gladstone and Gladstone/Callide FA used in this study is classified as special graded FA which is highly reactive FA that may be prepared by various processes including milling and centrifugal separation (Standard, 2016b). The chemical compositions of FA, determined using the X-Ray Fluorescence (XRF) analyser is given in Table 3.3.

Table 3.2 – Classification of Fly Ash as per the fineness percentage

Grade	Fineness % passing 45µm sieve (minimum)
Special grade limit	75
Grade 1 limit	65
Grade 2 limit	55
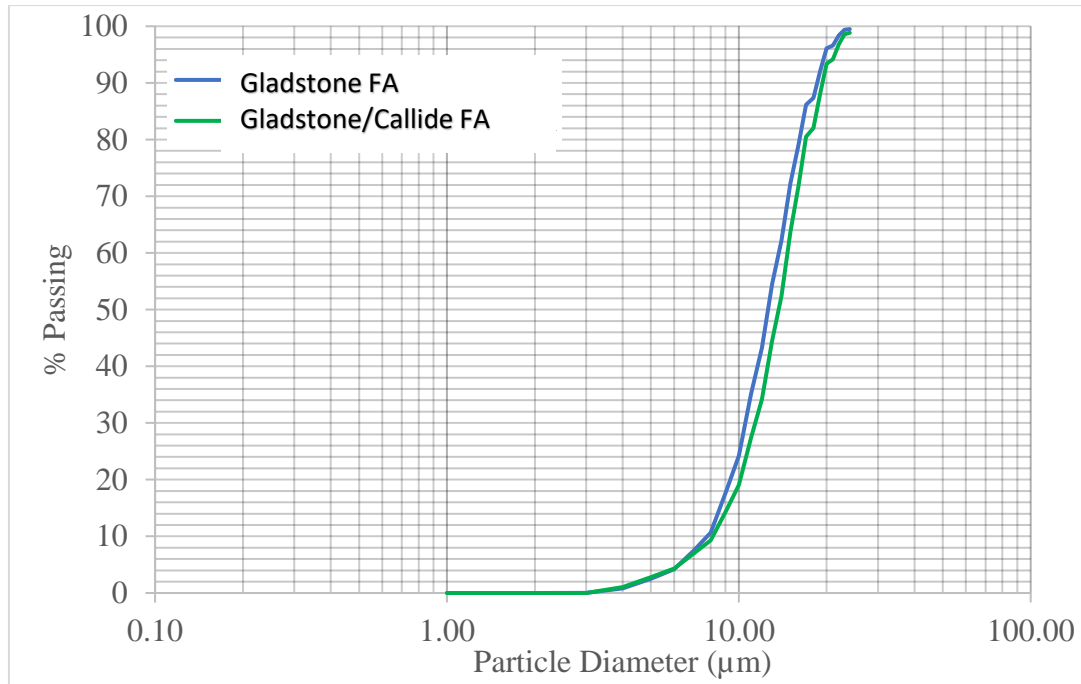
Figure 3.1–Particle size distribution curve of FA

Table 3.3 – Chemical composition of FA

Chemical	Gladstone Component (Wt %)	Gladstone/Callide Component (Wt %)
Al_2O_3	25.56	28.83
SiO_2	51.11	52.76
CaO	4.30	2.70
Fe_2O_3	12.48	9.99
K_2O	0.70	0.45
MgO	1.45	1.13
Na_2O	0.77	0.44
P_2O_5	0.89	0.49
TiO_2	1.32	1.71
BaO	0.09	0.08
MnO	0.15	0.08
SO_3	0.24	0.17
Loss of Ignition	0.95	1.18
Total	**100**	**100**

As is evident from Table 3.3, the two main differences between Gladstone and Gladstone/Callide FA are as follows: Gladstone/Callide FA has a higher Al_2O_3 and SiO_2 compared to Gladstone FA; Gladstone FA has a higher calcium and iron content compared to Gladstone/Callide FA. Figure 3.2 gives a top view of all cementitious materials used in the study.

Figure 3.2 – Top view of cementitious materials used in the study

3.2.2. Aggregate

Processed silica sand and silica flour were used as the aggregate in the study. 50N silica sand had a maximum particle size of 600μm and was supplied from *North Stradbroke Island, Australia*. Silica flour which was white in colour and was supplied from *Unimin Australia Ltd.* Figure 3.3 gives a top view of the silica sand and flour.

Figure 3.3 – Top view of aggregates used in the study

3.2.3. Liquid components

A silicate based alkaline activator was used in the study where a combination of Grade D sodium silicate (Na_2SiO_3) and 8M sodium hydroxide (NaOH) solution were used. Sodium silicate, also known as waterglass or liquid glass, was clear and colourless having a density of $1.53 g/cm^2$ and a pH of 12.7. Table 3.4 shows the chemical compositions of sodium silicate. Sodium Hydroxide solution was prepared by dissolving sodium hydroxide grains in deionised water approximately 24 hours prior to sample preparation. In reference to Rajamane and Jeyalakshmi (2014), 225 grams of NaOH grains were hand mixed with 745 grams of water to produce 1litre of 8M NaOH solution (Table 3.5). Dissolution of the NaOH grains continued until a clear solution was observed.

Table 3.4 Chemical compositions of Grade D sodium silicate.

Sodium Silicate Grade D	
% SiO_2 per kg	29.40
% Na_2O per kg	14.70
% H_2O per kg	55.90
pH	12.7
Wt. Ratio (SiO_2/Na_2O)	2
Density (g/cm^2)	1.53

Table 3.5 – Quantities of Sodium Hydroxide solids and water to produce Sodium Hydroxide Solution of given Molarity (Rajamane and Jeyalakshmi, 2014)

Molarity M mole/l Col (1)	For preparation of 1 kg of SHS			Concentration of SHS	
	SH Solids	Water	SHS		
	grams	grams	grams	ws, mass/mass	%
	Col (2)	Col (3)	Col (4)	Col (4)	Col (5)
1.00	39	961	1000	0.39	3.9
2.00	74	926	1000	0.74	7.4
3.00	108	892	1000	1.08	10.8
4.00	140	860	1000	1.40	14.0
5.00	171	829	1000	1.71	17.1
6.00	200	800	1000	2.00	20.0
7.00	228	772	1000	2.28	22.8
8.00	255	745	1000	2.55	25.5
9.00	281	719	1000	2.81	28.1
10.00	306	694	1000	3.06	30.6
11.00	331	669	1000	3.31	33.1
12.00	354	646	1000	3.54	35.4
13.00	377	623	1000	3.77	37.7
14.00	400	600	1000	4.00	40.0
15.00	422	578	1000	4.22	42.2
16.00	443	557	1000	4.43	44.3
17.00	464	536	1000	4.64	46.4
18.00	485	515	1000	4.85	48.5
19.00	505	495	1000	5.05	50.5

When considering the superplasticisers used for the preparation of RPC specimens, Sika ViscoCrete high range water reducer was used during the initial testing stages of testing, however due to higher water requirements Glenium 51 high range water reducer was utilized in latter stages of testing. This was done based on the work conducted by Menefy (2007).

3.3. Mix Designs

3.3.1. GP paste

Ten different combinations of FA and alkaline solution were used and named as GP01, GP02, GP03, etc. The first 05 mixes (GP01–GP05) had an alkaline solution to FA ratio of 0.4 whereas GP06-10 had a ratio 0.57 which implies that the first half of the set is less workable compared to the latter half. Additionally, five sodium silicate to sodium hydroxide ratios were tested, namely, 0.5, 1.0, 1.75, 2.0, 2.5. Mix design combinations are given in Table 3.6.

Table 3.6 – Mix Designs for GP pastes

ID	Name	FA (kg)	Alkaline Solution / FA Ratio	Alkaline Solution (kg)	Na_2SiO_3/ NaOH	8M NaOH (kg)	Sodium Silicate Grade D (kg)	Total Weight (kg)
GP 01	GP 0.4/0.5	1.00	0.400	0.400	0.500	0.267	0.133	1.400
GP 02	GP 0.4/1.0	1.00	0.400	0.400	1.000	0.200	0.200	1.400
GP 03	GP 0.4/1.75	1.00	0.400	0.400	1.750	0.145	0.255	1.400
GP 04	GP 0.4/2.0	1.00	0.400	0.400	2.000	0.133	0.267	1.400
GP 05	GP 0.4/2.5	1.00	0.400	0.400	2.500	0.114	0.286	1.400
GP 06	GP 0.57/0.5	1.00	0.570	0.570	0.500	0.380	0.190	1.570
GP 07	GP 0.57/1.0	1.00	0.570	0.570	1.000	0.285	0.285	1.570
GP 08	GP 0.57/1.75	1.00	0.570	0.570	1.750	0.207	0.363	1.570
GP 09	GP 0.57/2.0	1.00	0.570	0.570	2.000	0.190	0.380	1.570
GP 10	GP 0.57/2.5	1.00	0.570	0.570	2.500	0.163	0.407	1.570

3.3.2. RPC

In reference to the work of Gowripalan et al. (2003), Richard and Cheyrezy (1994) and Yazıcı et al. (2009), three RPC combinations were used in the study. Referenced mix combination are presented in Table 3.7. Initial mixing resulted in poor workable conditions, therefore, mix design combinations were refined and are presented in Table 3.8. The occurrence of poor workable mixtures were due to the aggregate particles being bone dry hence affecting the w/c ratio. Excess water was added to the aggregate particles to achieve saturated surface dry (SSD) conditions. SSD condition is where the particles are dry on the external surface, but saturated completely on the inside (internal voids filled with water). This prevents further absorption from occurring into the aggregate and hence not affect the free water content of the design.

Table 3.7 – Mix combinations of RPC in reference to past studies.

ID	Reference	Cement kg/m^3	Silica Fume kg/m^3	Silica Flour 200G kg/m^3	Silica Sand 50N kg/m^3	Super plasticiser L/m^3	Water kg/m^3	W/C
RPC 01	Gowripalan et al. (2003)	680.0	204.0	204.0	974.0	44.0	150.0	0.22
RPC 02	Richard and Cheyrezy (1994)	955.0	229.0	10.0	1051.0	13.0	153.0	0.16
RPC 03	Yazıcı et al. (2009)	830.0	291.0	488.0	489.0	55.0	151.0	0.18

Table 3.8 – Refined combinations of RPC and quantities required for Cubic meter

ID	Amount Needed m³	Total Weight Initial kg	Cement kg	Silica Fumes kg	Silica Flour kg	Silica Sand kg	SP ml	Water kg	Initial W/C
RPC 01-a	1.0	2212.0	680.0	204.0	204.0	974.0	44000.0	150.0	0.22
RPC 01-b	1.0	2212.0	680.0	204.0	204.0	974.0	44000.0	150.0	0.22
RPC 02	1.0	2398.0	955.0	229.0	10.0	1051.0	13000.0	153.0	0.16
RPC 03	1.0	2249.0	830.0	291.0	488.0	489.0	55000.0	151.0	0.18

ID	% Absorption by Total Sand	Added Water (kg) for Absorption	Added SP ml	Added Water kg	Final W/C	% Super of Cement + Fume	Final Weight kg
RPC 01-a	1.0	11.7	0	0	0.22	4.9	2223.7
RPC 01-b	1.0	11.7	2.0	0	0.22	4.9	2223.7
RPC 02	1.0	10.6	16.0	0	0.16	1.0	2408.6
RPC 03	1.0	9.7	0	0	0.18	4.9	2258.7

3.3.3. RPGC

RPGC mix design combinations were developed after conducting the initial testing and analysis stages on GP and RPC mixes. Combinations which displayed high performance in terms of strength, thermal cracking and mass loss were used for the development of the RPGC mix combinations. Gladstone FA was used in complete replacement to cement and due to the highly workable nature of the GP mixtures, both water and SP were omitted from the mix design. However, due to the requirement of the SSD conditions, extra water was added for absorption. As RPGC is a newly developed material trial and error testing method was conducted. Mix combinations are presented in Table 3.9.

Table 3.9 – Mix Design – RPGC Trial and Error

Mix Components	RPC01 + Gladstone GP-0.4/2.5	RPC02 + Gladstone GP-0.4/2.5	RPC01 + Gladstone GP-0.57/1.75	RPC02 + Gladstone GP-0.57/1.75	RPC01 + Gladstone GP-0.57/2.5	RPC02 + Gladstone GP-0.57/2.5
ID	RPGC 01	RPGC 02	RPGC 03	RPGC 04	RPGC 05	RPGC 06
Volume Needed (mm^3)	1.00	1.00	1.00	1.00	1.00	1.00
GP Cement (kg/m^3)	-	-	-	-	-	-
Silica Fume (kg/m^3)	204.0	229.0	204.0	229.0	204.0	229.0
Silica Flour 200G (kg/m^3)	204.0	10.0	204.0	10.0	204.0	10.0
Silica Sand 50N (kg/m^3)	974.0	1051.0	974.0	1051.0	974.0	1051.0
SP (L/m^3)	-	-	-	-	-	-
Water (kg/m^3)	-	-	-	-	-	-
Fly Ash (kg)	680.0	955.0	680.0	955.0	680.0	955.0
Alkaline Solution / Fly Ash Ratio	0.4	0.4	0.57	0.57	0.57	0.57
Alkaline Solution (kg)	272.0	382.0	387.6	544.3	387.6	544.3
Na$_2$SiO$_3$/NaOH	2.5	2.5	1.75	1.75	2.5	2.5
8M NaOH (kg)	77.7	109.1	140.9	197.9	110.7	155.5
Sodium Silicate Grade D (kg)	194.2	272.8	246.6	346.4	276.8	388.8
Total Wt (kg)	2334.0	2627.0	2449.6	2789.3	2449.6	2789.3
Aggregate/ binder ratio	2.03	1.35	2.03	1.35	2.03	1.35
Added Water due to absorption (kg)	11.7	10.6	11.7	10.6	11.7	10.6
Added Water due to workability (kg)	0.00	0.00	0.00	0.00	0.00	0.00

3.4. Specimen Preparation

Hardened cube specimens of 25×25×25 mm were used during the initial stages of testing and 50×50×50 mm cube specimens were used to understand the effects of specimen size of the performance of GPs.

During the preparation of alkaline solution, the two activators were hand mixed together for a period of 1 minute until a clear, transparent solution was obtained. This was allowed to rest for a further 3 minutes before machine mixed with FA. All mixing was carried out in a *Breville* mixer shown in Figure 3.4. The FA and alkaline solution was measured, and machine mixed first for 2 minutes at a working speed of 50 revolutions per minute (rpm) then for another 3 minutes at a working speed of 85 rpm. Fresh materials were used for density and workability measurements. Cubes of required dimensions were casted and cured accordingly.
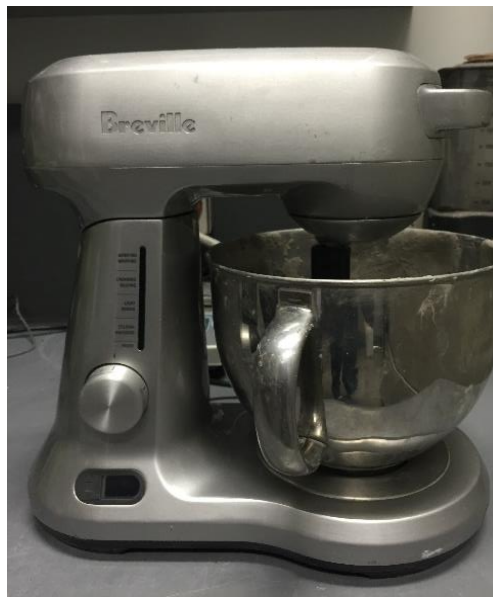
Figure 3.4 – Mixer used in the study

The mixing of RPC followed closely the procedures recommended by Menefy (2007), who, as previously mentioned in chapter two, followed a controlled method of mixing conducted by Bonneau et al. (1997b). Dry materials (cement, silica fumes, silica sand and silica flour) were initially measured and

machine mixed for 2 minutes at a working speed of 50 rpm until the dry materials reach homogeneity. The absorption water content required to reach SSD conditions for the aggregate particles was pre-calculated where 500g of silica sand and 500g of silica flour were separately oven dried at 105°C for 24 hours. Afterwards the two materials were separately machine mixed with different percentages of water ranging from 0.1% to 2.0% at 50 rpm. Each mix was compacted into a cone shape mould, tamped 25 times in circular motion for 3 layers after which the cone was removed vertically. The percentage of water required to allow the mixture to hold its shape, preventing it from collapsing is considered to be the percentage absorption of aggregate. This percentage was found to be 1% (Figure 3.5).

Figure 3.5 – Determination of absorption water required to achieve SSD condition of silica sand

After mixing the dry ingredients together, initial superplasticiser, initial water and absorption water contents, were measured, pre-mixed and added into dry mix. The RPC mix was machine mixed for a total of 30 minutes at 85 rpm until a workable mixture was obtained. Delayed addition of superplasticiser was conducted in RPC 01-a and RPC 02 mixtures to obtain a superplasticiser to cementitious material percentage of around 5%. The energy required to liquefy the mixture was obtained through extended mixing times.

Graybeal and Hartmann (2003) defined a term called 'breakpoint' during the mixing procedure as the point at which the dry nature of the mixture transits into a viscous, liquid, workable state. This is identified as the point at which

the superplasticiser and the water have adequately dispersed and reacted with the dry materials. This breakpoint could clearly be identified during the mixing procedures.

Similar mixing procedures were followed for the RPGC, where the dry materials were machine mixed until homogeneity was reached for a period of 2 minutes at 50 rpm after which the alkaline solution (sodium hydroxide and sodium silicate which were premixed for 1 minute) was added and machine mixed for a further 2 minutes at 50 rpm and then for 3 minutes at 85 rpm.

The mixtures were casted in Teflon coated steel cube moulds (Figure 3.6) and slightly tapped on the sides to remove any air bubbles or voids. To increase the accuracy of each result, 3 specimens were tested on for each data point in all experiments.
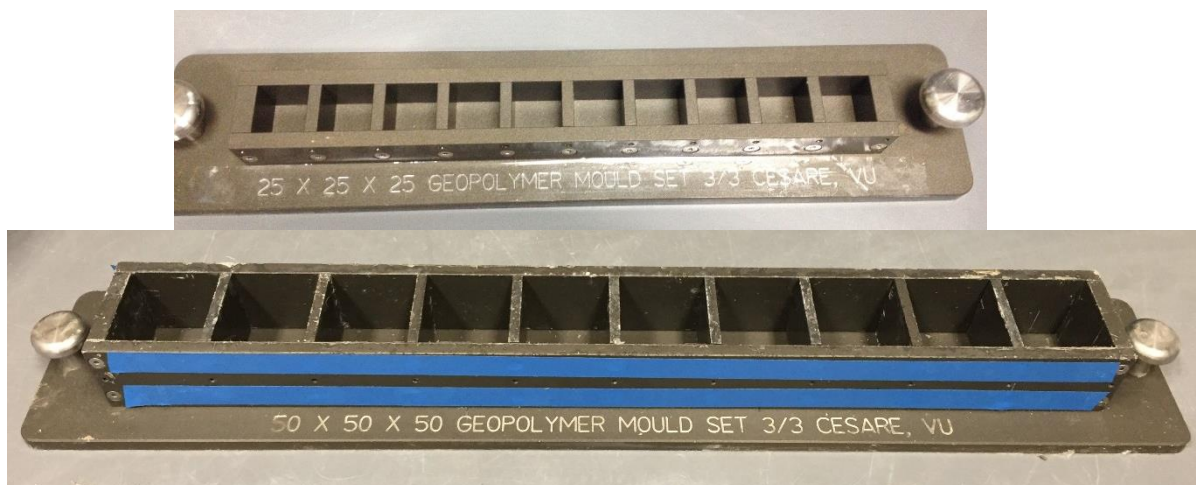
Figure 3.6 – Teflon coated steel cube moulds

3.5.   Curing regime

Curing was conducted in two methods for the Gladstone GP mixes, namely non-sealed and sealed dry oven curing at 60°C (Figure 3.7). This was conducted to investigate the effects of initial surface evaporation on the behaviour of hardened specimens.
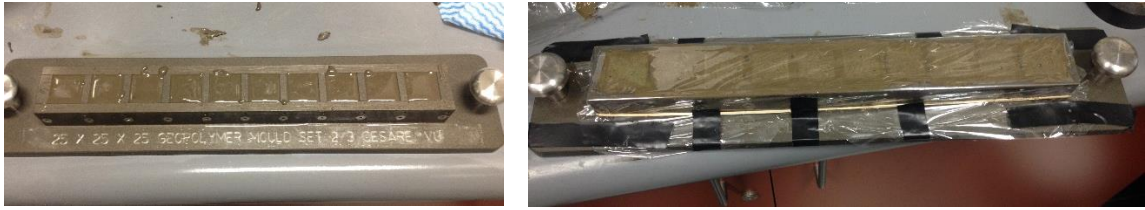
Figure 3.7 – Casted specimens in liquid state.

(Left) Non-sealed specimens. (Right) Sealed specimens

Samples which were subjected to sealed curing conditions were placed in oven bags immediately after casting and exposed to dry oven curing at 60°C for 24 hours in the *WEISS WVC Series* Temperature and Climatic Test Chamber (Figure 3.8a).

Sealed curing testing was only conducted on the 25mm Gladstone GP specimens which produced better results compared to the non-sealed specimens and therefore both Gladstone/Callide GP and RPGC samples were only subjected to sealed oven dry curing at 60°C for 24 hours.

When considering the curing regime used for the RPC samples, initially, RPC 01 was subjected to water curing in the *Thermoline Scientific* Water Bath (Figure 3.8b) under two different temperatures, at 20°C and at 75°C. This was conducted to test the effects of ambient temperature water curing on the compressive strength at 7 days. These samples were labelled RPC 01-a.

Figure 3.8a (left)–WEISS WVC Series Temperature and Climatic Test Chamber.
Figure 3.8b (right)–Thermoline Scientific Water Bath.

Gilbert (2000) tested the effects on the compressive strength of RPC without heat treatments and deduced that samples suffer shrinkage when not exposed to heat treatment methods which was similar to the findings of Roy and Gouda (1973) who found that high temperature curing greatly enhances the strength of RPC. RPC 01-b and RPC 02 samples were prepared as per the same procedure, but no curing variations were conducted. This means that samples RPC 01-b and RPC 02 were only subjected to ambient temperature water curing at 75°C. The RPC 03 mixture did not reach breakpoint, in other words, it did not transit to a workable state during the mixing procedure and hence, it was considered a failed attempt. An overview of the experiments in regard to different curing conditions and specification on specimen dimension are presented in Table 3.10.

Table 3.10 – Experiment Overview

State	Condition	Mixes	Test	Specimen dimensions
Liquid	–	All Gladstone and Gladstone/Callide GP mixes, RPC mixes and RPGC mixes	Density Workability	–
Solid	Dry Oven Curing (Non-Sealed)	All Gladstone GP mixes	Compressive Strength	25×25×25 mm
Solid	Dry Oven Curing (Sealed)	All Gladstone and Gladstone/Callide GP mixes	Compressive Strength	25×25×25 mm 50×50×50 mm
Solid	Dry Oven Curing (Sealed)	RPGC mixes	Compressive Strength	25×25×25 mm
Solid	Water curing at 25°C and 75°C	RPC mixes	Compressive Strength	25×25×25 mm
Solid	Residual	All Gladstone and Gladstone/Callide GP mixes	Compressive Strength Mass Loss	25×25×25 mm 50×50×50 mm
Solid	Residual	RPGC mixes	Compressive Strength Mass Loss	25×25×25 mm

3.6. Test methods and specifications

During the liquid stages, the density and workability values of all mixes were recorded in accordance with AS 1012.5:2014 – Determination of mass per unit volume of freshly mixed concrete (Standard, 2014b) and ASTM C230/230M-08 – Standard Specification for Flow Table for Use in Tests of Hydraulic Cement (ASTM, 2008), respectively.

For the density determination test, the empty container was first weighed and labelled as m_1. Immediately after the completion of the mixing process the sample was compacted into the container. Sample compaction of all GP pastes for the determination of density was conducted in accordance with Clause 7.3 of the standard AS 1012.5, due to its highly workable nature.

Similarly, sample preparation of RPC and RPGC mixes for the determination of density was conducted using the vibration method (Clause 7.2 of AS 1012.5). The fully compacted container plus sample was then reweighed and labelled as m_2 and the mass of sample was determined. The density was then calculated using Equation 1.

$$\rho=(m2-m1)/V \qquad \boxed{1}$$

Where, m_1 = mass of empty container

m_2 = mass of fully compacted material plus empty container

V = Volume of container

Workability was conducted using the flow table apparatus shown in Figure 3.9. First, the mould and flow table were wiped cleaned using a damp cloth. Material was then filled in 3 layers and tamped 25 times each in circular motion. After levelling the top and wiping any excess material from around the mould, the mould was lifted vertically. Immediately after lifting, the table was dropped 25 times within 15 seconds and two diameter readings perpendicular to each other were recorded (d_1, d_2). The slump flow (SF) values were then calculated using Equation 2 (Topccedil and Uygunoğlu, 2010).

$$SF=(d1+d2)/2 \qquad \boxed{2}$$

Where   SF = Slump flow

d_1 and d_2 = diameter readings perpendicular to each other.

Figure 3.9 – Flow Table Apparatus

Cubes were used for the determination of the strength in accordance with AS 1012.9.2014 - Methods of testing concrete Method 9: Compressive strength tests–Concrete, mortar and grout specimens (Standard, 2014a). 100kN *Instron* 1195 and 2000kN *Mori* testing machines at a loading rate of 20 ± 2 MPa/min were used to test the compression strength. Compression machine capacities are given in Table 3.11. All GP and RPGC specimens were tested for initial compressive strength 24 hours after casting and RPC specimens were tested 7days after casting. No samples were subjected to a rest period, which means that all samples were immediately cured after casting. The average of three test specimens was used for accuracy purposes. The strength was calculated using Equation 3 in accordance with the test standard.

$$\sigma = F/A \qquad \text{③}$$

Where, σ = compressive strength (MPa)

F = applied force (N)

A = cross sectional area (mm^2)

Table 3.11 – Compression Machine Capacities.

100kN Instron Limits			2000kN Mori Limits		
	25 mm Cube	50 mm Cube		25 mm Cube	50 mm Cube
Area (mm^2)	625	2500	Area (mm^2)	625	2500
Load (T)	10	10	Load (T)	20	20
Load (kg)	10000	10000	Load (kg)	200000	200000
Force (kN)	100	100	Force (kN)	2000	2000
Stress (MPa)	160	40	Stress (MPa)	3200	800

Residual strength is an important parameter to analyse when assessing structures which have been exposed to fire. Residual strength profiles can help understand the bearing capacity and also required repair work after exposure to elevated temperatures. When considering elevated temperature testing, 3 main steady-state test methods have been discussed by Phan and Peacock (1999) (Figure 3.10).
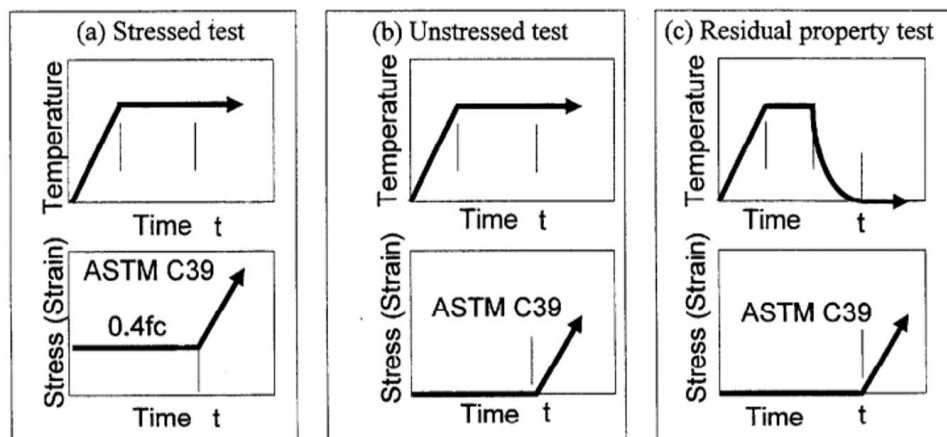
Figure 3.10 – Schematic temperature and load histories for steady state elevated temperature tests (Phan and Peacock, 1999)

In the Stressed test method, specimens are preloaded during room temperature and this load is sustained while heating occurs. Once the specimens are heated to the target temperature and upon reaching a steady state condition the specimens are loaded until failure. In the unstressed test method, specimens are not subjected to any such preloading. The specimens are heated to a target temperature and upon reaching a steady sate, they are loaded until failure. In the third method, the residual property test, the

specimens are heated to a target temperature at a steady rate and then allowed to cool down until room temperature after which they are loaded until failure. In this study, the residual property test was conducted on the GP and RPCG specimens 24 hours after casting and the RPC specimens 7 days after casting, as it is the most commonly used method.

Immediately after the curing processes, the specimens were subjected to elevated temperatures of either 400°C or 800°C increasing at a steady rate of 10°C/min using the muffle furnace which has a capacity of up to 1100°C. The specimens were exposed to these temperatures for a period of 60 minutes and then allowed to cool down to room temperature and then tested on. This method was maintained for all elevated temperature testing conducted throughout the study. Figure 3.11 shows specimens placed inside the furnace before exposure.

Figure 3.11 – Specimens placed inside the muffle furnace before exposure.

Mass loss was also investigated using two methods. In the first method, cube samples were weighed in an electronic balance before and after exposure to elevated temperature levels from which the difference in weights were calculated. In the second method, the *Mettler Toledo* TGA was used to determine the loss of mass. Powdered samples of 20mg in weight passing through the 0.425 µm sieve were placed in silica crucibles and subjected to a constant heating rate of 10°C/min up to 800°C, under air flow (Figure 3.12).

Mass loss is calculated as the percentage of change of mass with respect to initial mass.
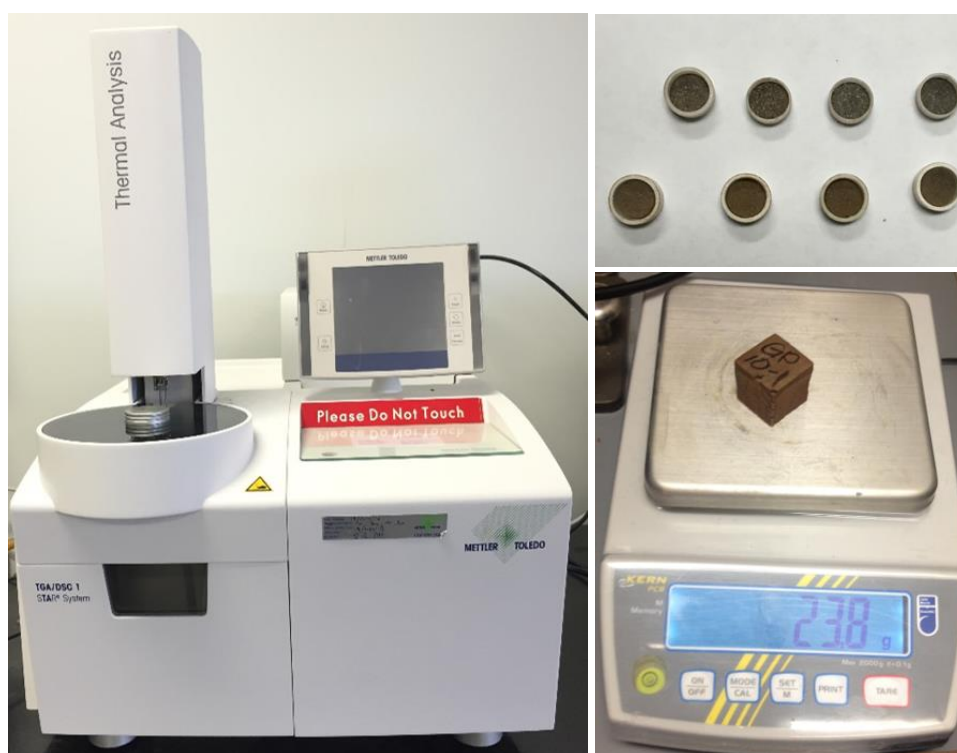
Figure 3.12 – (Left) Mettler Toledo TGA, (Top-Right) TGA samples in silica-based crucibles,

(Bottom-Right) Weight measurement using the electronic balance

CHAPTER 04

TEST RESULTS AND DISCUSSION

4.1. Workability and Initial setting times

The workability of fresh material is of vital importance when understanding the performance of a particular material. The Gladstone and Gladstone/Callide FA GP paste results and photographs are given in Tables 4.1 and 4.2 and Figures 4.1 and 4.2, respectively. The slump flow (SF) values were calculated in reference to the equations given in section 3.6.

Both Gladstone FA and Gladstone/Callide FA based pastes produced excellent workability conditions. This was expected as the mix matrix comprise of very fine and spherical shaped particles which provides a smooth flow. The first half of the mixtures (GP 01–05) produced slightly higher SF values from the Gladstone FA pastes compared to the Gladstone/Callide FA pastes with a maximum of 312.5 mm for the Gladstone FA pastes and 275 mm for the Gladstone/Callide FA pastes. This could be explained in terms of particle size as the number of particles passing each sieve was seen to be higher for the Gladstone FA which implies that it is finer and hence provide a more liquid mixture. Similar deductions have been reported from Kong et al. (2007).

This condition slightly changed in the latter half of the mixtures (GP 06–10) with the SF values of the Gladstone/Callide FA paste exceeding that of the Gladstone FA paste. Gladstone/Callide FA pastes resulted in a maximum SF of 337.5 mm whilst the Gladstone FA pastes resulted in a maximum SF of 335 mm. This could be due to the high liquidity of the latter half paired with the high calcium content of the Gladstone FA. Lee and Van Deventer (2002b) reported that a higher calcium content in a comparatively higher alkaline solution to FA ratio could cause additional nucleation during the dissolution process which

would accelerate the rate of hardening. Gomaa et al. (2017) also stated that a higher level of CaO may result in poor workability conditions however, high calcium alone is insufficient to produce poor workability conditions.

When considering the workability of the latter half of the mixtures (GP06–10) in both types of FA pastes are higher than the first half (GP01–05) which is due to the higher alkaline solution to FA ratio. The higher this ratio implies a higher fluid content in the mixture which in turn produces a paste more liquid in nature.

Table 4.1 – Workability Results Gladstone FA GP mixtures

Gladstone FA GP pastes					
ID	Mix	d1 (mm)	d2 (mm)	SF (mm)	Initial Setting Times (min)
GP01	GP-0.4/0.5	300	300	300	All mixtures were observed to be workable 30 minutes after casting.
GP02	GP-0.4/1	300	305	302.5	
GP03	GP-0.4/1.75	315	310	312.5	
GP04	GP-0.4/2	300	300	300	
GP05	GP-0.4/2.5	290	300	295	
GP06	GP-0.57/0.5	305	310	307.5	
GP07	GP-0.57/1	280	280	280	
GP08	GP-0.57/1.75	310	320	315	
GP09	GP-0.57/2	330	340	335	
GP010	GP-0.57/2.5	320	330	325	
Min		280	280	280	
Max		330	340	335	

Table 4.2 – Workability Results Gladstone/Callide FA GP mixtures

	Gladstone/Callide FAA GP pastes				
ID	**Mix**	**d1 (mm)**	**d2 (mm)**	**SF (mm)**	**Initial Setting Times (min)**
GP01	GP-0.4/0.5	235	235	235	3-5
GP02	GP-0.4/1	235	230	232.5	2-5
GP03	GP-0.4/1.75	235	235	235	5
GP04	GP-0.4/2	265	270	267.5	20+
GP05	GP-0.4/2.5	275	275	275	20+
GP06	GP-0.57/0.5	320	320	320	8
GP07	GP-0.57/1	315	320	317.5	15-20
GP08	GP-0.57/1.75	315	320	317.5	30+
GP09	GP-0.57/2	335	340	337.5	30+
GP010	GP-0.57/2.5	335	340	337.5	30+
Min		235	230	232.5	
Max		335	340	337.5	

Gladstone GP 01   Gladstone GP 02   Gladstone GP 03   Gladstone GP 04   Gladstone GP 05

Gladstone GP 06   Gladstone GP 07   Gladstone GP 08   Gladstone GP 09   Gladstone GP 10
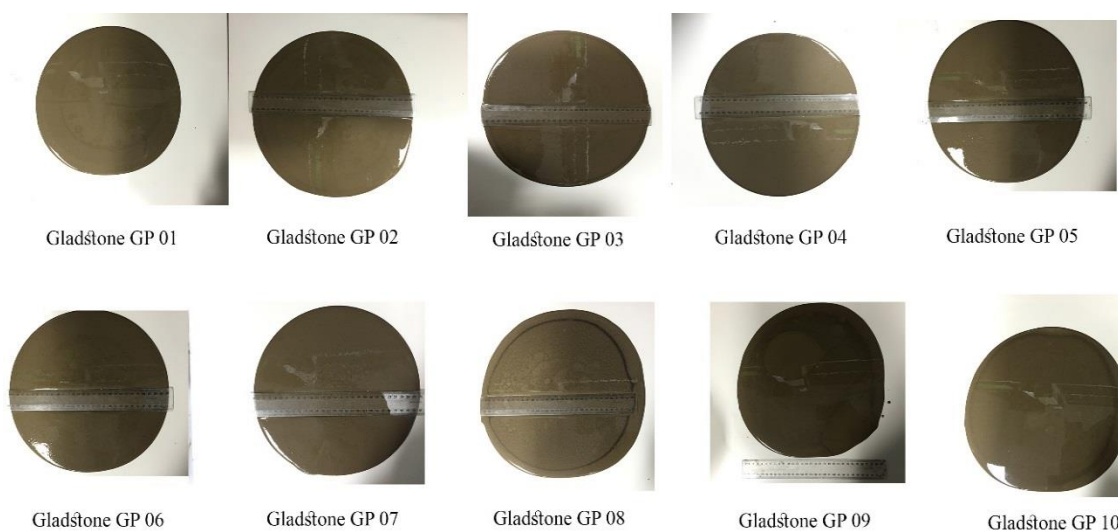
Figure 4.1 – Gladstone FA GP SF photographs
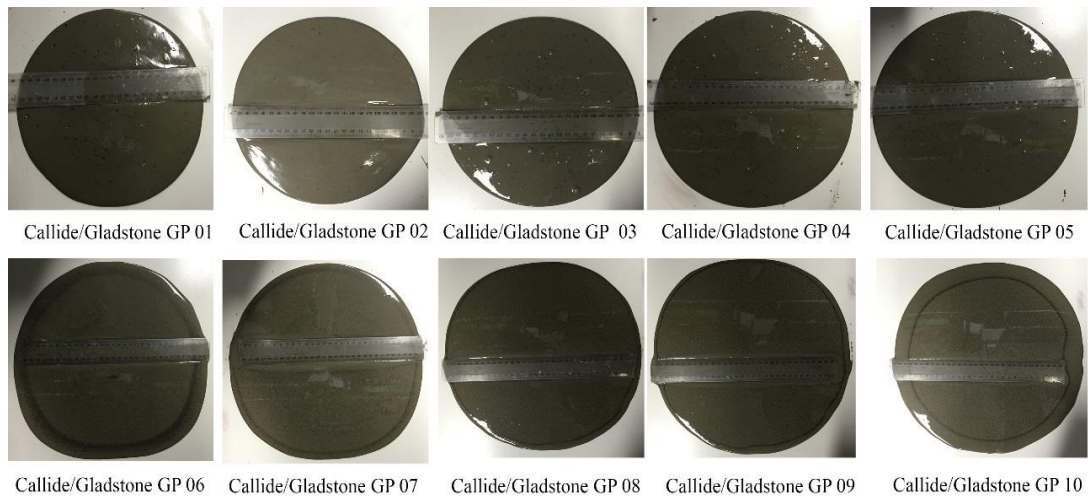
Figure 4.2 – Gladstone/ Callide FA GP SF photographs

It can be evidently seen from both Figures 4.1 and 4.2 that the both types of FA produce highly workable mixtures.

The RPC results and photographs are given in Table 4.3 and Figure 4.3, respectively. Compared to GP mixtures, RPC specimens displayed low workability conditions with a maximum SF of only 111 mm–132.5 mm. This condition can be expected due to the inclusion of aggregate particles which increases the friction among particles hence providing a thicker flow. In addition, the w/c ratio is kept to a minimum in RPC in order to obtain high strengths, which also contributes to providing low flow properties. Moreover, the RPC mixture was observed to be denser compared to the GP pastes which further reduces the workability conditions of the mixture. Similar flow results have been reported by Yazıcı et al. (2009). However, the flow Table results achieved in this study are lower than the ASTM C230 standard requirement which is 190 mm–250 mm after 20 drops. According to Gowripalan et al. (2003), this flow can be achieved with a mixing time of about 40 minutes at laboratory conditions. The RPC in this study underwent a mixing time of 30 minutes to reach breakpoint (see section 3.4).

Table 4.3 – Workability Results RPGC Mixtures

RPC Mixtures			
ID	**d1 (mm)**	**d2 (mm)**	**SF (mm)**
RPC 01-a	130	135	130
RPC 01-b	120	120	120
RPC 02	110	112	110
Min	110	112	111
Max	130	135	132.5

RPC 01–a   RPC 01–b   RPC 02
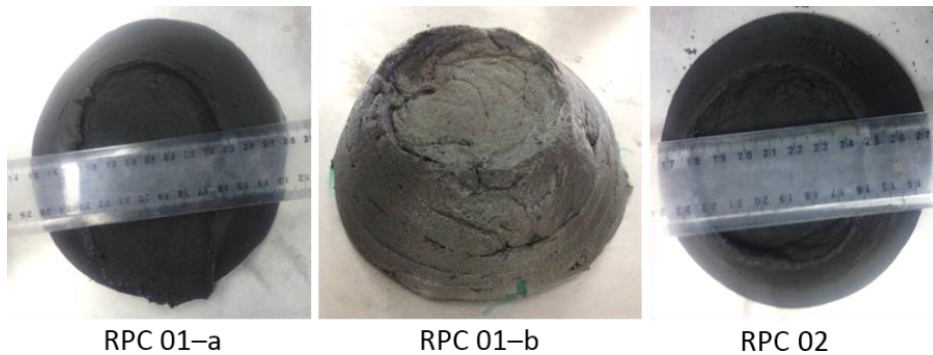
Figure 4.3 – RPC SF photographs

The RPC mixtures were observed to be viscous in nature as shown in the above Figure (4.3).

The workability test results and photographs for RPGC are given in Table 4.4 and Figure 4.4. Compared to RPC, RPGC showed better results with a highest SF of 252 mm and a lowest of 187.5 mm. This is due to the finer and spherical nature of the FA compared to OPC which improves the fluidity and workability conditions. Moreover, the RPGC displayed somewhat lower SF values compared to GP pastes. This is due to the inclusion on aggregate particles which thickens the mixture thus reducing the workability conditions.

Table 4.4 – Workability Results RPGC Mixtures

ID	Mix	d1 (mm)	d2 (mm)	SF (mm)
RPGC Mixtures				
RPGC 01	RPC01 + GP05	190	185	187.5
RPGC 02	RPC01 + GP08	220	220	220
RPGC 03	RPC02 + GP05	223	225	224
RPGC 04	RPC02 + GP08	225	225	225
RPGC 05	RPC01 + GP10	254	250	252
RPGC 06	RPC02 + GP10	250	250	250
Min		190	185	187.5
Max		254	250	252
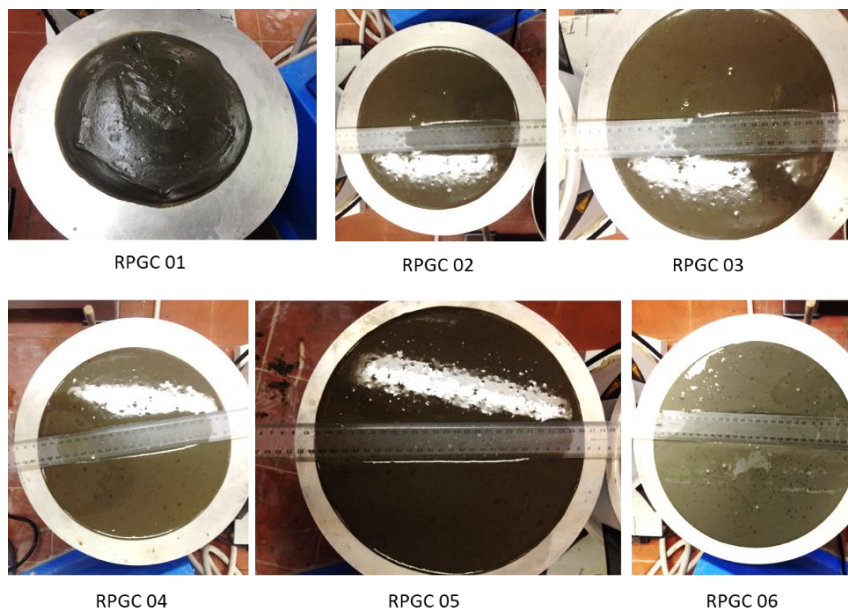
Figure 4.4 – RPGC SF photographs

As seen in Figure 44, the RPGC mixtures were observed to be highly workable in nature.

When considering the initial setting times, Gladstone FA GP lasted for over 30 minutes in liquid state, whereas the Gladstone/Callide FA GP pastes set comparatively fast. GP 01, 02 and 03 of the Gladstone/Callide set resulted in initial setting times of approximately 2–5 minutes, which made it difficult during the casting process and hence no results were obtainable. Figure 4.5 shows a comparison of Gladstone FA GP01 and Gladstone/Callide FA GP01 5 minutes after casting.

Figure 4.5 – Comparison of workability conditions
Gladstone FA GP01 (left)/ Gladstone/Callide FA GP01 (right)

The mixtures were observed to solidify slower as the Na_2SiO_3/NaOH ratio increased. This could be explained through the pH value of the solution. Sodium hydroxide has the ability to reduce the acidity of a solution, so, lower amounts of hydroxide imply lower pH values. Literature states that when the pH value is low the nature of the GP mixture is more fluid-like and more workable while for higher pH values the mix matrix remains more viscous which accelerates the setting times (Roy et al., 1995). This explains the low initial setting times of Gladstone/Callide FA mixtures with a lower Na_2SiO_3/NaOH ratios (samples having a higher hydroxide content).

However, a question may arise as to why this condition did not occur in the Gladstone FA mixtures which produced longer setting times despite the difference in the Na_2SiO_3/NaOH ratios. This can be explained by the difference in Al_2O_3 and SiO_2 compositions of the two FA materials. De Silva et al. (2007) reports that Al has a dominant effect on the setting times of the GP pastes, with shorter setting times reported for lower SiO_2: Al_2O_3 ratios and that minor changes in the Si and Al concentrations can drastically affect the setting of GPs. Gladstone FA has a higher ratio compared to Gladstone/Callide FA which implies that it takes a longer time to set.

4.2. Density

Density results are given in Tables 4.5 and 4.6 for the two FA GP types. The densities of the samples Gladstone FA GP samples which noticed to be lower than that of the Gladstone/Callide FA GP samples. While the Gladstone FA GP samples resulted in a maximum density of 2396 kg/m^3 and a lowest of 2154 kg/m^3, Gladstone/Callide FA GP samples resulted in a maximum density of 2102 kg/m^3 and a lowest of 1870 kg/m^3. Additionally, the densities of the GP mixtures were observed to increase with increasing Na_2SiO_3/NaOH ratios. This is quite reasonable because the increase in the Na_2SiO_3/NaOH ratio implies an increase in the sodium silicate amount which causes a more viscous and thicker mixture, thus increasing the density.

Table 4.5 – Density Results-Gladstone FA GP Mixtures

Density Calculation (kg/m^3)				
No	Name	Mass (kg)	Volume (m^3)	Density (kg/m^3)
GP 01	GP-0.4/0.5	0.2189	0.0001	2189.00
GP 02	GP-0.4/1	0.2272	0.0001	2272.00
GP 03	GP-0.4/1.75	0.2154	0.0001	2154.00
GP 04	GP-0.4/2	0.2335	0.0001	2335.00
GP 05	GP-0.4/2.5	0.2364	0.0001	2364.00
GP 06	GP-0.57/0.5	0.2203	0.0001	2203.00
GP 07	GP-0.57/1.0	0.2298	0.0001	2298.00
GP 08	GP-0.57/1.5	0.2308	0.0001	2308.00
GP 09	GP-0.57/2.0	0.2371	0.0001	2371.00
GP 10	GP-0.57/2.5	0.2396	0.0001	2396.00

Table 4.6 – Density Results-Gladstone/Callide FA GP Mixtures

Density Calculation (kg/m^3)				
No	Name	Mass (kg)	Volume (m^3)	Density (kg/m^3)
GP 04	GP-0.4/2	0.2046	0.0001	2046.00
GP 05	GP-0.4/2.5	0.2059	0.0001	2059.00
GP 06	GP-0.4/2.5	0.1870	0.0001	2102.00
GP 07	GP-0.57/1.0	0.1873	0.0001	1873.00
GP 08	GP-0.57/1.5	0.1886	0.0001	1886.00
GP 09	GP-0.57/2.0	0.1905	0.0001	1905.00
GP 10	GP-0.57/2.5	0.1968	0.0001	1968.00

The RPC samples displayed readings of 2546kg/m^3, 2752kg/m^3 and 2715kg/m^3 for RPC01-a, RPC01-b and RPC 02, respectively (shown in Table 4.7) which were higher than that of the GP samples and of conventional concretes. While conventional concretes have a density of about 2400kg/m^3, Richard and Cheyrezy (1994) reported that the density of RPC could be increased to as high as 3000kg/m^3.

Table 4.7 – Density Results-RPC Mixtures

Density Calculation (kg/m^3)				
No	Name	Mass (kg)	Volume (m^3)	Density (kg/m^3)
RPC01	RPC 01-a	0.2546	0.0001	2546.00
RPC01	RPC 01-b	0.2752	0.0001	2752.00
RPC02	RPC02	0.2715	0.0001	2715.00

Density results of the RPGC samples are given in Table 4.8. The RPGC samples displayed a maximum density of 2245kg/m^3 and a minimum of 2112kg/m^3.

Table 4.8 – Density Results-RPGC Mixtures

Density Calculation (kg/m^3)				
No	Name	Mass (kg)	Volume (m^3)	Density (kg/m^3)
RPC 01 + GP5	RPCG 1	0.2245	0.0001	2245.00
RPC 02 + GP5	RPCG 2	0.2193	0.0001	2193.00
RPC 01 + GP8	RPCG 3	0.2147	0.0001	2147.00
RPC 02 + GP8	RPCG 4	0.2112	0.0001	2112.00
RPC 01 + GP10	RPCG 5	0.2145	0.0001	2145.00
RPC 02 + GP10	RPCG 6	0.2120	0.0001	2120.00

4.3. Physical appearance

Figures 4.6–4.8 show the physical appearance of the Gladstone, Gladstone/Callide and RPGC specimens before temperature exposure, after 400°C exposure and after 800°C exposure. Initial GP specimens were observed to be grey in colour which changed to a slightly darker grey when exposed to a temperature of 400°C. This colour further changed to a reddish brown after exposure of 800°C. These changes in colour were reported to be due to the high levels of iron oxide in the FA (Zhang et al., 2014, Sarker et al., 2014, Wattimena et al., 2017, Ali et al., 2017). The Gladstone FA GP samples displayed deeper reddish-brown colour changes compared to the Gladstone/Callide FA GP samples. This was a result of the comparatively higher Fe_2O_3 contents of 12.48 wt.% in the Gladstone FA compared to 9.99 wt.% in the Gladstone/Callide FA. Similar changes were observed in the RPGC specimens which could also be due to the iron content of the FA.
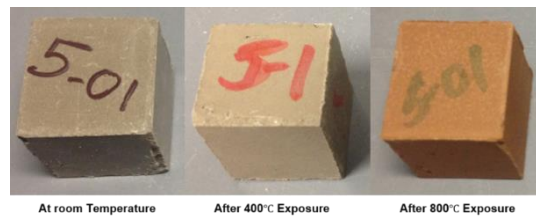
Figure 4.6 – Gladstone FA GP
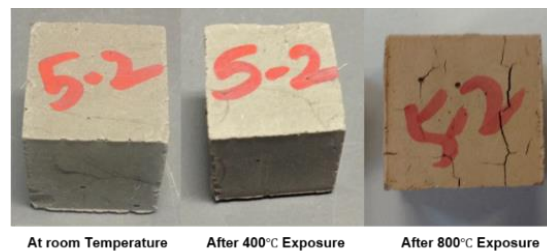
Figure 4.7 – Gladstone/Callide FA GP
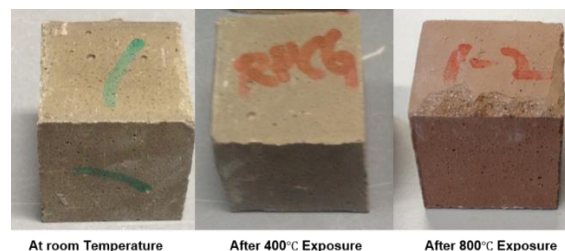
Figure 4.8 – RPGC specimens

4.4. Thermal performance and strength of GP.

Severe thermal cracking of Gladstone FA GP specimens which underwent non-sealed curing conditions were witnessed after exposure to elevated temperatures (Figure 4.9 and 4.10). This is can be explained in terms of initial dehydration of fluids which occurred during the curing process. Initial dehydration provides insufficient fluids for the geopolymerisation process causing the breaking down of the granular structure. This restricts the GP network from transforming to a more semicrystalline form hence causing severe cracking. Heah et al. (2011). Lee et al. (2016) reported that initial evaporation restricts the further development of strength producing weaker specimens which are more likely to crack due to differential thermal gradients between the inside and outside when exposed to elevated temperature levels.

Figure 4.9 – Non-sealed Gladstone FA GP 25mm specimens–Before temperature exposure

Gladstone GP01   Gladstone GP02   Gladstone GP03   Gladstone GP04   Gladstone GP05

Gladstone GP06   Gladstone GP07   Gladstone GP08   Gladstone GP09   Gladstone GP10

Figure 4.10 – Non-sealed Gladstone FA GP 25mm specimens–After 800ºC exposure

A comparison of the initial compressive strength between sealed and non-sealed GP specimens are given in Table 4.9 and Figure 4.11. When considering initial strength readings, approximately 25% lesser average initial strength readings were produced from the non-sealed samples compared to those of the sealed samples. This change in strength does indeed prove that initial dehydration plays an important role in the development of strength of GPs.

Table 4.9 – Comparison of the average compressive strengths at 24hours between non-sealed and sealed 25mm Gladstone FA GP cubes

Mixture	Non-sealed specimens		Sealed specimens	
	Initial Compressive Strength (**MPa**)	Standard Deviation	Initial Compressive Strength (**MPa**)	Standard Deviation
GP01	14.83	0.61	28.76	4.67
GP02	14.88	0.70	41.31	3.28
GP03	24.00	0.16	68.76	14.66
GP04	59.00	2.84	67.95	12.20
GP05	57.97	2.66	74.48	3.41
GP06	20.80	0.89	22.67	3.64
GP07	40.27	1.80	41.98	8.36
GP08	42.13	1.71	54.77	7.10
GP09	48.37	1.09	55.38	1.32
GP10	62.33	0.89	58.13	1.72
Min	**14.83**	**0.16**	**22.67**	**1.32**
Max	**62.33**	**2.84**	**74.48**	**14.66**
Average	**38.48**		**50.95**	
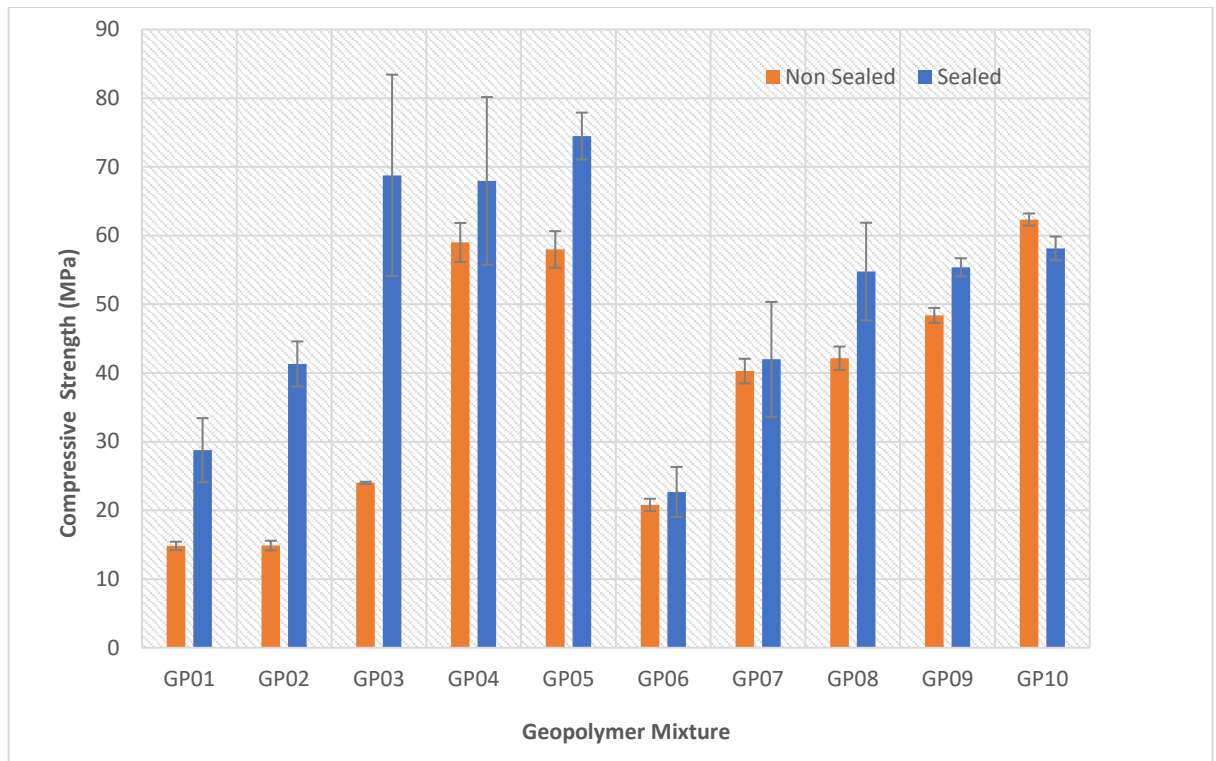
Figure 4.11 – Comparison of initial compressive strength between non-sealed and sealed 25mm Gladstone FA GP cubes

As evidenced in Table 4.9 non-sealed specimens produced strengths ranging from 14.83 MPa to 62.33 MPa, the highest being from GP10 having a Na2SiO3/NaOH ratio of 2.5 and an alkaline solution to FA ratio of 0.57. It must be noted that the highest initial strengths for non-sealed specimens was produced from the ones having a comparatively higher liquid content (0.57).

As mentioned before, early dehydration prevents the further development in strength due to the absence of sufficient fluids. However, due to the higher alkaline solution to FA ratio of the GP10 mixture (0.57) compared to GP05 (0.4), sufficient fluids are present for the dissolution and gelation processes even after early dehydration, thus producing high initial strength readings.

Mix	23°C	23°C STDEV	400°C	400°C STDEV	800°C	800°C STDEV	Thermal Cracking 800°C?
GP01	14.83	0.61	15.14	0.74	24.27	0.83	No
GP02	14.88	0.70	26.40	0.80	22.00	1.06	Yes
GP03	24.00	0.16	26.19	0.65	22.29	0.44	Yes
GP04	59.00	2.84	31.73	1.22	23.33	0.61	Yes
GP05	57.97	2.66	52.55	1.67	25.20	1.06	Yes
GP06	20.80	0.89	13.44	0.32	15.84	0.49	Yes
GP07	40.27	1.80	24.48	0.58	12.11	0.18	Yes
GP08	42.13	1.71	26.35	1.09	12.59	0.24	Yes
GP09	48.37	1.09	20.81	0.74	12.37	0.37	Yes
GP10	62.33	0.89	30.69	1.14	13.81	0.40	Yes
Min	**14.83**	**0.16**	**13.44**	**0.32**	**12.11**	**0.18**	
Max	**62.33**	**2.84**	**52.55**	**1.67**	**25.20**	**1.06**	
Av	38.48		27.81		18.43		

Additionally, the highest residual strength reading recorded at both 400°C and 800°C exposures were from GP05. A maximum residual strength of 52.66 MPa and 25.20 MPa was obtained after exposure to a temperature of 400°C and 800°C, respectively. This is graphically evident from the data presented in Figure 4.12.
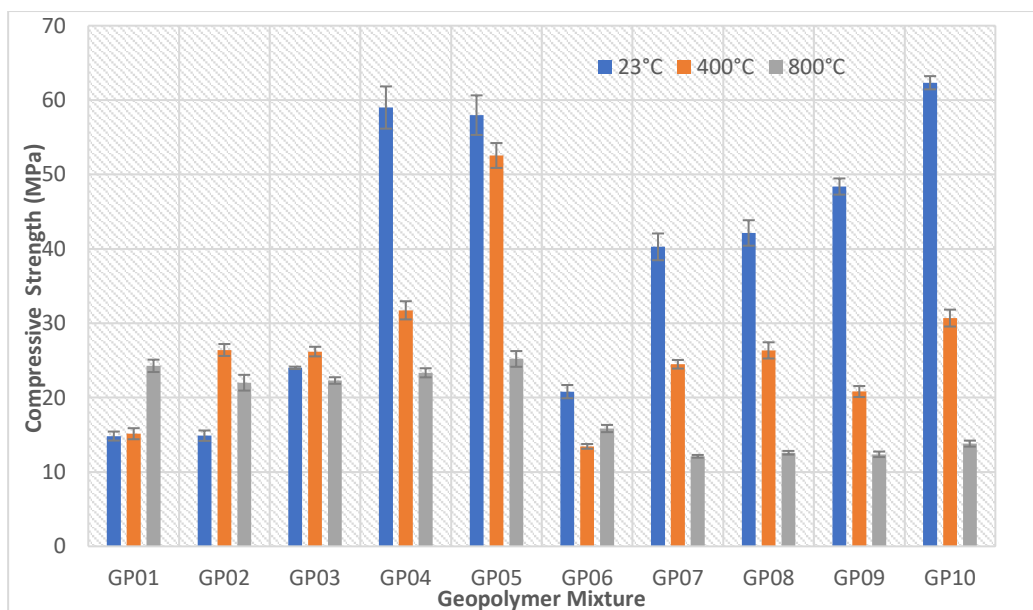
Figure 4.12 – Graph of compressive strength for non-sealed Gladstone FA GP cubes.

Lee et al. (2016) state that early evaporation of fluids hinders continuous reorganization of polycondensation processes and blocks further strength developments and structural evolution of GPs. This explains the reductions in strength of the non-sealed specimens.

Furthermore, early surface evaporation of fluids further creates a less dense structure within the GP which can in turn reduce the compressive strength. Similar findings and deductions have been made by Bakharev (2005) and Lee et al. (2016) who stated that the obstruction of the ongoing geopolymerisation process creates a less dense matrix with higher pores which produces poorer compressive strength readings.

The occurrence of carbonation can also be a probable cause behind the degradation of strength. When the material is openly exposed to the atmosphere during its early setting stages, CO_2 can easily penetrate and spread rapidly through the matrix. This results in the formation of sodium bicarbonate which reduces the pH value creating a less alkaline environment and reducing the rate of aluminosilicate gel formation. Pacheco-Torgal et al. (2008) states that higher alkaline concentrations are required for the development of strength in low calcium content binders. Similar findings have also been reported by Criado et al. (2005).

Figures 4.13–4.15 show 25mm Gladstone FA GP specimens before and after exposure to elevated temperature levels. Gladstone FA GP specimens which underwent sealed curing conditions showed far more promising results compared to non-sealed GP specimens. Majority of the sealed cured specimens were observed to be still intact displaying mild cracking even after an exposure of 800°C. And among these specimens, no cracking was witnessed in the 25mm Gladstone FA GP01-05 sealed specimens exposed to both 400°C and 800°C. However, mild cracking was witnessed in the latter half (GP06-10) which had a comparatively higher alkaline solution to FA ratio (0.57) after being exposed to 800°C.

Figure 4.13 – Sealed Gladstone FA GP 25mm specimens–Before temperature exposure
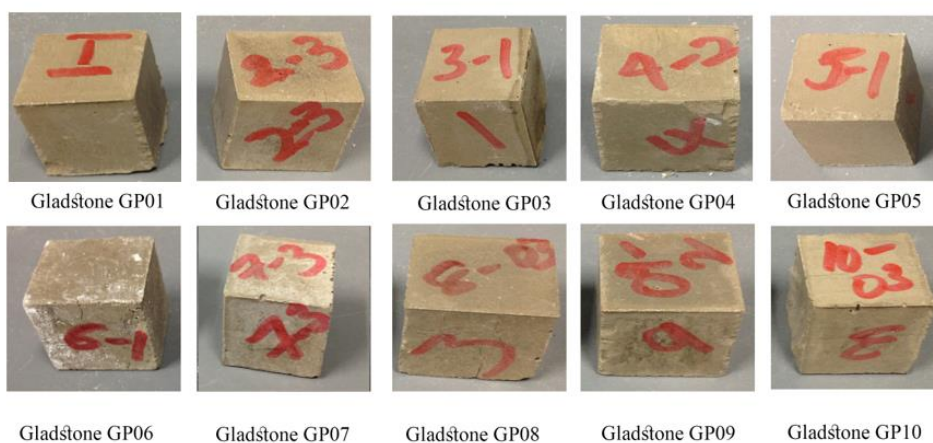
Figure 4.14 – Sealed Gladstone FA GP 25mm specimens 400ºC Exposure
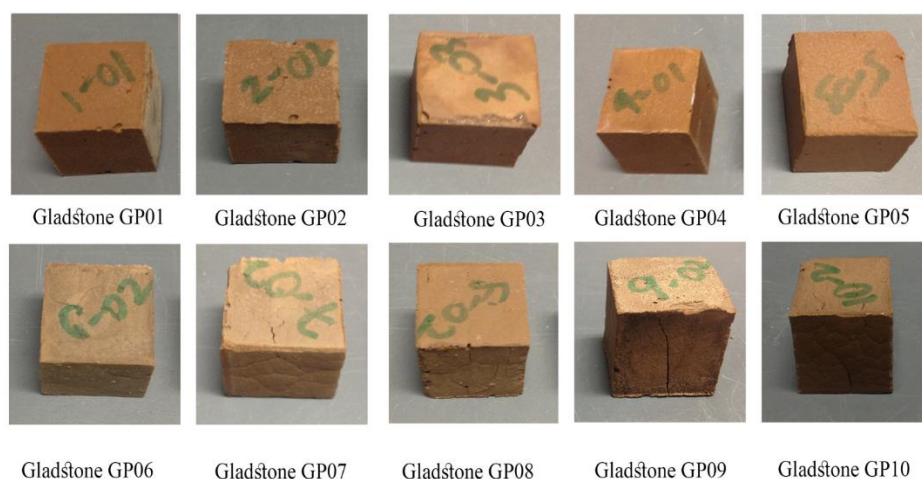
Figure 4.15 – Sealed Gladstone FA GP 25mm specimens 800ºC exposure

88

Figures 4.16 and 4.17 show 50mm Gladstone FA GP specimens after exposure to elevated temperature levels. Similar thermal cracking conditions to the 25mm Gladstone FA GP specimens were observed from the 50mm Gladstone FA GP specimens after being exposed to 400ºC. However, after being exposed to 800ºC, all 50mm specimens were observed to undergo thermal cracking as opposed to the 25mm specimens which displayed cracking from only the latter half (GP 06–GP10). The increase in thermal cracking with the increase in size could potentially be due to higher differential thermal gradients. As the specimen increases in size, heat conduction through the specimen significantly decreases. This increases the difference in thermal gradient between the surface and core of the specimens. This induces thermal stresses within the specimen which cause thermal cracking.
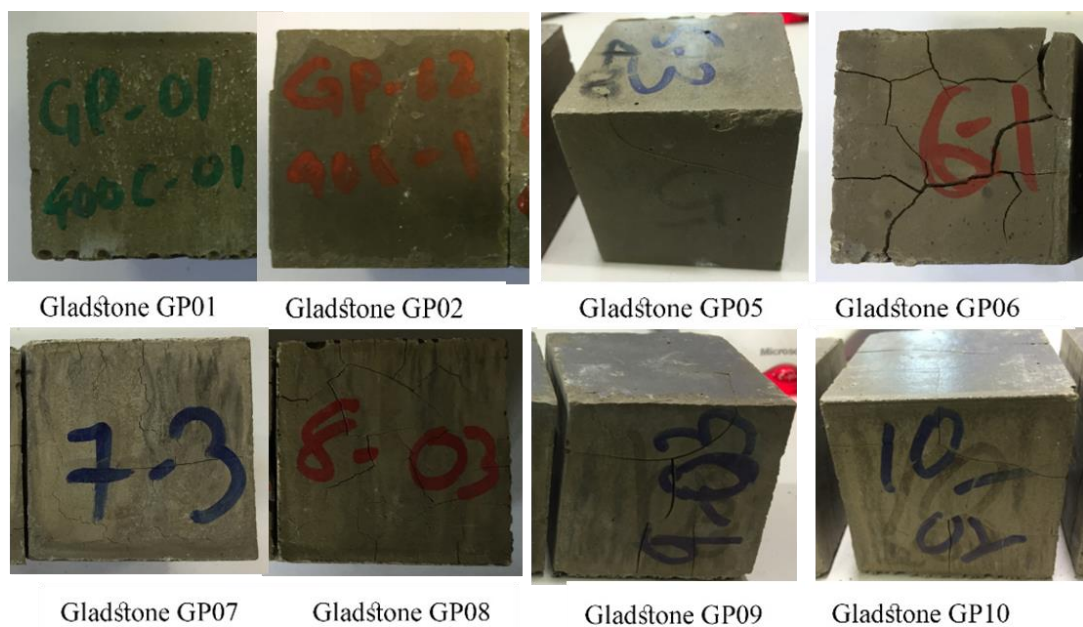
Figure 4.16 – Gladstone FA GP 50mm specimens after 400ºC exposure
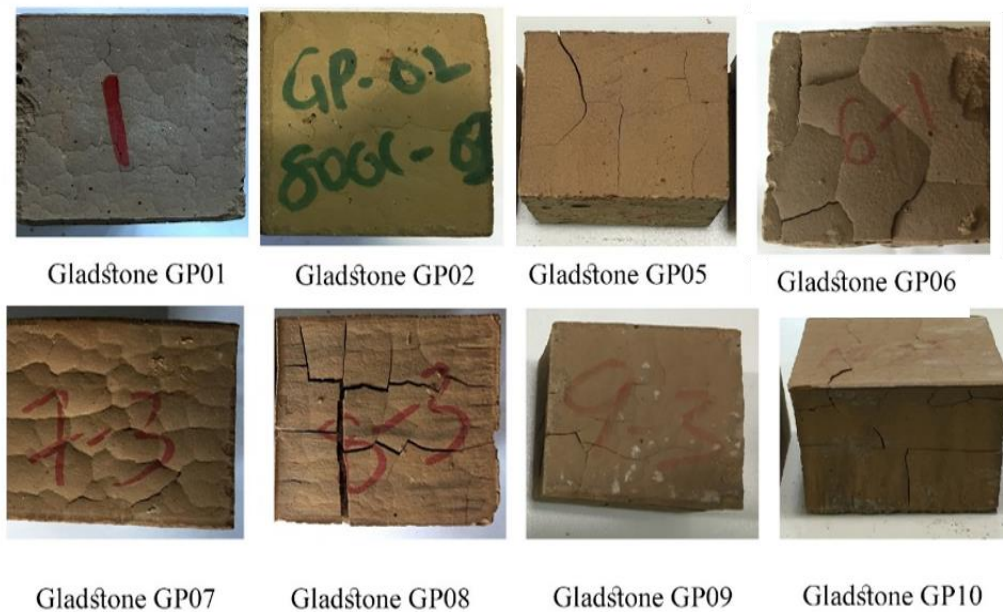
Figure 4.17 – Gladstone FA GP 50mm specimens after 800ºC exposure

When considering the initial strength results of the Gladstone FA GP specimens, at constant Na_2SiO_3/NaOH ratios, specimens having a lower alkaline solution to FA ratio of 0.4 achieved higher initial strengths compared to specimens having a higher alkaline solution to FA ratio of 0.57 (refer Table 4.11 and Figure 4.18). This condition was observed in both sealed and non-sealed curing conditions. This could potentially be due to the dense microstructure provided from utilizing a lower alkaline solution to FA ratio which result in fewer pores and high internal strength.

Table 4.11–Average compressive strengths. Sealed Gladstone FA GP pastes 25mm cubes

Mix	23°C	23°C STDEV	400°C	400°C STDEV	800°C	800°C STDEV	Thermal Cracking 400°C?	Thermal Cracking 800°C?
GP01	28.76	4.67	35.62	1.99	26.22	4.76	No	No
GP02	41.31	3.28	47.80	6.68	35.31	3.35	No	No
GP03	68.76	14.66	54.42	6.26	48.05	1.23	No	No
GP04	67.95	12.20	74.14	5.42	38.29	0.74	No	No
GP05	74.48	3.41	56.91	3.81	36.49	5.07	No	No
GP06	22.67	3.64	17.71	1.47	10.53	3.61	Yes	Yes
GP07	41.98	8.36	26.46	3.72	7.69	2.96	Yes	Yes
GP08	54.77	7.10	39.99	1.37	13.37	2.82	Yes	Yes
GP09	55.38	1.32	29.33	9.22	11.47	3.47	Yes	Yes
GP10	58.13	1.72	39.18	2.83	9.49	4.13	Yes	Yes
Min	**22.67**	**1.32**	**17.71**	**1.37**	**7.69**	**0.74**		
Max	**74.48**	**14.66**	**74.14**	**9.22**	**48.05**	**5.07**		
Av	**50.95**		**42.78**		**24.39**			
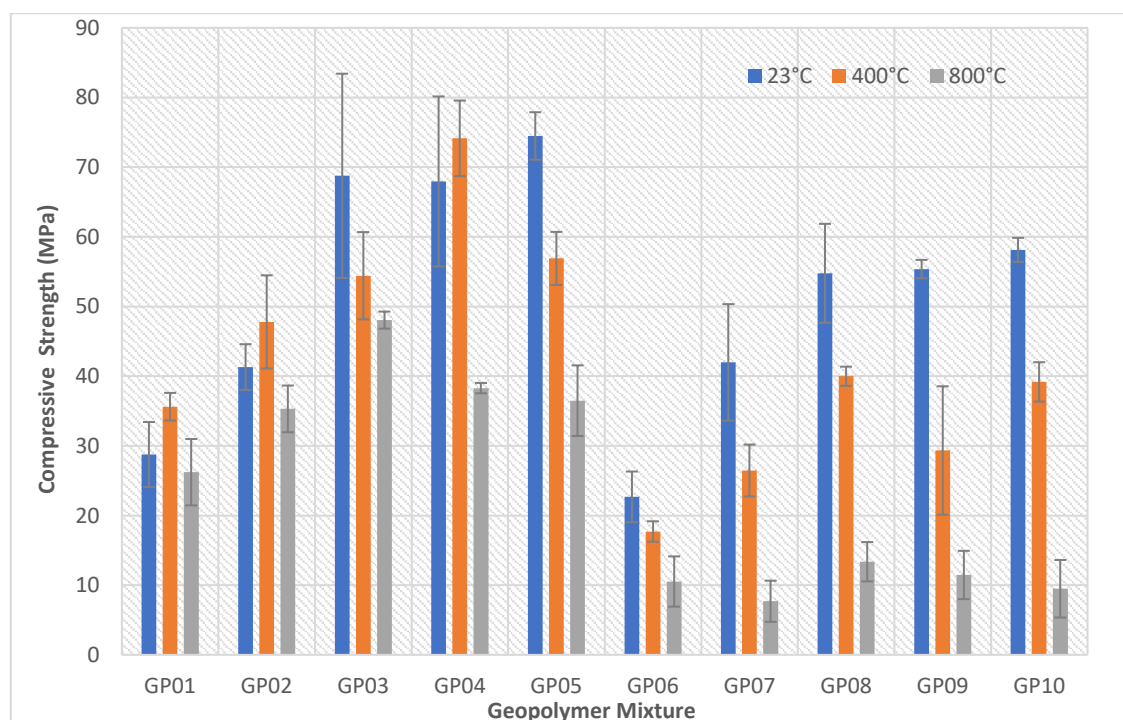
Figure 4.18 – Graph of compressive strength for sealed 25mm Gladstone FA GP cubes.

Additionally, at constant alkaline solution to FA ratio, as the Na_2SiO_3/NaOH ratio increased from 0.5 to 2.5 the initial strength readings also increased. Hardjito et al. (2004) and Hardjito et al. (2005b) reported similar findings where an increase in the Na_2SiO_3/NaOH ratio have resulted in an increase in strength. A possible explanation for this increase may be connected to the inclusion of more sodium silicate as the ratio increases.

Pacheco-Torgal et al. (2008) reported that more silica gel which favours the geopolymerisation reaction can result in higher mechanical strengths. Xu and Van Deventer (2000) also reported that the use of sodium silicate improves the geopolymerisation process by accelerating the dissolution of the FA. Additionally, Al Bakri et al. (2011) reported that increasing levels of sodium silicate increases the SiO_2 to Al_2O_3 ratio which in turn increases the number of Si-O-Si bonds and this contributes to better strength development. While Yao et al. (2009) stated that silicate has the ability to accelerate the geopolymerisation process by inducing the polymerization of leached materials and hence producing high early strength

However, Degirmenci (2017) recommended an optimum Na_2SiO_3/NaOH ratio of 2.5 and stated that at a ratio of 3.0 or greater, reductions in compressive strength were observed. This was due to the excess alkaline content retarding the geopolymerisation reaction.

This research results in similar trends with initial compressive strengths of the 25mm sealed Gladstone FA GP specimens increasing from 28.76 MPa to 74.48 MPa and from 22.67 MPa to 58.13 MPa as the Na_2SiO_3/NaOH ratio increased from 0.5 to 2.5, at alkaline solution to FA ratios of 0.4 and 0.57, respectively.

In considering the residual strength readings of the Gladstone FA GP, some mixtures recorded losses in strength while others were observed to gain strength with increasing temperatures.

Figure 4.19 and 4.20 show Gladstone specimens at room temperature and after exposure to elevated temperature levels before and after compression. While specimens compressed at room temperature were observed to fail as per the shear failure plane, specimens exposed to elevated temperature levels (800°C) were observed to crush in to small particles. This is due to the breaking down and the decomposition of gepolymeric bonds at high temperature levels.
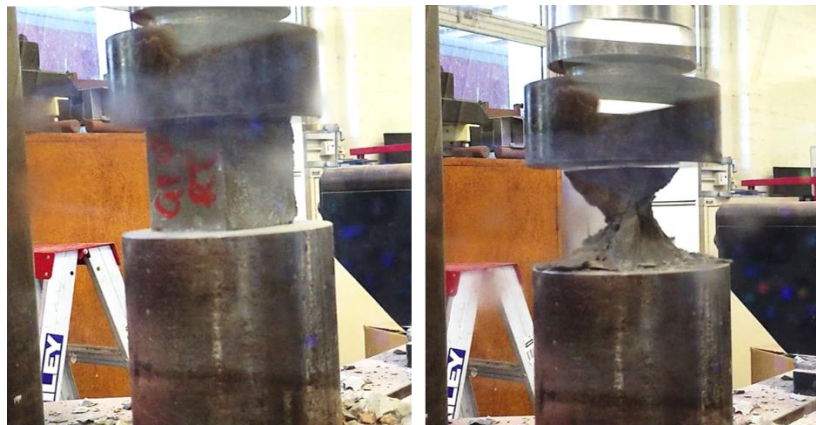
Figure 4.19– Specimen at room temperature before and after compression

Figure 4.20– Specimen after high heat exposure before and after compression

As the temperature increased to 400°C the strength of the 25mm sealed Gladstone FA GP06-10 specimens was seen to decrease while majority of the GP01-05 specimen strengths increased. This increased strength is due to the denser and viscose nature of the first set of mixtures (alkaline solution to FA ratio of 0.4), which provides a better bond system resulting in increased thermal resistance. Similar results have been reported by Barbosa and MacKenzie (2003) and Bakharev (2006). The specimens produced strengths

within the range of 17.71 MPa –74.14 MPa after being exposed to 400°C and 7.69 MPa–48.05 MPa after being exposed to 800°C. Amongst all GP specimens which were exposed to 800°C a highest strength was recorded from the sealed 25mm Gladstone FA GP03 samples (Table 4.11).

Table 4.12 shows he average compressive strength reading of 50mm sealed Gladstone FA GP specimens. Figure 4.21 shows the graph of compressive strength for 50mm sealed Gladstone specimens.

Initial strength results of the 50mm Gladstone FA GP specimens reached a highest of 63.87MPa from GP05 as shown in Table 4.12 which were somewhat similar to the 25 mm GP05 specimens. An average initial compressive strength of 45.16 MPa was recorded. The highly questionable result was the initial compressive strength obtained from the 50mm GP 06 cube which was recorded to be 5.99MPa. This was approximately 74% less initial strength between two sizes. This could potentially be due to severe cracking which occurred at both 400°C and 800°C (refer Figures 4.16 and 4.17).

Table 4.12 – Average compressive strengths.

Sealed Gladstone FA GP 50mm cubes

Mix	23°C	23°C STDEV	400°C	400°C STDEV	800°C	800°C STDEV	Thermal Cracking 400°C?	Thermal Cracking 800°C?
GP01	35.05	3.06	34.35	1.74	20.32	2.23	No	Yes
GP02	50.80	6.29	41.33	1.40	21.65	2.24	No	Yes
GP05	63.87	3.40	65.20	1.74	34.31	5.12	No	Yes
GP06	5.99	2.27	12.13	2.44	5.75	0.46	Yes	Yes
GP07	51.47	3.63	25.83	0.73	7.94	0.30	Yes	Yes
GP08	59.73	5.10	33.30	3.07	8.88	1.49	Yes	Yes
GP09	59.07	0.92	27.23	0.97	11.75	1.01	Yes	Yes
GP10	55.73	9.83	37.11	3.43	19.91	2.28	Yes	Yes
Min	**5.99**	**0.92**	**12.13**	**0.73**	**5.75**	**0.30**		
Max	**63.87**	**9.83**	**65.20**	**3.43**	**34.31**	**5.12**		
Av	**45.16**		**35.38**		**17.05**			
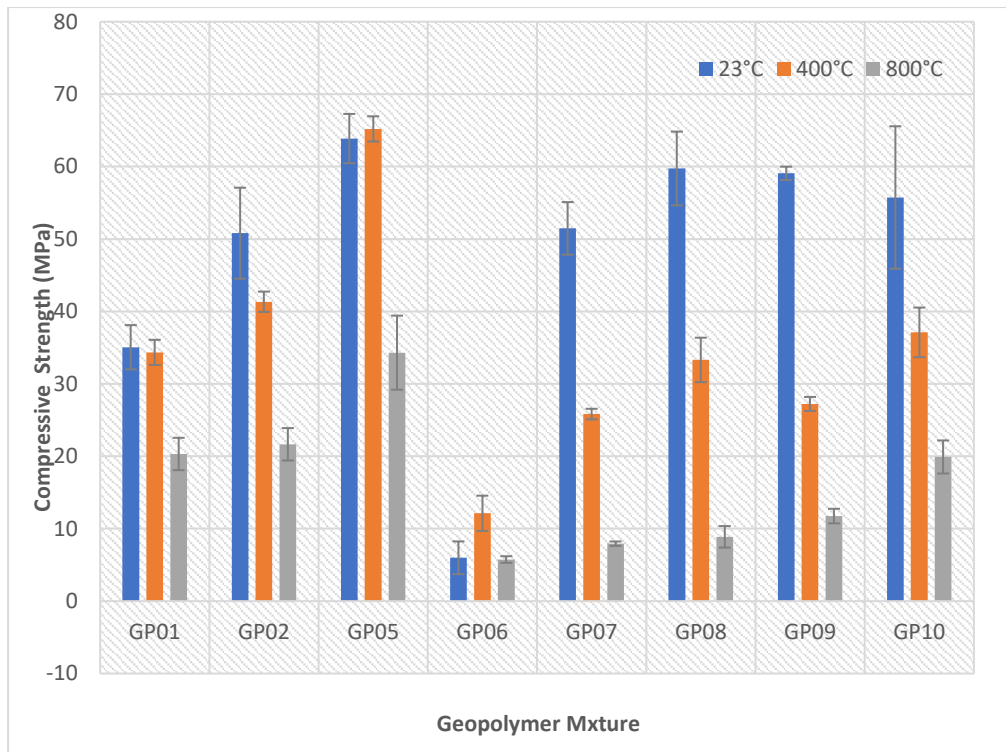
Figure 4.21 – Graph of compressive strength for sealed 50mm Gladstone FA GP cubes.

Table 4.13 and Figure 4.22 show a comparison of the initial and residual strength readings between the two sizes for Gladstone FA GP cube specimens. 50 mm Gladstone FA cube samples displayed lesser strengths compared to the 25mm cubes with a maximum of 65.20MPa from GP05 after exposure to 400ºC. This was approximately a 2% increment in strength compared to initial strength results of the 50mm GP05 specimen. Additionally, 50mm GP05 cubes were observed to have strength loss of approximately 36% after exposure to 800ºC.

Table 4.13 – Comparison of the average Compressive Strength between 25 mm & 50mm Gladstone FA GP pastes specimens

Gladstone GP (Oven Bag)							
Comparison Average Compressive Strengths - 25 mm & 50mm (MPa)							
Mixture	Size	23°C	23°C STDEV	400°C	400°C STDEV	800°C	800°C STDEV
GP01	25	28.76	4.67	35.62	1.99	26.22	4.76
	50	35.05	3.06	34.35	1.74	20.32	2.23
GP02	25	41.31	3.28	47.80	6.68	35.31	3.35
	50	50.80	6.29	41.33	1.40	21.65	2.24
GP05	25	74.48	3.41	56.91	3.81	36.49	5.07
	50	63.87	3.40	65.20	1.74	34.31	5.12
GP06	25	22.67	3.64	17.71	1.47	10.53	3.61
	50	5.99	2.27	12.13	2.44	5.75	0.46
GP07	25	41.98	8.36	26.46	3.72	7.69	2.96
	50	51.47	3.63	25.83	0.73	7.94	0.30
GP08	25	54.77	7.10	39.99	1.37	13.37	2.82
	50	59.73	5.10	33.30	3.07	8.88	1.49
GP09	25	55.38	1.32	29.33	9.22	11.47	3.47
	50	59.07	0.92	27.23	0.97	11.75	1.01
GP10	25	58.13	1.72	39.18	2.83	9.49	4.13
	50	55.73	9.83	37.11	3.43	19.91	2.28
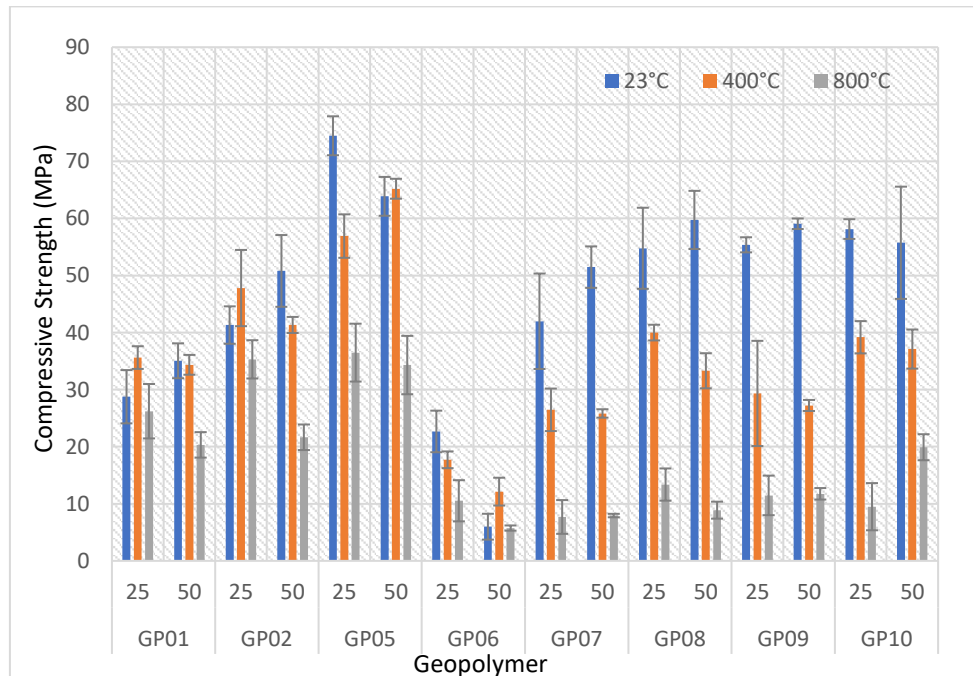
Figure 4.22 – Comparison of strength-25mm and 50mm Gladstone FA GP cubes

These occurrences indicate higher thermal gradients between the centre and surface of the 50mm specimens causing a higher degree of cracking and hence, strength losses. Kong and Sanjayan (2010) reported similar findings where elevated temperature exposure adversely effected larger paste specimens prepared using class F FA. They reported that larger samples have less dissipation of trapped moisture from within the GP matrix and dissipated moisture causes discontinuous microspores which in turn improves strength. As the dissipated moisture reduces, the development of strength also reduces. Additionally, Guerrieri (2009) reported that larger alkali activated slag paste specimens produce lower strengths compared to smaller samples due to higher thermal shrinkage occurring in response to the evaporation of chemically combined water. This differential movement of vaporized water causes significant internal cracking which degrades the overall strength.

Gladstone/Callide FA GP specimens behaved somewhat similar to the Gladstone FA GP specimens in terms of thermal cracking. However, no data could be obtained from the Gladstone/Callide FA GP01, 02 and 03 mixtures due to rapid initial setting times, hence, no investigations were carried out on mix number GP01, 02 and 03.

The 25mm Gladstone/Callide FA GP specimens displayed no cracking when exposed to 400°C but showed considerable amounts of cracking when exposed to 800°C (Figures 4.23 – 4.25). This degree of cracking at 800°C was greater for the Gladstone/Callide specimens compared to the Gladstone specimens which could be explained in terms of particle size. As mentioned in section 3.2.1, Gladstone FA is finer in nature having a fineness of 86.136% passing the 45μm sieve compared to Gladstone/Callide FA which has a finesse of 80.488%. This produces a stronger matrix and a better bond system between particles when activated with alkaline solution. As temperature increases, the thermal stresses developed within the specimens due to differential thermal gradients, would have a greater effect on the Gladstone/Callide FA GP specimens because of the low bondage properties compared to the Gladstone FA.

Mild thermal cracking was observed from the 50mm Gladstone/Callide FA GP specimens after exposure to 400°C. However, unlike the 25mm specimens, large cracking of specimens were observed from the 50mm specimens after exposure to 800°C (Figures 4.26 – 4.27). Similar to the 50mm Gladstone specimens, the increase in thermal cracking of the 50mm Gladstone/Callide specimens could potentially be due to an increase in thermal gradients between the outer surface and the inner core with the increase in size (distance). Ali and Zurisman (2015) reported that larger specimens displayed higher amounts of spalling compared to smaller specimens due to the increase in thermal gradients within the specimen which pressurizes the outer surface to crack under thermal stresses.
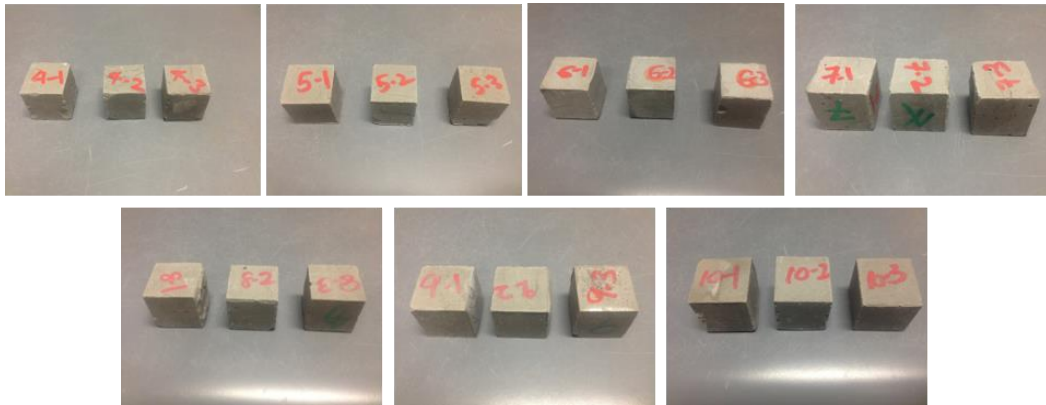
Figure 4.23 – Gladstone/Callide FA GP 25mm specimens before temperature exposure

Figure 4.24 – Gladstone/Callide FA GP 25mm specimens after 400°C exposure

Gladstone/Callide
GP04

Gladstone/Callide
GP05

Gladstone/Callide
GP06

Gladstone/Callide
GP07

Gladstone/Callide
GP08

Gladstone/Callide
GP09

Gladstone/Callide
GP10

Figure 4.25 – Gladstone/Callide FA GP 25mm specimens after 800ºC exposure

Gladstone/Callide
GP04

Gladstone/Callide
GP05

Gladstone/Callide
GP06

Gladstone/Callide
GP07

Gladstone/Callide
GP08

Gladstone/Callide
GP09

Gladstone/Callide
GP10

Figure 4.26 – Gladstone/Callide FA GP 50mm specimens after 400ºC exposure

99

Gladstone/Callide
GP04

Gladstone/Callide
GP05

Gladstone/Callide
GP06

Gladstone/Callide
GP07

Gladstone/Callide
GP08

Gladstone/Callide
GP09

Gladstone/Callide
GP10

Figure 4.27 – Gladstone/Callide FA GP 50mm specimens after 800ºC exposure

Figure 4.28 shows graphically presented strength results of the 25mm Gladstone/Callide FA GP paste specimens. Initial strengths achieved from the Gladstone/Callide FA GP 25mm cube specimens were a maximum of 61.38 MPa with an average of 51.29 MPa. Maximum strength readings were produced from GP08 having a Na_2SiO_3/NaOH ratio of 1.75 and an alkaline solution to FA ratio of 0.57 (Table 4.14). This is similar to the findings of Lee and Van Deventer (2002b) who reported that after a ratio of 1.75, excessive silicate will retard the geopolymerisation process by the precipitation of Al-Si phase by preventing contact between the FA and alkaline solution.

Table 4.14 – Average compressive strengths. Gladstone/Callide FA GP pastes 25mm cubes

Mix	23°C	23°C STDEV	400°C	400°C STDEV	800°C	800°C STDEV	Thermal Cracking 400°C?	Thermal Cracking 800°C?
GP04	56.75	11.53	76.43	9.01	25.91	1.00	No	Yes
GP05	49.91	7.84	90.02	6.87	30.43	2.31	No	Yes
GP06	41.15	4.76	56.51	2.52	18.51	3.68	No	Yes
GP07	43.35	3.51	56.62	3.34	19.84	3.71	No	Yes
GP08	61.38	11.68	47.73	6.57	14.43	3.73	No	Yes
GP09	54.53	1.74	59.10	9.21	13.61	1.37	No	Yes
GP10	51.99	1.93	41.03	6.50	15.22	13.37	No	Yes
Min	**41.15**	**1.74**	**41.03**	**2.52**	**13.61**	**1.00**		
Max	**61.38**	**11.68**	**90.02**	**9.21**	**30.43**	**13.37**		
Av	**51.29**		**62.05**		**20.22**			
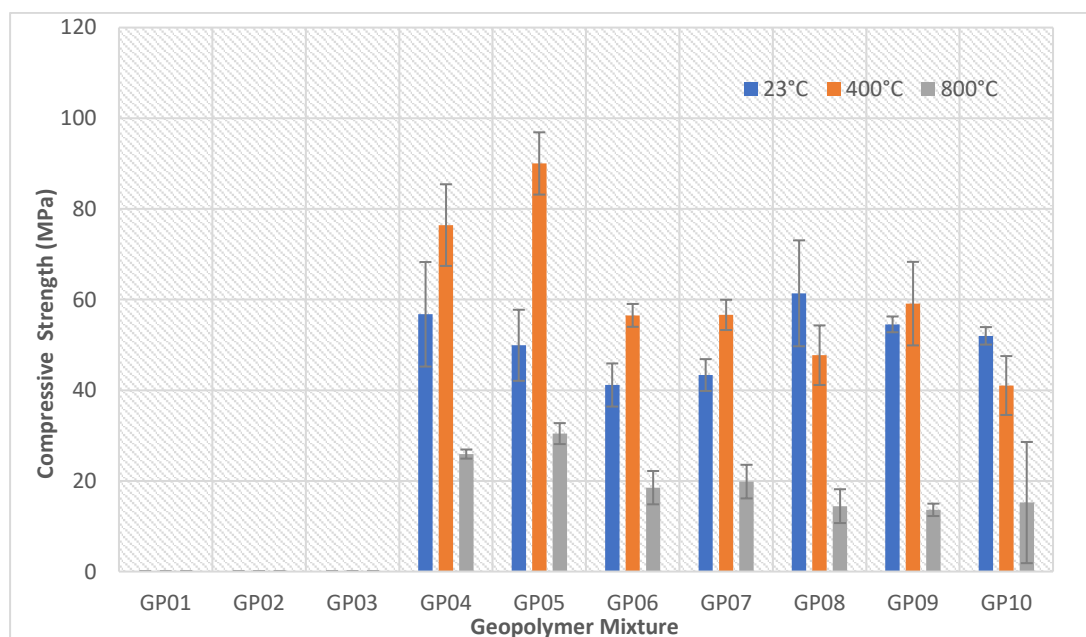
Figure 4.28 – Graph of compressive strength for 25mm Gladstone/Callide FA GP cubes.

Significantly, majority of the Gladstone FA specimens have higher initial strengths compared to Gladstone/Callide FA specimens which could be explained through the differences in particle size. Gladstone FA has a fineness of 86.136% passing the 45μm sieve compared to 80.488% of the Gladstone/Callide FA. This means that the number of particles passing each

sieve is higher for the Gladstone FA or in other words Gladstone FA has finer particles compared to Gladstone/Callide FA. Wijaya and Ekaputri (2017) reports that finer particles have a higher rate of dissolution during the geopolymerisation process thus producing higher compressive strengths which is evidence of obtaining higher strength readings for the Gladstone FA specimens. Figure 4.29 shows the comparison between the two types of FA GP cubes.
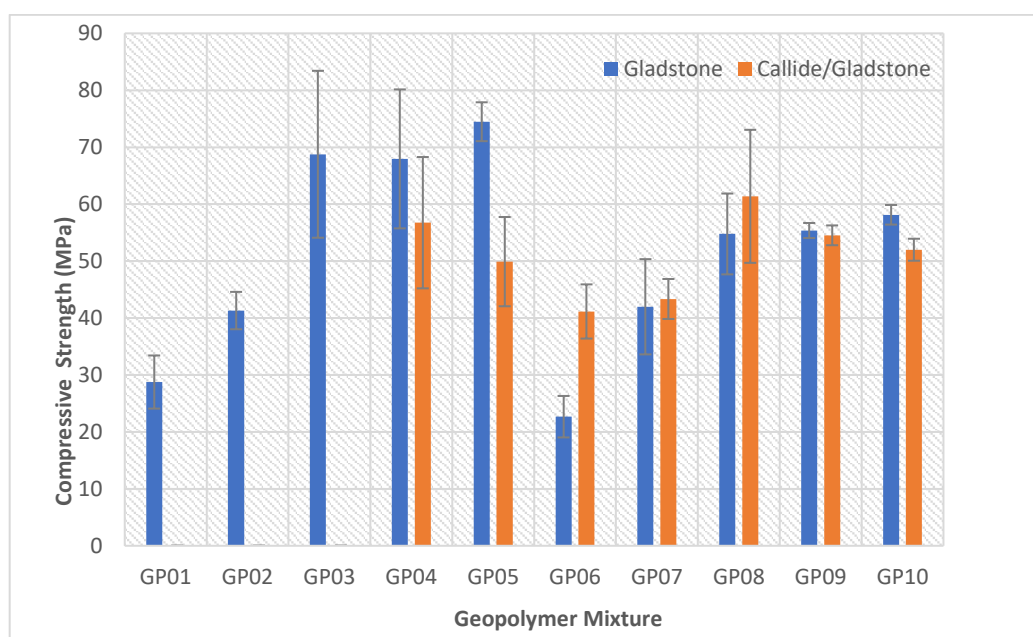
Figure 4.29 – Comparison of initial compressive strength between Gladstone and Gladstone/Callide 25mm FA GP cubes.

It can be easily noted from the graph that four out of seven mixtures produced higher initial strengths from the Gladstone FA GP specimens, whereas GP 06, 07 and 08 produced higher strengths from the Gladstone/Callide FA GP specimens. Additionally, it can be assumed that GP 01, 02 and 03 would have followed similar trends had they been casted. The key point to be noted is that specimens which produced higher strengths consisted of a Na_2SiO_3/NaOH ratio of ≤ 1.75. This seconds the findings of Lee and Van Deventer (2002b) who, as mentioned before, reported that after a Na_2SiO_3/NaOH ratio of 1.75, the excessive silicate will retard the geopolymerisation process resulting in lower strength readings.

Though initial strength results proved Gladstone FA to be the better of the two materials for a majority of the mixtures, 25mm Gladstone/Callide FA GP specimens displayed excellent residual strength results at 400°C, with a striking maximum strength of 90.02 MPa (Table 4.14). This was the highest recorded strength amongst all the GP specimens. Furthermore, this recorded strength exceeded the maximum strength of Gladstone FA GP specimens at 400°C which was limited to 74.14 MPa.

Similar results have been reported by Bakharev (2006), Sarker et al. (2014) and Zulkifly et al. (2017) who reported that low strength GPs produce higher thermal performance whereas high strength GPs produce low residual strengths. This condition is closely attributed to the chemical compositions and the microstructural changes at elevated temperatures.

Gladstone/Callide has a higher level of silicon and aluminium compared to Gladstone FA which play a major role in the geopolymerisation process forming the gel layer on the surface of the particles. As temperature increases sintering of this gel phase is reported which produces high internal strengths, better homogeneity and a denser microstructure. Furthermore, higher contents of silicon and aluminium result in higher conductivity. This allows a better heat flow through the matrix which result in lower thermal gradients between the inside and outside of the specimen. And hence, the ability to produce higher bearing capacities. Similar deductions have been made by Sarker et al. (2014) and Shaikh and Vimonsatit (2015).

At elevated temperatures, low levels of Si-Al minerals can result in poor bonding properties and a higher thermal incompatibility within the specimen due to reduced conductivity. This can result in thermal cracking which can in turn produce poorer strengths. Additionally, this condition can be explained further in terms of ductility which was reported by Pan et al. (2009) and Guerrieri and Sanjayan (2010). Specimens having low initial strengths were observed to display high levels of ductility, thus, improving strength and vice versa for brittle samples. However, the ductility or brittleness which effects the gain/loss in strength after temperature exposure was reported to be governed

by the dominant process of two parallel processes, further geopolymerisation of unreacted FA particles with increasing ductility, thus increasing strength and thermal incompatibility within the matrix with decreasing ductility, thus decreasing strength (see section 2.3.5.).

After an exposure of 800°C the highest strength amongst the 25mm Gladstone/Callide FA specimens was 30.43 MPa (Table 4.14) which was a loss of approximately 40% compared to the initial strength of the same specimen. It must be noted that the highest residual strength at both 400°C and 800°C exposure was recorded from GP05 which had an alkaline solution to FA ratio of 0.4 and more importantly, the highest Na_2SiO_3/NaOH ratio (2.5).

Table 4.15 and Figure 4.30 show data of the compressive strengths of the 50mm Gladstone/Callide FA GP specimens.

Table 4.15 – Average compressive strengths. Gladstone/Callide FA GP paste 50mm cubes

Mix	23°C	23°C STDEV	400°C	400°C STDEV	800°C	800°C STDEV	Thermal Cracking 400°C?	Thermal Cracking 800°C?
GP04	48.53	6.40	57.33	6.48	31.72	1.32	Yes	Yes
GP05	57.87	7.72	56.40	1.44	36.85	4.70	Yes	Yes
GP06	31.46	1.46	25.27	12.34	9.24	1.12	Yes	Yes
GP07	40.68	3.19	38.45	1.76	0.00	0.00	Yes	Yes
GP08	58.53	3.23	49.73	0.61	18.47	1.05	Yes	Yes
GP09	55.07	3.00	52.67	3.45	20.36	2.62	Yes	Yes
GP10	55.87	6.77	42.53	3.00	22.36	0.08	Yes	Yes
Min	**31.46**	**1.46**	**25.27**	**0.61**	**9.24**	**0.08**		
Max	**58.53**	**7.72**	**57.33**	**12.34**	**36.85**	**4.70**		
Av	**48.67**		**45.00**		**23.14**			

The 50mm Gladstone/Callide FA GP specimens, a maximum initial strength 58.53 MPa was achieved from GP08, with an average initial strength of 48.67 MPa. Furthermore, the 50mm Gladstone/Callide specimens recorded a maximum residual strength of 57.33MPa at 400ºC exposure. Residual strengths at 800ºC reached a maximum of 36.85MPa from GP05 with an average of 23.14 MPa.
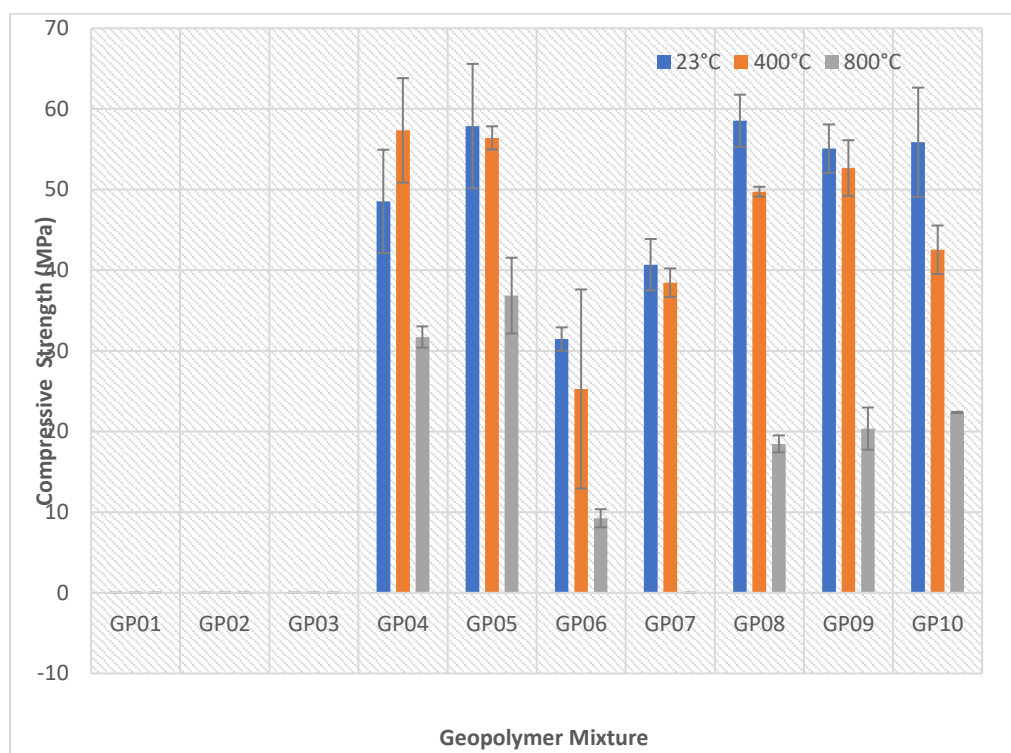
Figure 4.30 – Graph of compressive strength for sealed 50mm Gladstone/Callide FA GP cubes.

Given in Table 4.16 is a comparison of compressive and residual strength between the 25mm and 50mm Gladstone/Callide FA GP specimens.

Apart from GP04, all other 50mm specimens displayed strength losses at 400ºC and all specimens displayed strength losses at 800ºC. This was quite different to the 25mm Gladstone/Callide FA GP specimens which displayed both strength losses as well as strength gains. Moreover, at 400ºC, a loss of approximately 2.5% was recorded from the 50mm specimens as oppose to a strength gain of approximately 80% recorded from the same mixture (GP05) of the 25mm specimens.

Table 4.16 – Comparison of the average Compressive Strength between 25 mm & 50mm Gladstone/Callide FA GP pastes specimens

Gladstone/Callide GP (Oven Bag)							
Comparison Average Compressive Strengths - 25 mm & 50mm (MPa)							
Mixture	Size	23°C	23°C STDEV	400°C	400°C STDEV	800°C	800°C STDEV
GP04	25	56.75	11.53	76.43	9.01	25.91	1.00
	50	48.53	6.40	57.33	6.48	31.72	1.32
GP05	25	49.91	7.84	90.02	6.87	30.43	2.31
	50	57.87	7.72	56.40	1.44	36.85	4.70
GP06	25	41.15	4.76	56.51	2.52	18.51	3.68
	50	31.46	1.46	25.27	12.34	9.24	1.12
GP07	25	43.35	3.51	56.62	3.34	19.84	3.71
	50	40.68	3.19	38.45	1.76	-	-
GP08	25	61.38	11.68	47.73	6.57	14.43	3.73
	50	58.53	3.23	49.73	0.61	18.47	1.05
GP09	25	54.53	1.74	59.10	9.21	13.61	1.37
	50	55.07	3.00	52.67	3.45	20.36	2.62
GP10	25	51.99	1.93	41.03	6.50	15.22	13.37
	50	55.87	6.77	42.53	3.00	22.36	0.08
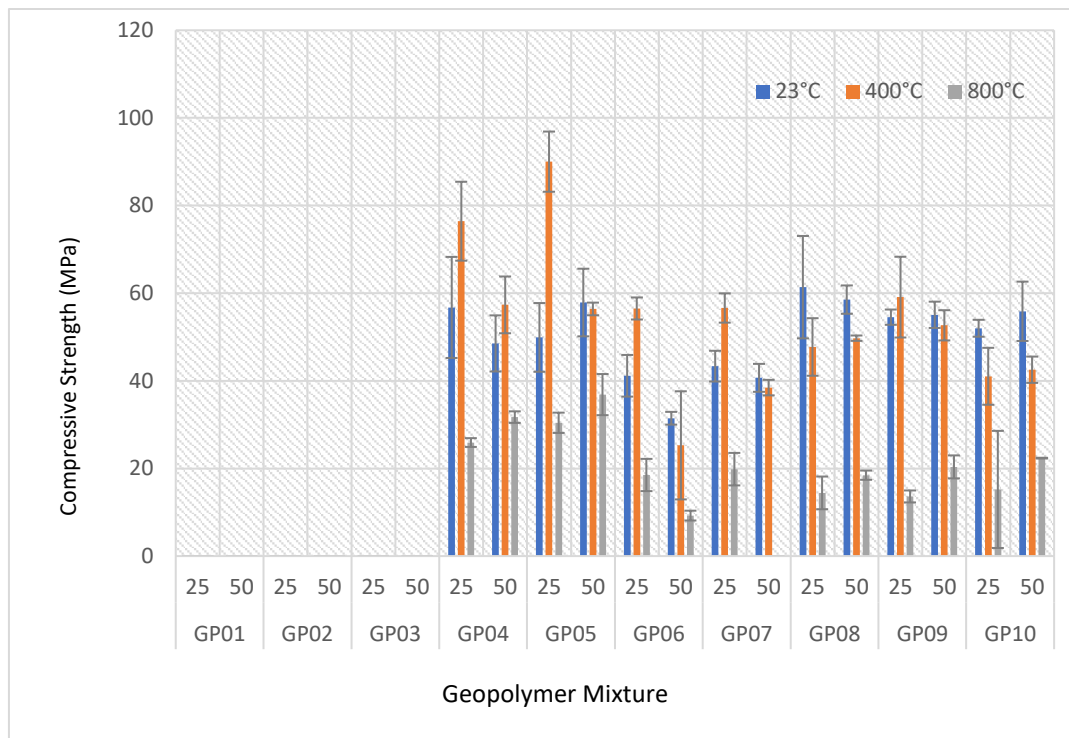
Figure 4.31 – Comparison of strength-25mm and 50mm Gladstone/Callide FA GP cubes

Similar to the Gladstone FA GP specimens, this condition can be due to higher differences in thermal gradients between the core and outer surface which resulted in a significant internal cracking. Additionally, referring Tables 4.14

and 4.15 it is evident that thermal cracking occurred in all 50mm samples at both 400°C and 800°C due to the high thermal stresses built up within the specimen. These thermal stresses can hinder the sintering process which and the ductility of the material which, as reported by Pan et al. (2009) can result in an increase in strength after temperature exposure. In this case, it can be assumed that the in the larger specimens, the thermal incompatibility within the matrix overcame further geopolymerisation of the unreacted FA particles, thus, resulting in strength losses (Pan et al., 2009).

4.5. Thermal performance and strength of RPC

RPC samples experienced explosive spalling conditions when exposed to elevated temperature levels. The specimens were noted to display explosive spalling conditions when the furnace temperature reached approximately 360°C. Figure 4.32 shows the RPC samples before exposure to elevated temperatures and Figure 4.33 shows the explosive spalling conditions which occur inside the furnace.

Figure 4.32 – RPC specimens

Figure 4.33 – RPC specimens after elevated temperature exposure

Tabulated and graphical data on the average compressive strengths of the 25mm RPC specimens are presented in Table 4.17 and Figure 4.34, respectively.

Table 4.17 – Average compressive strengths RPC 25mm cubes

Mixture	Compressive strength (MPa)	Average Compressive strength (MPa)	STDEV	400°C	800°C
RPC01a (25°C)	95.34	85.98	11.11	-	-
	73.70			-	-
	88.90			-	-
RPC01a (75°C)	138.74	140.66	12.72	-	-
	129.01			-	-
	154.22			-	-
RPC01b (75°C)	80.75	95.10	31.67	-	-
	131.41			-	-
	73.14			-	-
RPC02 (75°C)	136.78	108.15	31.17	-	-
	74.94			-	-
	112.72			-	-
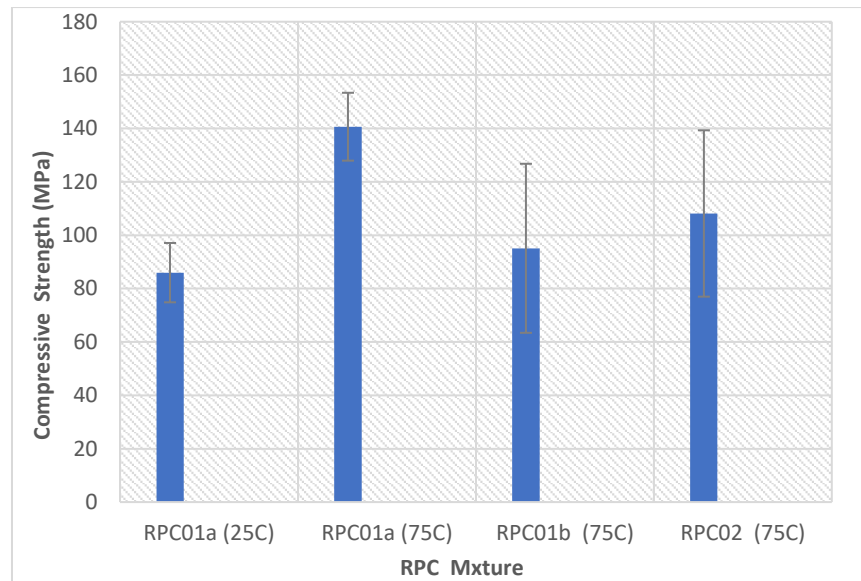
Figure 4.34 – Graph of compressive strength for RPC cubes.

All initial compressive strength results of RPC specimens were obtained at 7 days testing. RPC01-a specimens which were exposed to water curing conditions at 20°C displayed an average strength of 85.98 MPa having a highest reading of 95.34 MPa and lowest of 73.70 MPa. Specimens exposed to 75°C water curing conditions displayed an average strength of 140.66 MPa with a highest of 154.22 MPa and a lowest of 129.01 MPa. Which proved water curing conditions at 75°C to be the better condition of the two.

Hiremath and Yaragal (2017) reported similar declinations in strength when RPC samples were cured under normal water conditions. They reported that under normal water curing conditions the pozzolanic activity is slow and this, together with the formation of ettringite can hinder the rate of hydration thus, reducing the rate of strength development. Similar results have been reported by Menefy (2007) and Khadiranaikar and Muranal (2012) where it was reported that the insufficient supply of heated water, a lesser percentage of C-S-H gel is produced which leads to reduced strength.

When subjected to elevated temperature water curing conditions the hydrothermal conditions have the ability to rapidly increase the pozzolonic reaction of the silica fumes thus, increasing the amount of hydrated compounds occurring through the formation of secondary hydrated products

Menefy (2007). Courtial et al. (2013) also stated that when RPC is cured under elevated temperature conditions the rate of production of secondary hydrated products from reactive silica fumes and quartz powder can increase. This can increase the bond between the cement paste and the aggregate particles and in turn enhance the internal strength.

Menefy (2007) and Hiremath and Yaragal (2017) reported that the continuous supply of moisture result in a higher consumption of portlandites (transforming portlandites to tobermorites) which further result in a higher degree of hydrated products. This higher degree of hydrated products acts as an inert filler which fills in the voids and gel pores within the matrix, hence, producing a denser microstructure with a better interlocking structure and fewer capillary pores. The study conducted by Hiremath and Yaragal (2017) further reported that the results obtained at 28 days under normal water curing can be obtained within 24 hours of hot water curing due to the continuous development of C-S-H chains.

Due to higher results obtained after exposing the specimens to water curing conditions at 75°C, RPC01-b and RPC 02 specimens were not exposed to water curing conditions at 20°C.

The only difference between RPC 01-a and RPC 01-b was an extra 2ml superplasticizer being added in to RPC 01-b. This resulted in an average compressive strength drop of approximately 32% from the RPC 01-b specimens when cured under the same conditions. An average compressive strength of 95.10 MPa achieved from the RPC01-b specimens. Mostofinejad et al. (2016) reported that the microstructure of the RPC can be drastically weakened with the excess dosage of superplasticizer (because of the formation of spherical pores). This could be a possible reason behind the reductions in strength between RPC 01-a and RPC 01-b.

As mentioned before, RPC specimens suffered explosive spalling conditions inside the furnace itself upon reaching a temperature of around 360°C. Hence, no residual strength results could be obtained from the RPC specimens.

Similar trends have been reported by Liu et al. (2010). Preliminary testing done by Ju et al. (2016) found that RPC specimens burst in to a pile of small debris at approximately 380°C. As mentioned before, the RPC specimens have a highly dense microstructure. As the temperature increases the built-up vapour, formed through the evaporation of water molecules, release pressure (pore pressure) within the specimens due to limited escape routes. Concurrently, as temperature increase, the thermal gradients between the outside and the inside of the specimens increases within a very short period. At ambient temperatures of about 380°C, the centre temperature would be about 240°C-250°C. This increasing pore pressure and thermal stresses exceed the tensile strength and cause the specimens to burst. In addition to these two simultaneously occurring conditions, (Ju et al., 2011) reports that above 200°C, the vibrational energy within the solid RPC specimens increase which amplifies the vibrational amplitude causing volume expansions thus, inducing cracks.

Opposing results were reported from Liu and Huang (2009) who found that RPC specimens incorporation no fibre particles exhibited higher fire endurance compared to both normal strength concretes and high performance concretes with RPC specimens displaying no spalling conditions until around 790°C. However, it must be noted that the 28-day compressive strength of the RPC specimens reached only 75 MPa, which, in theory, cannot be considered as RPC.

It must be noted that all strength readings recorded in this research were at 7days which would generally be around 65–70% of full strength. Hence, full average strengths of over 150 MPa can be expected at 28 days.

4.6. Thermal performance and strength of RPGC

RPGC specimens were observed to behave exceptionally well after exposure to high temperatures. No cracking was witnessed from any of the specimens after exposure to 400°C. Additionally, apart from RPGC 03 and RPGC 05 specimens which displayed slight cracking, no other specimens displayed any cracking after being exposed to 800°C. (Figures 4.35 and 4.36).

These results are different to both the GP and the RPC specimen results. While the former experienced mild-moderate cracking, the latter experienced explosive spalling conditions. Thermal cracking conditions would have been limited to a minimum due the sintering of the silica which forms a gel between the paste and aggregate particles thus, improving the internal bondage. This eliminates the occurrence of explosive spalling conditions altogether. The reduced thermal cracking of the RPGC specimens when compared to the GP specimens could potentially be due to the higher levels of silica in the RPGC from the silica fumes. This can further increase the sintering of unreacted products and contribute to an increase in ductility. Bakharev (2006) reported that increased SiO_4 tetrahedral units can reduce pore sizes within the concrete making it denser with better internal strength which can reduce cracking.

RPGC 01   RPGC 02   RPGC 03

RPGC 04   RPGC 05   RPGC 06
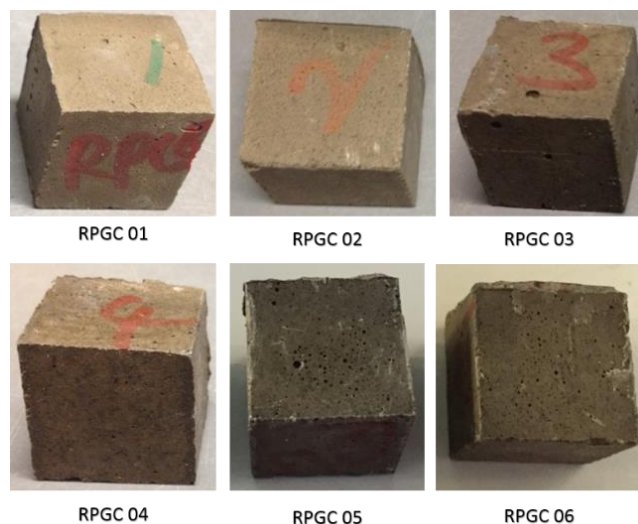
Figure 4.35 – RPGC specimens before temperature exposure
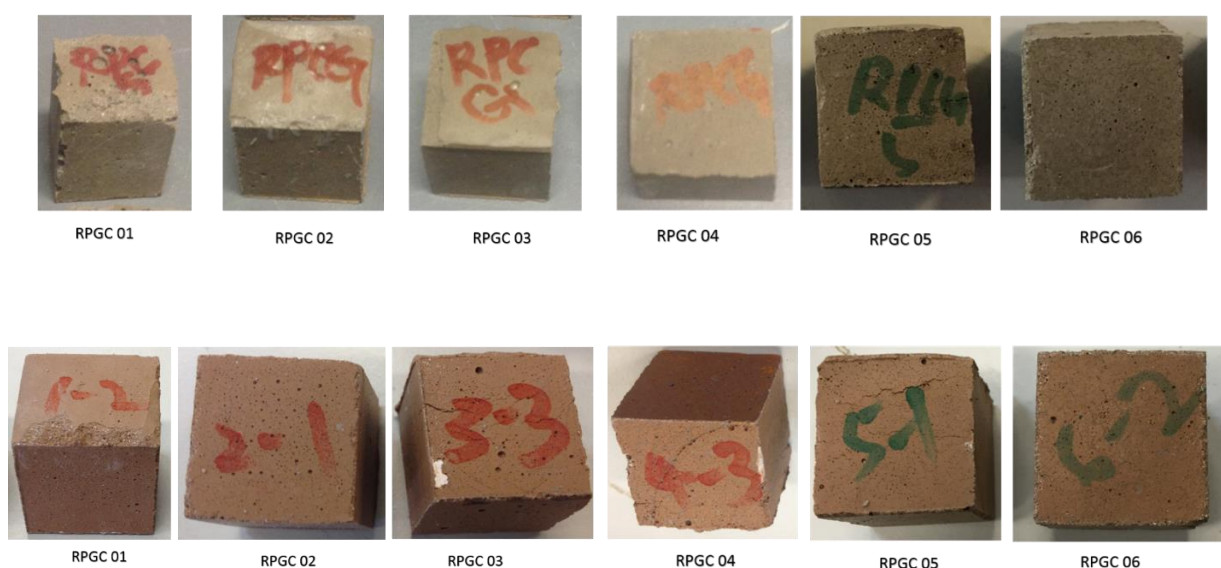
Figure 4.36 – RPGC specimens. Above – After 400ºC exposure, below – After 800ºC exposure

The strength results of the RPGC specimens are given in Table 4.18 and Figure 4.37. Amongst the six RPGC trial and error mixtures, the highest initial strength was recorded from RPGC01 specimens which was 76.25 MPa. All other mixtures were observed to display comparatively lower initial strength readings. The weakest being RPGC 06 specimens producing an average initial strength of 19.55 MPa.

Table 4.18 – Average compressive strengths RPGC 25mm cubes

Mix	23C	23C STDEV	400°C	400°C STDEV	800°C	800°C STDEV	Thermal Cracking 400°C?	Thermal Cracking 800°C?
RPCG01	76.25	3.83	60.58	0.69	50.52	3.58	No	No
RPCG02	64.54	3.53	44.43	3.98	30.58	0.83	No	No
RPCG03	51.37	2.58	36.90	0.68	36.29	3.43	No	Yes
RPCG04	29.47	1.99	20.63	3.54	27.61	3.05	No	No
RPCG05	38.59	0.56	21.67	1.25	14.90	3.02	No	Yes
RPCG06	19.55	0.90	18.34	0.46	14.42	1.31	No	No
Min	**19.55**	**0.56**	**18.34**	**0.46**	**14.42**	**0.83**		
Max	**76.25**	**3.83**	**60.58**	**3.98**	**50.52**	**3.58**		
Av	**46.94**		**35.19**		**29.91**			
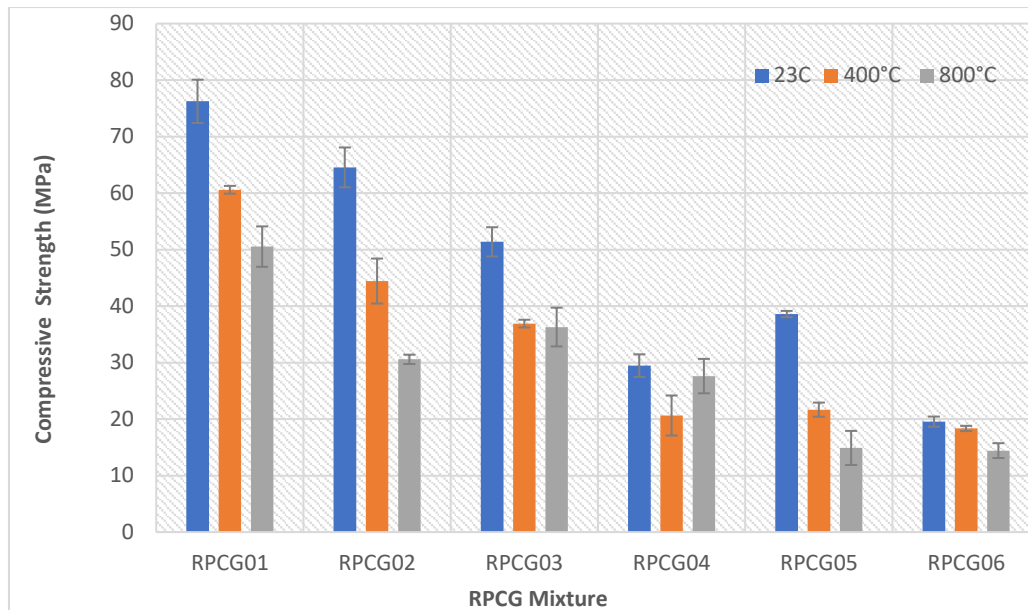
Figure 4.37 – Graph of compressive strength for RPGC cubes.

As given in section 3.3.3, RPGC 01 is a combination of GP05 and RPC01-a which were the highest performing mixtures amongst the Gladstone GP specimens and the RPC specimens. Hence, the achievement of the highest strength resulting from RPGC 01 could have been expected.

When comparing the RPGC specimens, it was observed that increments in the silica flour together with decrements in the alkaline solution to FA resulted in poorer strength readings. The low alkaline solution to FA ratio provides a denser microstructure with reduced porosity and thus, increases the bondage between the paste and the aggregate particles. The high flour content can be advantageous as the silica content in the silica flour can increase the pozzolanic reaction and act as a filler which can further increase internal strength (Morsy et al., 2010).

RPGC specimens produced strengths within the range of 18.34–60.58 MPa at 400°C and 14.42–50.52 MPa at 800°C. The highest residual strength was recorded from RPGC 01 at both 400°C and 800°C with maximum strength drops of approximately 20% and 33% at 400°C and 800°C, respectively. RPGC 06 proved to be the weakest mixture producing the lowest initial and residual strength readings. This condition could also be associated with the

high silica content which provides increased sintering during exposure to elevated temperature levels. Additionally, Sharma and Ahmad (2017) reported that similar to normal concretes, as the liquid to solid ratio increases compressive strength decreases. At higher alkaline solution to FA ratios the specimens are vulnerable to reductions in strength due to the substantial increase in pores which in turn reduce the load bearing capacity of the specimens.

4.7. Mass loss

Mass loss is an important factor in analysing when measuring the performance of a material. Several researchers have deduced a high rate of mass loss upon reaching $150^{\circ}C$ due to the evaporation of moisture, after which the rate reduced and somewhat stabilized (Pan et al., 2009, Mane and Jadhav, 2012, Kong and Sanjayan, 2010, Abdulkareem et al., 2014) . Su et al. (2016) reported that weight loss occurs significantly within the ranges from room temperature to $200^{\circ}C$, due to the escape of free water, and $600^{\circ}C$-$800^{\circ}C$, due to the decomposition of $CaCO_3$.

Table 4.19 gives the scale measurements of the percentage mass loss of non-sealed Gladstone FA GP specimens. 25mm non-sealed Gladstone FA GP 01–08 specimens recorded an average mass loss of up to approximately 10% when subjected to both $400^{\circ}C$ and $800^{\circ}C$. However, specimens 09 and 10 resulted in higher losses of approximately 18% when subjected to $400^{\circ}C$ and $800^{\circ}C$.

Table 4.19 – Scale measurements of percentage mass loss
25mm non-sealed Gladstone FA GP cubes

Sample ID	400°C	400°C STDEV	800°C	800°C STDEV
GP01	5.19	0.05	6.71	0.06
GP02	6.56	0.31	7.41	0.37
GP03	7.02	0.15	7.66	0.08
GP04	8.41	0.79	9.41	0.10
GP05	8.57	0.16	9.33	0.16
GP06	6.55	0.88	7.57	0.02
GP07	7.03	0.28	7.91	0.25
GP08	7.21	0.02	8.19	0.16
GP09	18.18	0.17	18.24	0.23
GP10	18.13	0.11	18.50	0.32
Min	**5.19**	**0.02**	**6.71**	**0.02**
Max	**18.18**	**0.39**	**18.50**	**0.37**
Average	**9.55**	**0.17**	**10.09**	**0.17**

Due to the higher fluid content in mixtures 06-10, a larger loss of mass was recorded compared to mixtures 01-05. This is understandable as the high fluid content makes up a larger portion of the specimens hence, resulting in higher losses. Additionally, with increasing Na_2SiO_3/NaOH ratios an increase in mass loss was recorded. Furthermore, it has been reported that after a Na_2SiO_3/NaOH ratio of 1.75, the silicate in the mixture retards the geopolymerisation process and reduces the bondage between the FA and alkaline solution (Lee and Van Deventer, 2002b). Therefore, a combination of a Na_2SiO_3/NaOH ratio ≥ 1.75 and high alkaline solution to FA ratio of 0.57, a greater loss of mass can be explained.

Table 4.20 shows the percentage mass loss of both TGA (powdered specimens) and scale (25mm cube specimens) measurements of the sealed Gladstone FA GP specimens. Figure 4.38 gives the graph of weight loss vs temperature for the RPGC specimens which clearly indicate step losses upon reaching about 150°C.

Table 4.20 – Percentage mass loss (TGA & Scale results) Sealed Gladstone FA

Gladstone FA GP specimens				
	TGA % mass loss		**Scale % mass loss**	
Sample ID	**400°C**	**800°C**	**400°C**	**800°C**
GP01	6.47	8.45	14.10	15.88
GP02	6.59	8.09	14.61	15.34
GP03	7.16	8.73	14.08	14.86
GP04	6.66	7.78	15.09	15.37
GP05	6.73	7.84	15.08	15.79
GP06	7.89	10.56	22.39	21.68
GP07	8.66	11.76	20.33	20.99
GP08	8.36	10.69	19.27	19.52
GP09	8.64	10.22	19.66	19.31
GP10	7.89	9.65	19.75	20.04
Min	**6.47**	**7.78**	**14.08**	**14.86**
Max	**8.66**	**11.76**	**22.39**	**21.68**
Average	**7.51**	**9.38**	**17.43**	**17.88**

Scale measurements for average mass loss was approximately 17% for the sealed Gladstone FA GP specimens exposed to both 400°C and 800°C. This shows evidence of non-sealed specimens displaying lower losses in mass compared to the sealed specimens of 10% and 17%, respectively. This is due to a large portion of the free water content in the non-sealed samples having already evaporated during initial dehydration process thus reducing the amount of free water readily available for evaporation at elevated temperatures.

TGA specimens produced very much lesser losses with averages of approximately 7.5% and 9.4% for 400°C and 800°C exposure, respectively (Table 4.20). This could be due the severe thermal cracking which may have caused minor corner spalling conditions to occur in the cube specimens, in addition to the loss of chemically bound water.
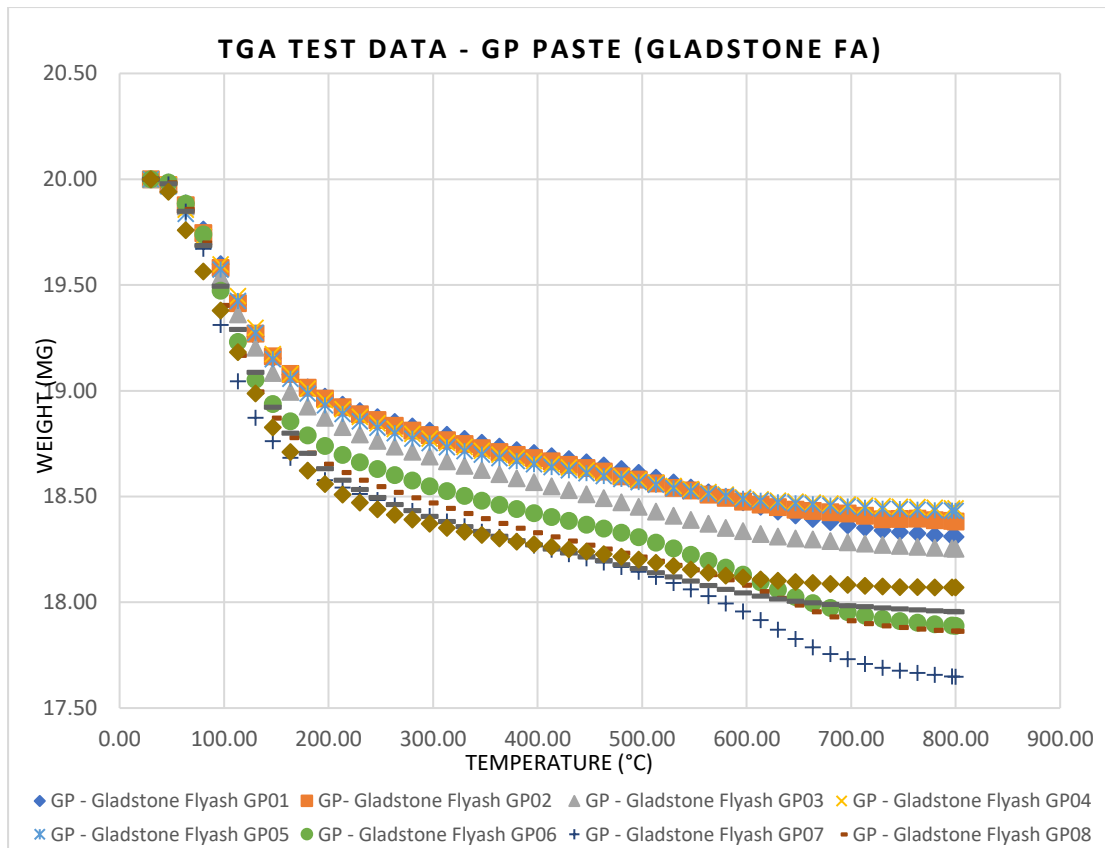
Figure 4.38 – TGA test data, Gladstone FA GP

Table 4.21 gives the scale measurements of the percentage mass loss of sealed 50mm Gladstone FA GP specimens. The 50mm specimens were observed to have average mass losses slightly higher to that of the 25mm.

When comparing the scale measurements of the two sizes, Gladstone FA specimens produced an average loss of 17.43% in 25mm specimens and 20.25% in 50mm specimens at 400°C and 17.88% in 25mm specimens and 21.52% in 50mm specimens at 800°C (Table 4.20 and 4.21). This increment in mass loss of the larger specimens could potentially be due to the occurrence of surface and corner spalling. Due to high differential thermal gradients which created thermal incompatibility within the specimens, the larger samples displayed a comparatively higher degree of thermal cracking and thus, a breaking down of surface layers. As TGA uses powdered samples, spalling is an irrelevant condition to consider when evaluating TGA results.

Table 4.21 – Scale measurements of percentage mass loss
50mm sealed Gladstone FA GP cubes

Percentage mass loss – 50mm Gladstone FA GP				
Sample ID	400°C	400°C STDEV	800°C	800°C STDEV
GP01	18.87	0.09	18.97	0.07
GP02	18.02	0.04	18.97	0.02
GP05	16.61	0.08	17.00	0.07
GP06	23.99	0.30	24.47	0.06
GP07	21.53	0.35	23.13	0.15
GP08	17.96	0.17	21.52	0.76
GP09	22.45	0.05	24.28	0.08
GP10	22.58	0.03	23.83	0.09
Min	**16.61**	**0.03**	**17.00**	**0.02**
Max	**23.99**	**0.35**	**24.47**	**0.76**
Average	**20.25**	**0.14**	**21.52**	**0.16**

Table 4.22 show the percentage mass loss of both TGA (powdered specimens) and scale (25mm cube specimens) measurements of the sealed Gladstone/Callide FA GP specimens. Figure 4.39 gives the graph of weight loss vs temperature for the RPGC specimens which clearly indicate step losses upon reaching about 150°C.

Table 4.22 –Percentage mass loss (TGA & Scale results)–Gladstone/Callide FA

Gladstone/Callide FA GP Specimens				
	TGA mass loss		**Scale mass loss**	
Sample ID	**400C**	**800C**	**400C**	**800C**
GP04	8.61	11.69	14.63	16.46
GP05	8.69	11.39	14.15	16.13
GP06	10.63	13.50	17.82	19.57
GP07	10.13	12.72	18.21	20.07
GP08	9.56	12.43	18.23	20.66
GP09	10.28	12.95	18.68	20.70
GP10	9.45	12.35	17.27	17.90
Min	**8.61**	**11.39**	**14.15**	**16.13**
Max	**10.63**	**13.50**	**18.68**	**20.70**
Average	**9.62**	**12.43**	**17.00**	**18.79**

Scale measurements of the Gladstone/Callide 25mm specimens resulted in an average mass loss of 17% and 18.79% when exposed to 400ºC and 800ºC, respectively. This was rather similar to the losses recorded from the Gladstone FA which shows evidence that changes in the chemical composition is not being a main governing factor behind loss the mass. Furthermore, similar to the Gladstone specimens, it was also evident that as the alkaline solution to FA ratio increased, the loss of mass also increased which again proved that the loss of moisture is a governing factor behind mass loss. A higher alkaline solution to FA ratio would result in more fluid within the specimens thus resulting in a higher amount of evaporation.

Similar trends to that of the Gladstone specimens were observed when considering the TGA results of the Gladstone/Callide specimens with percentage mass losses of 9.62% and 12.43% at 400ºC and 800ºC exposure, respectively recorded.
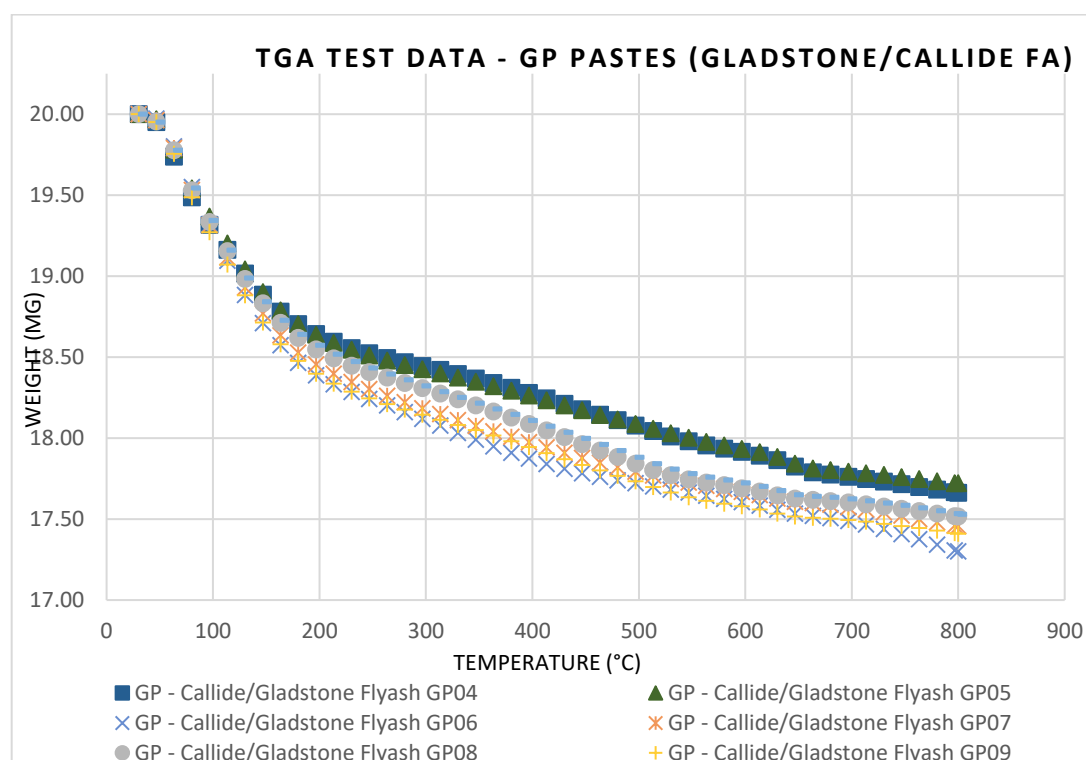
Figure 4.39 – TGA test data, Gladstone/Callide FA GP

Table 4.23 gives the scale measurements of the percentage mass loss of sealed 50mm Gladstone/Callide FA GP specimens. The Gladstone/Callide FA specimens produced an average loss of 17.00% in 25mm specimens and 21.03% in 50mm specimens at 400ºC and 18.79% in 25mm specimens and 23.04% in 50mm specimens at 800ºC. 50mm cubes measurement results are given in Tables 4.30. Similar to the Gladstone FA GP specimens, the thermal incompatibility within the specimens would have caused surface and corner spalling which could potentially be the reason for increased mass loss in the larger specimens.

Table 4.23 – Scale measurements of percentage mass loss
50mm sealed Gladstone/Callide FA GP cubes

Percentage mass loss – 50mm Callide/Gladstone FA GP				
Sample ID	400°C	400°C STDEV	800°C	800°C STDEV
GP04	17.33	0.08	19.81	0.12
GP05	17.32	0.08	19.66	0.12
GP07	23.93	0.07	26.26	1.10
GP08	22.54	0.04	24.37	0.03
GP09	22.45	0.05	24.28	0.08
GP10	22.58	0.03	23.83	0.09
Min	**17.32**	**0.03**	**19.66**	**0.03**
Max	**23.93**	**0.08**	**26.26**	**1.10**
Average	**21.03**	**0.06**	**23.04**	**0.26**

Table 4.24 show the percentage mass loss of both TGA (powdered specimens) and scale (25mm cube specimens) measurements of the sealed RPGC specimens. Figure 4.40 gives the graph of weight loss vs temperature for the RPGC specimens which clearly indicate steep losses upon reaching about 150ºC.

Table 4.24– Percentage mass loss (TGA & Scale results)–RPGC

Percentage mass loss RPGC Specimens				
	TGA		**Scale**	
Sample ID	**400C**	**800C**	**400C**	**800C**
RPGC 01	3.06	3.97	6.75	5.60
RPGC 02	3.75	4.81	8.06	8.07
RPGC 03	4.67	5.90	8.30	8.36
RPGC 04	6.26	7.74	10.13	8.80
RPGC 05	5.00	5.86	9.00	9.03
RPGC 06	5.95	6.64	11.23	11.32
Min	**3.06**	**3.97**	**6.75**	**5.60**
Max	**6.26**	**7.74**	**11.23**	**11.32**
Average	**4.78**	**5.82**	**8.91**	**8.53**

RPGC recorded the lowest percentages in mass loss for TGA and scale measurements compared to both Gladstone and Gladstone/Callide FA GP specimens which were valuable findings (Tables 4.20, 4.22 and 4.24).

Compared to the GP specimens, which are having a higher percentage of water molecules, the RPGC specimens have a comparatively higher percentage of solid particles within the cube specimens. Therefore, after exposure to elevated temperature levels the amount of water molecules available for evaporation is low. Hence, the overall loss of mass is potentially reduced as mass loss is mainly associated with the loss of moisture.

However, similar to the GP specimens, the rate of mass loss was high upon reaching 100°C which gradually decreased afterwards. After about 150°C, this rate stabilized exceptionally well, more so compared to GP. Average drops of 4.78% at 400°C and 5.82% at 800°C were recorded from the TGA with maximum losses of 6.26% and 7.74% and minimum losses of 3.06% and 3.97% at 400°C and 800°C, respectively. Scale measurements recorded an average of 8.91% and 8.53% with maximums of 11.23% and 11.32% and minimums of 6.75% and 5.60% at 400°C and 800°C, respectively.

It is evident from Figure 4.40 that RPGC 01 and RPGC 02 displayed the lowest mass loss percentages. This could be due to the lower alkaline solution to FA ratio in these two samples which reduces the amount of water molecules available for evaporation. Additionally, amongst these two samples (RPGC 01 and RPGC 02), a lower mass loss was recorded from RPGC 01. This could be due to the higher silica flour content which aid in the sintering process of geopolymerisation. Moreover, RPGC 01 cube specimens recorded to be the heaviest amongst all RPGC specimens with a density of 2245kg/m^3. This means that a lower percentage of moisture is available within the specimens for evaporation at elevated temperature levels, and hence, would result in lower losses in mass.

RPGC 04 was observed to have the steepest drop in mass compared to all other RPGC specimens. RPGC 04 has the highest sodium hydroxide content amongst all RPCG specimens together with an alkaline solution to FA ratio of 0.57. This could contribute to the significant percentage loss in mass.
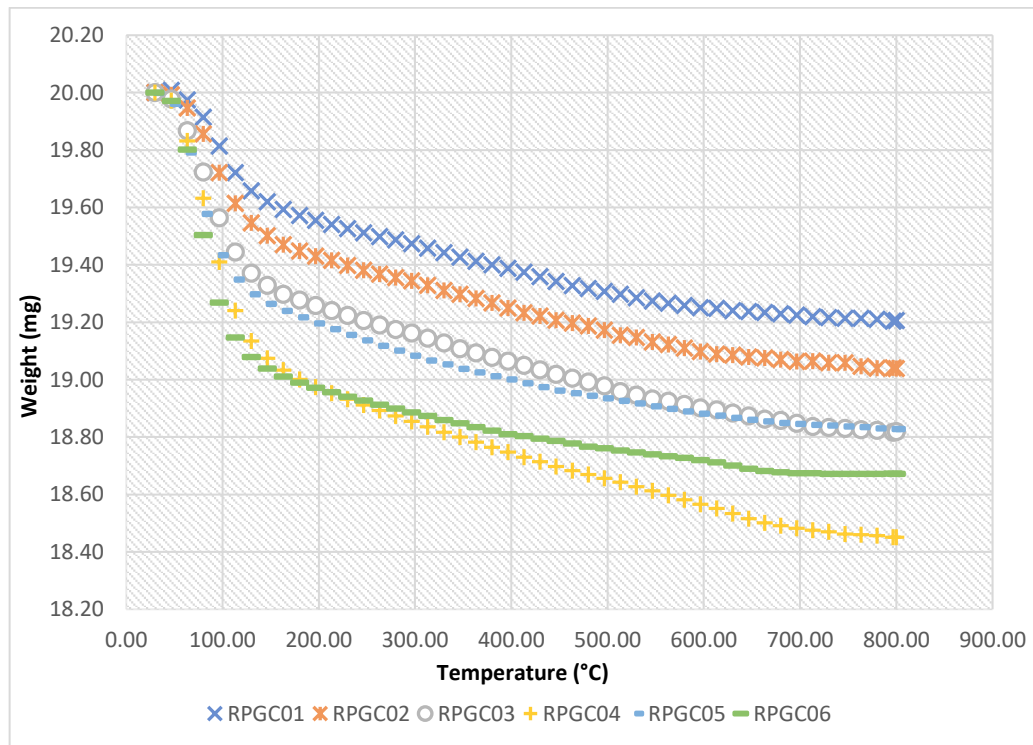
Figure 4.40 – TGA test data, RPGC

Additionally, compared to OPC concretes which continue to have a consistent rate of mass loss up to $650^{\circ}C$ due to the dehydration of $Ca(OH)_2$ (Sarker et al., 2014, Mendes et al., 2008), RPGC have a reducing rate above a temperature of $400^{\circ}C$ which indicate that RPGC specimens have a high storage capacity and thermal stability which helps maintain its structural integrity at high temperatures.

4.8. Summary of Results

Given in Table 4.25 is a summarisation and classification of the performance of GP, RPC and RPGC specimens which were evaluated in this study.

Table 4.25 – Summary and classification table of GP, RPC and RPGC specimens

Parameter	Density	Workability	Initial setting	Compressive strength	Residual strength After 400ºC	Residual strength After 800ºC	Thermal cracking	Mass loss Scale After 400ºC	Mass loss Scale After 800ºC	TGA	Conclusion
Non-sealed Gladstone GP	Minimum of 2145 kg/m³ and a maximum of 2396 kg/m³ was obtained	Slump flow values within the range of 280–335 mm were obtained	Lasted for over 30 minutes in liquid state	25% less strength compared to the sealed Gladstone specimens	Average of 27.81 MPa	Average of 18.43 MPa	Underwent severe thermal cracking where specimens were observed to split open	A mass loss of approximately 10% was reached		No data was obtained	Comparatively poor initial strengths. Severe cracking caused large reductions in strength
Sealed Gladstone GP 25mm				Strength results within the range of 22.67-74.48 MPa were obtained	Minimum of 42.78 MPa and a maximum of 74.14 MPa was obtained	Minimum of 24.39 MPa and a maximum of 48.05 MPa was obtained	No thermal cracking after 400ºC and mild thermal cracking in the GP06-10 specimens after 800ºC exposure	A mass loss of approximately 17% was reached		Average losses of approximately 7.5% and 9.4% were obtained for 400℃ and 800℃ exposures	High initial strength and low losses in strength after exposure to 400ºC. Low thermal cracking with non at 400ºC.

Sealed Gladstone GP 50mm				Strength results reached a maximum initial strength of 63.87 MP	Minimum of 1.2.13 MPa and maximum of 65.20 MPa was obtained	Minimum of 5.75 MPa and a maximum of 34.31 MPa was obtained	No thermal cracking after 400ᵒC and moderate thermal cracking in all specimens after 800ᵒC exposure	An average loss of 20.25% was recorded	An average loss of 21.52% was recorded		High in losses in strength was recorded compared to 25 mm specimens. Majority displayed high thermal cracking
Sealed Gladstone/Call ide GP 25mm	Minimum of 1870 kg/m³ and a maximum of 2059 kg/m³ was obtained	Slump flow values within the range of 232.5–337.5 mm were obtained	GP 01, 02 and 03 set within 2-5 minutes	Achieved a maximum initial strength of 61.38 MPa from GP08	Achieved the highest residual strength result amongst all others in the study with a maximum strength of 90.02 MPa	Achieved a maximum strength of 30.43 MPa	No thermal cracking after 400ᵒC and moderate thermal cracking in all specimens after 800ᵒC exposure	An average mass loss of 17% was obtained	An average mass loss of 18.79% was obtained	Average losses of approximat ely 9.62% and 12.43% were obtained for 400℃ and 800℃ exposure	Though initial strength was not as high as compared to Gladstone specimens, very high residual strength was recorded at 400ᵒC. The highest amongst all others

Sealed Gladstone/Call ide GP 50mm				Achieved a maximum initial strength of 58.53 MPa from GP08	Achieved a maximum strength of 57.33 MPa and a minimum of 25.27 MPa	Achieved a maximum strength of 36.85 MPa and a minimum of 9.24 MPa	No thermal cracking after 400°C and sever thermal cracking with splitting open of specimens after 800°C exposure	An average loss of 21.03% was recorded	An average loss of 23.04% was recorded		Residual strength readings were low compared to the 25mm specimens with highly severe thermal cracking at high temperature levels.
RPC	Values of 2546kg/m3, 2715 kg/m³ and 2752 kg/m³ was obtained	Slump flow values of only 111–132.5mm were obtained	Though the mixtures were highly vicious compared to the Gladstone paste mixtures, RPC lasted for over 30minutes in liquid state	Achieved the highest strength results in the study with a maximum initial strength of 140.66 MPa	Null results due to explosive spalling conditions.		Explosive spalling conditions occurred in a temperature of about 360°C	Null results due to explosive spalling conditions.			Though the initial strength was high, explosive spalling conditions occurred at high temperatures.

RPGC	Minimum of 2112 kg/m³ and maximum of 2245 kg/m³ was obtained	Slump flow values of 187.5-252mm were obtained	RPGC lasted for over 30minutes in liquid state	Achieved the maximum strength of 76.25 MPa and a minimum of 19.55 MPa, with RPGC 01 achieving the highest strength	Achieved an average strength of 35.19 MPa with a maximum strength of 60.58 MPa from RPGC 01 and a percentage residual strength of 73.77 MPa.	Achieved an average strength of 29.91 MPa with a maximum strength of 50.52 MPa from RPGC 01 and a percentage residual strength of 65.33 MPa.	No thermal cracking after 400°C and mild thermal cracking in RPGC 03 and RPGC 05 specimens after 800°C exposure	An average loss of 8.91% with a maximum of 11.23% and a minimum of 6.75%	An average loss of 8.53% with a maximum of 11.32% and a minimum of 5.60%	An average mass loss of 4.78% was recorded with a maximum loss of 6.26% at 400°C and an average mass loss of 5.82% was recorded with a maximum loss of 7.74%	Achieved the highest initial strength among all GP specimens. Though it did not achieve the highest residual strength reading, RPGC 01 did not crack at all after exposure to high temperatures. Additionally, loss of mass was recorded to be the lowest in the RPGC specimens.

RPGC specimens tested at 24 hours displayed fair strength readings with a highest recording of 76.25 MPa from RPGC01. This is rather similar to the initial strength reading recorded from GP05 with an increase of about 2 MPa, with RPGC 01 being the higher of the two. Higher strengths were expected for the RPGC specimens as RPC alone reached an average of about 140 MPa at 7 days. Abdulkareem et al. (2014) reported similar results with both paste and mortar samples displaying almost identical initial compressive strength readings to those obtained in this study. This is reasonable due to the somewhat similar densities and a high rate of geopolymerisation.

A key point to note however is the strength loss of the RPGC specimens when exposed to elevated temperatures compared to the GP specimens. While Gladstone GP specimens had maximum strength losses of 47% and 84%, RPGC specimens displayed maximum strength losses of 44% and 61% when exposed to 400°C and 800°C, respectively. Though some GP specimens recorded strength gains upon reaching 400°C, high strength losses were witnessed when exposed to 800°C. Whereas, the rate of strength loss reduced significantly for the RPGC specimens after 400°C. The drops in strength for all RPGC specimens can be attributed to the differential thermal expansions of the paste and aggregate which causes thermal incompatibility within the matrix thus, reduces the internal strength. Kong and Sanjayan (2010) studied the effects of aggregate inclusion in class F FA based GP samples and deduced that the thermal incompatibility between the paste and the aggregate particles cause reductions in strength when exposed to elevated temperatures.

However, unlike the GP specimens, none of the RPGC specimens experienced thermal cracking at 400°C, which are positive results. Reductions in strength loss of the RPGC specimens compared to the GP specimens may be attributed to the increased levels of silica in the RPGC mix matrix. Silica fume has a SiO_2 content of 95.5 wt.% which can further increase the homogeneity of the gel layer during the sintering process of unreacted products. And this can also increase the ductility of the concrete matrix thus,

increasing the load bearing capacity at elevated temperatures. Furthermore, majority of the RPGC specimens did not undergo thermal cracking after exposure to 800°C. Bakharev (2006) reported a high increase in the average pore size at 800°C as a key reason behind thermal cracking and hence, rapid deterioration of strength in GPs. Increased SiO_4 tetrahedral; units can reduce pore sizes within the concrete making it denser with better internal strength which in turn can reduce cracking.

When comparing the thermal performance of the RPC and the RPGC, FA has high levels of Si and Al and low levels of calcium unlike OPC. And these low levels of calcium in the FA may be completely consumed for the formation of the C-S-H bonds which coexist in the GP matrix (Dombrowski et al., 2007). As the temperature increases, silicon undergoes sintering which hardens the internal network thus reducing, or in the case of the RPGC specimen, completely eliminating explosive spalling

These can be considered valuable findings giving evidence of the high performance of the RPGC specimens in extreme temperatures compared to the RPC specimens, which underwent explosive spalling, and the GP pastes, which experienced thermal cracking.

In conclusion, this chapter covers the overall performance and discussions of the GP, RPC and RPGC materials. Through the course of this testing and analysis stage it can be deduced that RPGC 01, which is a combination of GP 05 and RPC01-a, is the optimum mix designation to produce a high strength and high fire resistant sustainable material. The mix combination of RPGC 01 given in section 3.3.3 (Table 3.9) produced the highest initial strength reading amongst all GP specimens. Though an ultra-high strength of over 150 MPa was not achievable from the RPGC 01 specimens, it must be noted that RPGC 01 specimens were tested at 24 hours after casting compared to RPC specimens which were tested at 7 days after casting. Additionally, the absences of spalling conditions and minimal thermal cracking makes RPGC 01 a superior and sustainable material.

CHAPTER 05

CONCLUSION AND RECOMMENDATIONS FOR FUTURE WORK

5.1. Conclusion

This research was focused on investigating the performance of a newly developed material called RPGC. Class F (low calcium) FA was used as the source material to completely eliminate the use of cement in the production of this high strength concrete with superior fire resistance properties. RPGC was a combination of the best performing GP paste and RPC mix designations selected through a series of testing. Though several studies have been conducted on GPs and RPCs as separate materials, research gaps were identified on the fire performance of the combination of the two materials, hence no experimental evidence or reports were available on the mechanical properties of RPGCs after exposure to elevated temperatures. Through the course of this study several major conclusions were derived and are presented below.

1. Gladstone FA GPs display higher levels of workability compared to Gladstone/Callide FA GPs regardless of the high level of calcium. This is due to the fineness in particle size which produces a better SF.

2. High calcium FA can account for poor workability conditions despite having a higher alkaline solution to FA ratio.

3. RPC samples produce low workability conditions having an average SF of about 120mm which can only be achieved through long mixing periods of ≥30 minutes in a high-speed machine mixture.

4. RPGC specimens displayed high workability conditions with SF having a highest flow of 252mm and a lowest of 187.5mm. This was somewhat lower

than that of the GP mixtures due to the inclusion of aggregate and higher than that of the RPC mixtures due to the smaller particle size of the FA compared to OPC.

5. Gladstone/Callide FA GP pastes displayed quicker initial setting times compared to all others. This is due to the pH values the mix matrix which can accelerate the setting times of GPs.

6. All GP and RPGC specimens underwent changes in colour from grey to reddish brown after fire exposure due to the high iron content in the FA. Both Gladstone FA GP and RPGC specimens displayed deeper reddish-brown colour changes compared to the Gladstone/Callide FA GP due to the comparatively higher iron contents in the Gladstone FA.

7. Initial surface evaporation has a major effect on the final performance of the GP specimens. This was tested by using sealed and non-sealed specimens exposed to identical dry-oven curing conditions. Non-sealed specimens performed poorly compared to the sealed specimens. Approximately 25% lesser average initial strength readings and 35% and 25% lesser average residual strength readings at 400°C and 800°C respectively, were recorded from the non-sealed specimens, including a comparably higher degree of thermal cracking and splitting.

8. Lower alkaline solution to FA ratios produced better results in both Gladstone and Gladstone/Callide FA GP specimens. This is due to the comparatively denser microstructure which produces a more homogenous material with fewer pores.

9. As the Na_2SiO_3/NaOH ratio increased from 0.5 to 2.5 the initial strength readings also increased, due to the increasing levels of sodium silicate. This increases the SiO_2 to Al_2O_3 ratio and caused acceleration of the geopolymerisation process by inducing the polymerization of leached materials and hence producing high early strength.

10. Majority of Gladstone FA specimens produced higher initial strengths compared to Gladstone/Callide FA specimens, due to the finer particles that

eased the dissolution stage in the geopolymerisation process thus producing higher compressive strengths.

11. Large increments in strength were observed in the Gladstone/Callide FA specimens compared to Gladstone FA after exposure to 400°C. These increments in the Gladstone/Callide specimens was due to higher level of silicon and aluminium which produces better internal strength through a higher degree of sintering at high temperature levels. Silicon and aluminium also provided better conductivity which help reduce the differential thermal gradient thus producing higher strengths. However, after 400°C, losses in strength were recorded with several samples undergoing severe cracking. This is primarily due to the increase in pore pressure causing high stresses at elevated temperatures.

12. Larger GP samples displayed comparatively higher strength losses when exposed to elevated temperatures. This is due to the slow rate of thermal conduction causing higher thermal gradients between the core and surface of the specimen inducing cracking and degrading the strength.

13. RPC specimens cured in hot water at 75°C until testing produced higher results compared to those cured in water at 20°C. This is due to hydrothermal conditions rapid increases in the number of hydrated compounds which produces a denser microstructure with a better interlocking structure.

14. RPC specimens experienced explosive spalling conditions at a temperature of around 360°C due to the limited amount of escape routes for the built-up vapour and the rapidly increasing differential thermal gradients.

15. RPGC specimens tested at 24hours displayed a highest initial strength reading of 76.25 MPa (RPGC01). Though this was only slightly higher than the maximum initial strength reading from GP paste specimens, the strength loss of the RPGC when exposed to elevated temperatures was comparatively low. GP specimens had maximum strength losses of 47%

and 84% whereas RPGC specimens displayed maximum strength losses of 44% and 61% after exposure to 400°C and 800°C respectively.

16. Unlike the RPC specimens, no explosive spalling conditions surfaced in the RPGC specimens with no thermal cracking at 400°C and only one-third of the specimens undergoing thermal cracking at 800°C. This was due to the higher levels of silicon in the FA compared to OPC which hardens the internal network at elevated temperatures thus reducing the risks of explosive spalling.

17. Non-sealed specimens resulted in an average mass loss of approximately 10% compared to the sealed specimens which resulted in an average mass loss of approximately 17% at both 400°C and 800°C. This is primarily due to a large portion of the free water content of the non-sealed samples having already evaporated during initial surface evaporation during the curing process.

18. A high rate of mass loss was recorded for all specimens upon reaching 400°C which reduced afterwards. Complete evaporation of free water is considered to the main cause for the loss of mass which occurs up to temperatures of about 150°C. Slow evaporation of zeolitic water and hydroxyl groups OH after 150°C reduces the rate of mass loss.

19. RPGC specimens recorded the lowest percentage losses in mass amongst all GP specimens. In scale measurements, average losses of 8.91% at 400°C and 8.53% at 800°C were recorded from the RPGC specimens compared to approximately 17-18% of both Gladstone and Gladstone/Callide GP specimens. Mass losses from TGA resulted in average losses of 4.78% at 400°C and 5.82% at 800°C for the RPGC specimens compared to approximately 7.5-12.5% of both Gladstone and Gladstone/Callide GP specimens. This was due to the inclusion of aggregate particles in the mix matrix compared to GP pastes which reduces the amount of free water molecules that is responsible for steep losses in mass.

20. Compared to OPC concretes which continue to have a consistent rate of mass loss, RPGC specimens had large reductions in the rate of mass loss after 400℃ which indicates that RPGC specimens have a high storage capacity and thermal stability.

In conclusion, RPGG 01 showed promising results with the highest initial compressive strength reading of 76.25 MPa recorded at 24-hour testing amongst all Gladstone and Gladstone/Callide based GP specimens and RPGC specimens. Further, although there were no strength gains observed in any of the RPGC specimens at elevated temperature exposure, RPGC 01 displayed excellent resistance to fire with no thermal cracking at both 400°C and 800°C and the lowest percentage mass loss compared to all GP specimens. The highest residual strength at 400°C was recorded from Gladstone/Callide GP 05 with a striking 90.02 MPa (45% gain in strength). Also, the highest residual strength at 800°C was recorded from RPGC01 which reached an average of 50.52 MPa (33.7% loss in strength).

RPGC01 displayed high workability conditions with an average slump flow of approximately 190mm which falls in line with the requirements of ASTM C230-Standard specification for flow table for the use in testing hydraulic cement. RPC, on the other hand, displayed excellent initial strength readings with a highest average strength of approximately 130 MPa at 7-day testing, but unfortunately displayed explosive spalling conditions where specimens were observed to shatter into pieces when exposed to elevated temperature levels of about 360°C.

5.2.   Recommendations for future work

Given below are several potential areas for future research work which are identified through the course of this research project.

1. To date there are limited studies conducted on the development of RPGC. This particular study is limited to the investigation of GP paste and micro sized particles. Hence, it is of vital importance to broaden the scope of the study to using GP paste mixed RPGC specimens with the inclusion of steel, glass or natural fibres for the enhancement of strength.

2. All RPGC testing in this study is conducted at 24 hours which should be broadened to 7 or 28 days to fully understand the long-term changes in RPGCs.

3. The fire performance RPGC should be further investigated using potassium-based activators and different source materials such as slag, metakaolin and class C FA.

4. Extensive research needs to be carried on larger specimens or structural elements such as beams, columns and/or slabs to deduce the behaviour of RPGC when exposed to simultaneous heating and loading conditions.

REFERENCES

ABDULKAREEM, O. A., AL BAKRI, A. M., KAMARUDIN, H., NIZAR, I. K. & ALA'EDDIN, A. S. 2014. Effects of elevated temperatures on the thermal behavior and mechanical performance of fly ash geopolymer paste, mortar and lightweight concrete. *Construction and building materials,* 50**,** 377-387.

AHMARUZZAMAN, M. 2010. A review on the utilization of fly ash. *Progress in energy and combustion science,* 36**,** 327-363.

AITCIN, P.-C., LACHEMI, M., ADELINE, R. & RICHARD, P. 1998. The Sherbrooke reactive powder concrete footbridge. *Structural Engineering International,* 8**,** 140-144.

AL BAKRI, A. M., KAMARUDIN, H., OMAR, A., NORAZIAN, M., RUZAIDI, C. & RAFIZA, A. 2011. The effect of alkaline activator ratio on the compressive strength of fly ash-based geopolymers. *Australian Journal of Basic and Applied Sciences,* 5**,** 1916-1922.

ALDRED, J. & DAY, J. 2012a. The data available suggest that geopolymer concretes in general including this particular. *37th Conference on Our World in Concrete & Structures.*

ALDRED, J. & DAY, J. 2012b. IS GEOPOLYMER CONCRETE A SUITABLE ALTERNATIVE TO TRADITIONAL CONCRETE? *37th Conference on Our World in Concrete & Structures.*

ALI, A. M., SANJAYAN, J. & GUERRIERI, M. 2017. Performance of geopolymer high strength concrete wall panels and cylinders when exposed to a hydrocarbon fire. *Construction and Building Materials,* 137**,** 195-207.

ALI, F., CONNOLLY, R. & SULLIVAN, P. 1997. Spalling of high strength concrete at elevated temperatures. *Journal of Applied Fire Science,* 6**,** 3-14.

ALI, M. & ZURISMAN, A. 2015. *Performance of geopolymer concrete in fire.* Swinburne University of Technology.

ANAND, S., VRAT, P. & DAHIYA, R. 2006. Application of a system dynamics approach for assessment and mitigation of CO 2 emissions from the cement industry. *Journal of environmental management,* 79**,** 383-398.

ANDERBERG, Y. Spalling phenomena of HPC and OC. NIST Workshop on Fire Performance of High Strength Concrete in Gaithersburg, 1997. 69-73.

ASSOCIATION, A. C. A. 2017. Coal Ash Recycling Reaches Record 56 Percent Amid Shifting Production and Use Patterns.

ASTM 2008. ASTM C230 / C230M-08 Standard Specification for Flow Table for Use in Tests of Hydraulic Cement,. *ASTM International, West Conshohocken, PA,.*

ASTM, C. 618-03. Standard specification for coal fly ash and raw or calcined natural pozzolan for use as a mineral admixture in Portland cement concrete. American Society for Testing and Materials, 2003.

ASTM, E. 1999. 119, Standard Test Methods for Fire Tests of Building Construction and Materials. *1995 Annual Book of ASTM Standards,* 4**,** 436.

BAKHAREV, T. 2005. Geopolymeric materials prepared using Class F fly ash and elevated temperature curing. *Cement and concrete research,* 35**,** 1224-1232.

BAKHAREV, T. 2006. Thermal behaviour of geopolymers prepared using class F fly ash and elevated temperature curing. *Cement and Concrete Research,* 36**,** 1134-1147.

BARBOSA, V. F. & MACKENZIE, K. J. 2003. Thermal behaviour of inorganic geopolymers and composites derived from sodium polysialate. *Materials Research Bulletin,* 38**,** 319-331.

BARBOUR, R. L. 1991. Synthetic class C fly ash and use thereof as partial cement replacement in general purpose concrete. Google Patents.

BAŽANT, Z. P. & CHERN, J.-C. 1987. Stress-induced thermal and shrinkage strains in concrete. *Journal of engineering mechanics,* 113**,** 1493-1511.

BEEBY, A. W. & NARAYANAN, R. 2005. *Designers' Guide to EN 1992-1-1 and EN 1992-1-2. Eurocode 2: Design of Concrete Structures: General Rules and Rules for Buildings and Structural Fire Design*, Thomas Telford.

BEHLOUL, M. & LEE, K. 2003. Ductal® Seonyu footbridge. *Structural Concrete,* 4**,** 195-201.

BONDAR, D., LYNSDALE, C. J., MILESTONE, N. B., HASSANI, N. & RAMEZANIANPOUR, A. A. 2010. Geopolymer Cement from Alkali-Activated Natural Pozzolans: Effect of Addition of Minerals. *Second International Conference on Sustainable Construction Materials and Technologies.*

BONNEAU, O., LACHEMI, M., DALLAIRE, E., DUGAT, J. & AITCIN, P.-C. 1997a. Mechanical properties and durability of two industrial reactive powder concretes. *Materials Journal,* 94**,** 286-290.

BONNEAU, O., LACHEMI, M., DALLAIRE, E., DUGAT, J. & AÏTCIN, P.-C. 1997b. Mechanical properties and durability of two industrial reactive powder concretes. *ACI Materials journal,* 94**,** 286-290.

BONNEAU, O., POULIN, C., DUGAT, M. & TCIN, P.-C. A. 1996. Reactive powder concretes: from theory to practice. *Concrete International,* 18**,** 47-49.

BOSTRÖM, L., WICKSTRÖM, U. & ADL-ZARRABI, B. 2007. Effect of specimen size and loading conditions on spalling of concrete. *Fire and materials,* 31**,** 173-186.

BRAHAMMAJI, G. & MUTHYALU, P. V. 2015. A study on performance of Fly Ash Based Geopolymer concrete in Chemical Atmosphere. *International Journal of Advances in Engineering & Technology,* 8**,** 574.

BROUGH, A. & ATKINSON, A. 2002. Sodium silicate-based, alkali-activated slag mortars: Part I. Strength, hydration and microstructure. *Cement and Concrete Research,* 32**,** 865-879.

BUCHANAN, A. H. & ABU, A. K. 2017. *Structural design for fire safety*, John Wiley & Sons.

BUCHWALD, A. & SCHULZ, M. 2005. Alkali-activated binders by use of industrial by-products. *Cement and concrete research,* 35**,** 968-973.

CAVILL, B. & CHIRGWIN, G. The world's first RPC road bridge at Shepherds Gully Creek, NSW. Austroads Bridge Conference, 5th, 2004, Hobart, Tasmania, Australia, 2004.

CHAN, Y.-W. & CHU, S.-H. 2004. Effect of silica fume on steel fiber bond characteristics in reactive powder concrete. *Cement and Concrete Research,* 34**,** 1167-1172.

CHEN, W., XIA, J.-H., LAO, L.-L. & SHEN, P.-L. 2012. Design and Mechnical Properties of Geopolymer-based Reactive Powder Concrete. *Bulletin of the Chinese Ceramic Society,* 6**,** 002.

CHENG, T. W. & CHIU, J. P. 2006. Fire-resistant geopolymer produced by granulated blast furnace slag. *Minerals Engineering.*

CHINDAPRASIRT, P., CHAREERAT, T., HATANAKA, S. & CAO, T. 2010. High-strength geopolymer using fine high-calcium fly ash. *Journal of Materials in Civil Engineering,* 23**,** 264-270.

COLLEPARDI, S., COPPOLA, L., TROLI, R. & COLLEPARDI, M. 1997. Mechanical properties of modified reactive powder concrete. *ACI Special Publications,* 173**,** 1-22.

CONNOLLY, R. J. 1995. *The spalling of concrete in fires.* Aston University.

CONSOLAZIO, G. R., MCVAY, M. C. & RISH III, J. W. 1998. Measurement and prediction of pore pressures in saturated cement mortar subjected to radiant heating. *Materials Journal,* 95**,** 525-536.

COOK, G. 2009. Climate Change and the Cement Industry. *Climate Strategies, Cambridge, UK [available at www. climatestrategies. org].*

COPPOLA, L., TROLI, R., BORSOI, A., ZAFFARONI, P. & COLLEPARDI, M. Influence of superplasticizer type on the compressive strength of RPM. Proceedings of the Fifth CANMET/ACI International Conference on Superplasticizers and other Chemical Admixtures in Concrete, Roma, 1997. 512-36.

COURTIAL, M., DE NOIRFONTAINE, M.-N., DUNSTETTER, F., SIGNES-FREHEL, M., MOUNANGA, P., CHERKAOUI, K. & KHELIDJ, A. 2013. Effect of polycarboxylate and crushed quartz in UHPC: microstructural investigation. *Construction and Building Materials,* 44**,** 699-705.

CRIADO, M., PALOMO, A. & FERNÁNDEZ-JIMÉNEZ, A. 2005. Alkali activation of fly ashes. Part 1: Effect of curing conditions on the carbonation of the reaction products. *Fuel,* 84**,** 2048-2054.

CROW, J. M. 2008. The concrete conundrum. *Chemistry World,* 5**,** 62-66.

CWIRZEN, A., PENTTALA, V. & VORNANEN, C. 2008. Reactive powder based concretes: Mechanical properties, durability and hybrid use with OPC. *Cement and Concrete Research,* 38**,** 1217-1226.

DAVIDOVITS, J. Properties of geopolymer cements. First international conference on alkaline cements and concretes, 1994. 131-149.

DAVIDOVITS, J. Chemistry of geopolymeric systems, terminology. Geopolymer, 1999. 9-39.

DAVIDOVITS, J. 30 years of successes and failures in geopolymer applications. Market trends and potential breakthroughs. Keynote Conference on Geopolymer Conference, 2002.

DAVIDOVITS, J. 2008. *Geopolymer chemistry and applications*, Geopolymer Institute.

DAVIDOVTS, J. 2013. GEOPOLYMER CEMENT. France.

DE SILVA, P., SAGOE-CRENSTIL, K. & SIRIVIVATNANON, V. 2007. Kinetics of geopolymerization: role of Al 2 O 3 and SiO 2. *Cement and Concrete Research,* 37**,** 512-518.

DEGIRMENCI, F. N. 2017. EFFECT OF SODIUM SILICATE TO SODIUM HYDROXIDE RATIOS ON DURABILITY OF GEOPOLYMER MORTARS CONTAINING NATURAL AND ARTIFICIAL POZZOLANS. *Ceramics–Silikáty,* 61**,** 340-350.

DOMBROWSKI, K., BUCHWALD, A. & WEIL, M. 2007. The influence of calcium content on the structure and thermal performance of fly ash based geopolymers. *Journal of Materials Science,* 42**,** 3033-3043.

DUGAT, J., ROUX, N. & BERNIER, G. 1996. Mechanical properties of reactive powder concretes. *Materials and structures,* 29**,** 233-240.

DUXSON, P., FERNÁNDEZ-JIMÉNEZ, A., PROVIS, J. L., LUKEY, G. C., PALOMO, A. & VAN DEVENTER, J. 2007. Geopolymer technology: the current state of the art. *Journal of Materials Science,* 42**,** 2917-2933.

EDWARDS, P. 2015. The Rise and Potential Peak of Cement Demand in the Urbanized World. *Cornerstone-The Official Journal of the World Coal Industry.*

FERNÁNDEZ-JIMÉNEZ, A. & PALOMO, A. 2005. Composition and microstructure of alkali activated fly ash binder: Effect of the activator. *Cement and concrete research,* 35**,** 1984-1992.

FERNÁNDEZ-JIMÉNEZ, A. & PUERTAS, F. 2001. Setting of alkali-activated slag cement. Influence of activator nature. *Advances in Cement Research,* 13**,** 115-121.

FLOWER, D. J. & SANJAYAN, J. G. 2007. Green house gas emissions due to concrete manufacture. *The international Journal of life cycle assessment,* 12**,** 282.

FU, Y. & LI, L. 2011. Study on mechanism of thermal spalling in concrete exposed to elevated temperatures. *Materials and structures,* 44**,** 361-376.

FU, Y., WONG, Y., POON, C. & TANG, C. 2005. Stress-strain behaviour of high-strength concrete at elevated temperatures. *Magazine of Concrete Research,* 57**,** 535-544.

GAN, M. 1997. *Cement and concrete*, CRC Press.

GLUKHOVSKY, V. 1959. Soil silicates. *Gostroiizdat Publish. Kiev, USSR.*

GLUKHOVSKY, V., ROSTOVSKAJA, G. & RUMYNA, G. High strength slag-alkaline cements. Proceedings of the 7th international congress on the chemistry of cement, Paris, 1980. 164-168.

GOMAA, E., SARGON, S., KASHOSI, C. & ELGAWADY, M. 2017. Fresh properties and compressive strength of high calcium alkali activated fly ash mortar. *Journal of King Saud University-Engineering Sciences,* 29**,** 356-364.

GOURLEY, J. & JOHNSON, G. Developments in geopolymer precast concrete. World Congress Geopolymer, 2005. 139-143.

GOWRIPALAN, N., WATTERS, R., GILBERT, I. & CAVILL, B. Reactive Powder Concrete (Ductal®) for Precast Structural Concrete–Research and Development in Australia. 21st Biennial Conference of the CIA, Brisbane, 2003.

GRAYBEAL, B. & HARTMANN, J. Ultra-high performance concrete material properties. Transportation Research Board Conference, 2003. 2-14.

GREGG, J. S., ANDRES, R. J. & MARLAND, G. 2008. China: Emissions pattern of the world leader in CO2 emissions from fossil fuel consumption and cement production. *Geophysical Research Letters,* 35.

GRIFFIN, R. 1987. CO2 Release from Cement Production 1950-1985. *Ed. G. Marland et al. Oak Ridge, TN, Oak Ridge National Laboratory.*

GUERRIERI, M. 2009. *Fire Performance of Alkali Activated Slag and Geopolymers.* Monash University.

GUERRIERI, M. & SANJAYAN, J. G. 2010. Behavior of combined fly ash/slag-based geopolymers when exposed to high temperatures. *Fire and materials,* 34**,** 163-175.

HARDJITO, D. 2005. Studies on Fly Ash-Based Geopolymer Concrete

HARDJITO, D. & RANGAN, B. V. 2005. Development and properties of low-calcium fly ash-based geopolymer concrete.

HARDJITO, D., WALLAH, S., SUMAJOUW, D. & RANGAN, B. Introducing fly ash-based geopolymer concrete: manufacture and engineering properties. 30th Conference on our World in Concrete and Structures, 2005a. 23-4.

HARDJITO, D., WALLAH, S. E., SUMAJOUW, D. M. & RANGAN, B. V. 2004. On the development of fly ash-based geopolymer concrete. *ACI Materials Journal-American Concrete Institute,* 101**,** 467-472.

HARDJITO, D., WALLAH, S. E., SUMAJOUW, D. M. & RANGAN, B. V. 2005b. Fly ash-based geopolymer concrete. *Australian Journal of Structural Engineering,* 6**,** 77-86.

HARRIS, D. 2017. Ash as an internationally traded commodity. *Coal Combustion Products (CCP's)*, 509-529.

HEAH, C., KAMARUDIN, H., AL BAKRI, A. M., BINHUSSAIN, M., LUQMAN, M., NIZAR, I. K., RUZAIDI, C. & LIEW, Y. 2011. Effect of curing profile on kaolin-based geopolymers. *Physics Procedia,* 22, 305-311.

HEIDRICH, C. Ash Utilisation-An Australian Perspective. Geopolymers 2002 International Conference, Melbourne, Australia, Siloxo, 2002.

HELMI, M., HALL, M. R., STEVENS, L. A. & RIGBY, S. P. 2016. Effects of high-pressure/temperature curing on reactive powder concrete microstructure formation. *Construction and Building Materials,* 105, 554-562.

HERTZ, K. D. 2003. Limits of spalling of fire-exposed concrete. *Fire safety journal,* 38, 103-116.

HIREMATH, P. N. & YARAGAL, S. C. 2017. Effect of different curing regimes and durations on early strength development of reactive powder concrete. *Construction and Building Materials,* 154, 72-87.

HSU, J.-H. & LIN, C.-S. 2008. Effect of fire on the residual mechanical properties and structural performance of reinforced concrete beams. *Journal of Fire Protection Engineering,* 18, 245-274.

İPEK, M., YILMAZ, K. & UYSAL, M. 2012. The effect of pre-setting pressure applied flexural strength and fracture toughness of reactive powder concrete during the setting phase. *Construction and Building Materials,* 26, 459-465.

IZQUIERDO, M. & QUEROL, X. 2012. Leaching behaviour of elements from coal combustion fly ash: an overview. *International Journal of Coal Geology,* 94, 54-66.

JIANFANG, Z. & WEI, L. 2003. STUDY ON PREPARATION OF GEOPOLYMER-BASED REACTIVE POWDER CONCRETE AND PROPERTIES THEREOF [J]. *Architecture Technology,* 2, 023.

JO, B.-W., PARK, S.-K. & PARK, M.-S. 2007. Strength and hardening characteristics of activated fly ash mortars. *Magazine of concrete research,* 59, 121-129.

JOSHI, R. & LOHTIA, R. 1993. Types and Properties of Fly Ash. *Mineral Admixtures in Cement and Concrete (Ed,* 119-157.

JU, Y., LIU, H., LIU, J., TIAN, K., WEI, S. & HAO, S. 2011. Investigation on thermophysical properties of reactive powder concrete. *Science China Technological Sciences,* 54, 3382-3403.

JU, Y., LIU, H., TIAN, K., LIU, J., WANG, L. & GE, Z. 2013. An investigation on micro pore structures and the vapor pressure mechanism of explosive spalling of RPC exposed to high temperature. *Science China Technological Sciences,* 56**,** 458-470.

JU, Y., LIU, J., LIU, H., TIAN, K. & GE, Z. 2016. On the thermal spalling mechanism of reactive powder concrete exposed to high temperature: Numerical and experimental studies. *International Journal of Heat and Mass Transfer,* 98**,** 493-507.

KALIFA, P., MENNETEAU, F.-D. & QUENARD, D. 2000. Spalling and pore pressure in HPC at high temperatures. *Cement and concrete research,* 30**,** 1915-1927.

KHADIRANAIKAR, R. & MURANAL, S. 2012. Factors affecting the strength of reactive powder concrete (RPC). *Int. J Civil Engg. and Tech,* 3**,** 455-464.

KHALIQ, W. & KODUR, V. 2012. High Temperature Mechanical Properties of High-Strength Fly Ash Concrete with and without Fibers. *ACI Materials Journal,* 109.

KHOURY, G. A. 2000. Effect of fire on concrete and concrete structures. *Progress in Structural Engineering and Materials,* 2**,** 429-447.

KIM, J., PARK, J. & KYONGGI, S. 2003. Experimental measurement of concrete thermal expansion. *Journal of the Eastern Asia Society for Transportation Studies,* 5**,** 1036-1048.

KODUR, V. 2014. Properties of concrete at elevated temperatures. *ISRN Civil engineering,* 2014.

KODUR, V. & RAUT, N. 2010. Performance of concrete structures under fire hazard: emerging trends. *The Indian Concrete Journal,* 84**,** 23-31.

KONG, D. L. & SANJAYAN, J. G. 2010. Effect of elevated temperatures on geopolymer paste, mortar and concrete. *Cement and concrete research,* 40**,** 334-339.

KONG, D. L., SANJAYAN, J. G. & SAGOE-CRENTSIL, K. 2007. Comparative performance of geopolymers made with metakaolin and fly ash after exposure to elevated temperatures. *Cement and Concrete Research,* 37**,** 1583-1589.

LEE, M.-G., WANG, Y.-C. & CHIU, C.-T. 2007. A preliminary study of reactive powder concrete as a new repair material. *Construction and Building Materials,* 21**,** 182-189.

LEE, S., VAN RIESSEN, A. & CHON, C.-M. 2016. Benefits of Sealed-Curing on Compressive Strength of Fly Ash-Based Geopolymers. *Materials,* 9**,** 598.

LEE, W. & VAN DEVENTER, J. 2002a. The effect of ionic contaminants on the early-age properties of alkali-activated fly ash-based cements. *Cement and Concrete Research,* 32**,** 577-584.

LEE, W. & VAN DEVENTER, J. 2002b. The effects of inorganic salt contamination on the strength and durability of geopolymers. *Colloids and Surfaces A: Physicochemical and Engineering Aspects,* 211**,** 115-126.

LI, C., SUN, H. & LI, L. 2010. A review: The comparison between alkali-activated slag (Si+ Ca) and metakaolin (Si+ Al) cements. *Cement and Concrete Research,* 40**,** 1341-1349.

LI, G. & WU, X. 2005. Influence of fly ash and its mean particle size on certain engineering properties of cement composite mortars. *Cement and Concrete Research,* 35**,** 1128-1134.

LI, Z. 2011. *Advanced concrete technology*, John Wiley & Sons.

LI, Z., DING, Z. & ZHANG, Y. Development of sustainable cementitious materials. Proceedings of international workshop on sustainable development and concrete technology, Beijing, China, 2004. 55-76.

LIU, C.-T. & HUANG, J.-S. 2009. Fire performance of highly flowable reactive powder concrete. *Construction and Building Materials,* 23**,** 2072-2079.

LIU, H., LI, K., JU, Y., WANG, H.-J., WANG, J.-B., TIAN, K.-P. & WEI, S. 2010. Explosive spalling of steel fiber reinforced reactive powder concrete subject to high temperature. *Concrete,* 8**,** 6-8.

LIZCANO, M., KIM, H. S., BASU, S. & RADOVIC, M. 2012. Mechanical properties of sodium and potassium activated metakaolin-based geopolymers. *Journal of Materials Science,* 47**,** 2607-2616.

LLOYD, N. & RANGAN, B. Geopolymer concrete with fly ash. Second international conference on sustainable construction materials and technologies, 2010. 1493-1504.

LONG, G., WANG, X. & XIE, Y. 2002. Very-high-performance concrete with ultrafine powders. *Cement and concrete research,* 32**,** 601-605.

MA, J., ORGASS, M., DEHN, F., SCHMIDT, D. & TUE, N. Comparative investigations on ultra-high performance concrete with and without coarse aggregates. Proceedings of international symposium on ultra high performance concrete, Germany, 2004. 205-212.

MANE, S. & JADHAV, H. 2012. Investigation of geopolymer mortar and concrete under high temperature. *Magnesium,* 1**,** 5.

MASSIDDA, L., SANNA, U., COCCO, E. & MELONI, P. 2001. High pressure steam curing of reactive-powder mortars. *Special Publication,* 200**,** 447-464.

MCLELLAN, B. C., WILLIAMS, R. P., LAY, J., VAN RIESSEN, A. & CORDER, G. D. 2011. Costs and carbon emissions for geopolymer pastes in comparison to ordinary portland cement. *Journal of Cleaner Production,* 19**,** 1080-1090.

MEHTA, K. P. 2001. Reducing the environmental impact of concrete. *Concrete international,* 23**,** 61-66.

MEHTA, P. K. 1986. Concrete. Structure, properties and materials.

MEHTA, P. K. High-performance, high-volume fly ash concrete for sustainable development. Proceedings of the international workshop on sustainable development and concrete technology, 2004. Iowa State University Ames, IA, USA, 3-14.

MEHTA, P. K. & BURROWS, R. W. 2001. Building durable structures in the 21 st century. *Indian Concrete Journal,* 75**,** 437-443.

MENDES, A., SANJAYAN, J. & COLLINS, F. 2008. Phase transformations and mechanical strength of OPC/Slag pastes submitted to high temperatures. *Materials and structures,* 41**,** 345.

MENEFY, L. 2007. *Investigation of reactive powder concrete and it's damping characteristics when utilised in beam elements.* Griffith University, Gold Coast.

MEYER, C. 2009. The greening of the concrete industry. *Cement and concrete composites,* 31**,** 601-605.

MORSY, M., ALSAYED, S. & AQEL, M. 2010. Effect of elevated temperature on mechanical properties and microstructure of silica flour concrete. *International journal of civil & environmental engineering,* 10**,** 1-6.

MOSTOFINEJAD, D., NIKOO, M. R. & HOSSEINI, S. A. 2016. Determination of optimized mix design and curing conditions of reactive powder concrete (RPC). *Construction and Building Materials,* 123**,** 754-767.

NEVILLE, A. M. 1995. *Properties of concrete*, Longman London.

NG, K. M., TAM, C. M. & TAM, V. 2010. Studying the production process and mechanical properties of reactive powder concrete: a Hong Kong study. *Magazine of Concrete Research,* 62**,** 647-654.

NG, T. S., VOO, Y. L. & FOSTER, S. J. 2012. Sustainability with ultra-high performance and geopolymer concrete construction. *Innovative materials and techniques in concrete construction.* Springer.

ONER, A., AKYUZ, S. & YILDIZ, R. 2005. An experimental study on strength development of concrete containing fly ash and optimum usage of fly ash in concrete. *Cement and Concrete Research,* 35**,** 1165-1171.

PACHECO-TORGAL, F., CASTRO-GOMES, J. & JALALI, S. 2008. Alkali-activated binders: a review. Part 2. About materials and binders manufacture. *Construction and Building Materials,* 22**,** 1315-1322.

PALOMO, A., GRUTZECK, M. & BLANCO, M. 1999. Alkali-activated fly ashes: a cement for the future. *Cement and concrete research,* 29**,** 1323-1329.

PAN, Z., SANJAYAN, J. G. & RANGAN, B. V. 2009. An investigation of the mechanisms for strength gain or loss of geopolymer mortar after exposure to elevated temperature. *Journal of Materials Science,* 44**,** 1873-1880.

PENG, G.-F., KANG, Y.-R., HUANG, Y.-Z., LIU, X.-P. & CHEN, Q. 2012. Experimental research on fire resistance of reactive powder concrete. *Advances in Materials Science and Engineering,* 2012.

PHAN, L. T. 2008. Pore pressure and explosive spalling in concrete. *Materials and structures,* 41**,** 1623-1632.

PHAN, L. T. & CARINO, N. J. 1998. Review of mechanical properties of HSC at elevated temperature. *Journal of Materials in Civil Engineering,* 10**,** 58-65.

PHAN, L. T. & CARINO, N. J. 2001. Mechanical properties of high-strength concrete at elevated temperatures. *NIST Interagency/Internal Report (NISTIR)-6726.*

PHAN, L. T. & PEACOCK, R. D. 1999. *Experimental plan for testing the mechanical properties of high-strength concrete at elevated temperatures*, Building and Fire Research Laboratory, National Institute of Standards and Technology Gaithersburg, Maryland.

PIMRAKSA, K., CHAREERAT, T., CHINDAPRASIRT, P., MISHIMA, N. & HATANAKA, S. Composition and microstructure of fly ash geopolymer containing metakaolin. Excellence in Concrete Construction through Innovation: Proceedings of the conference held at the Kingston University, United Kingdom, 9-10 September 2008, 2008. CRC Press, 201.

POON, C., SHUI, Z., LAM, L., FOK, H. & KOU, S. 2004. Influence of moisture states of natural and recycled aggregates on the slump and compressive strength of concrete. *Cement and Concrete Research,* 34**,** 31-36.

PROVIS, J. L. & VAN DEVENTER, J. S. J. 2009. *Geopolymers: structures, processing, properties and industrial applications*, Elsevier.

RAHMAN, S., MOLYNEAUX, T. & PATNAIKUNI, I. 2005. Ultra high performance concrete: recent applications and research. *Australian journal of civil engineering,* 2**,** 13-20.

RAJAMANE, N. & JEYALAKSHMI, R. 2014. Quantities of sodium hydroxide solids and water to prepare sodium hydroxide solution of given molarity for geopolymer concrete mixes. *The Indian Concrete Journal Aug–Sep.*

RAMACHANDRAN, V. S. 1996. *Concrete admixtures handbook: properties, science and technology*, William Andrew.

RANGAN, B. V., WALLAH, S., SUMAJOUW, D. & HARDJITO, D. 2006. Heat-cured, low-calcium, fly ash-based geopolymer concrete. *Indian Concrete Journal,* 80**,** 47.

RESPLENDINO, J. & TOULEMONDE, F. 2013. *Designing and Building with UHPFRC*, John Wiley & Sons.

RICHARD, P. & CHEYREZY, M. 1995. Composition of reactive powder concretes. *Cement and concrete research,* 25**,** 1501-1511.

RICHARD, P. & CHEYREZY, M. H. 1994. Reactive powder concretes with high ductility and 200-800 MPa compressive strength. *Special Publication,* 144**,** 507-518.

RICKARDA, W. D. A., GLUTHB, G. J. G. & PISTOLB, K. 2016. In-situ thermo-mechanical testing of fly ash geopolymer concretes made with quartz and expanded clay aggregates. *Cement and Concrete Research,* 80**,** 33-43.

ROVNANÍK, P. 2010. Effect of curing temperature on the development of hard structure of metakaolin-based geopolymer. *Construction and Building Materials,* 24**,** 1176-1183.

ROY, A., SCHILLING, P. J. & EATON, H. C. 1995. Alkali activated class C fly ash cement. Google Patents.

RYU, G. S., LEE, Y. B., KOH, K. T. & CHUNG, Y. S. 2013. The mechanical properties of fly ash-based geopolymer concrete with alkaline activators. *Construction and Building Materials,* 47**,** 409-418.

SAKKAS, K., NOMIKOS, P., SOFIANOS, A. & PANIAS, D. 2015a. Sodium-based fire resistant geopolymer for passive fire protection. *Fire and Materials,* 39**,** 258-270.

SAKKAS, K., SOFIANOS, A., NOMIKOS, P. & PANIAS, D. 2015b. Behaviour of passive fire protection K-geopolymer under successive severe fire incidents. *Materials,* 8**,** 6096-6104.

SANJAYAN, G. & STOCKS, L. 1993. Spalling of high-strength silica fume concrete in fire. *Materials Journal,* 90**,** 170-173.

SARKER, P. & MCBEATH, S. Reinforced Geopolymer Concrete after Exposure to Fire. Proceedings of the 2011 PCI Convention and National Bridge Coference, 2011. Precast/Prestressed Concrete Institute.

SARKER, P. K., KELLY, S. & YAO, Z. 2014. Effect of fire exposure on cracking, spalling and residual strength of fly ash geopolymer concrete. *Materials & Design,* 63**,** 584-592.

SHAH, A. H. & SHARMA, U. 2017. Fire resistance and spalling performance of confined concrete columns. *Construction and Building Materials,* 156**,** 161-174.

SHAIKH, F. & VIMONSATIT, V. 2015. Compressive strength of fly-ash-based geopolymer concrete at elevated temperatures. *Fire and Materials,* 39**,** 174-188.

SHARMA, A. & AHMAD, J. 2017. FACTORS AFFECTING COMPRESSIVE STRENGTH OF GEOPOLYMER CONCRETE-A REVIEW.

SHORTER, G. & HARMATHY, T. 1961. Discussion on the fire resistance of prestressed concrete beams. *Proceedings of the Institution of Civil Engineers,* 20**,** 313-315.

SHRESTHA, P. 2014. Development Of Geopolymer Concrete For Precast Structures.

SHUAIBU, R. 1950. Compressive Strength of Low Calcium Fly Ash Geopolymer Concrete-A Review.

SIDDIQUE, R. 2008. Cement Kiln Dust. *Waste Materials and By-Products in Concrete.* Springer.

SIDERIS, K. K. 2007. Mechanical characteristics of self-consolidating concretes exposed to elevated temperatures. *Journal of materials in civil engineering,* 19**,** 648-654.

SINDHUNATA, G. C. L., SJ, X. J., WEISS, J., KOVLER, K., MARCHAND, J. & MINDESS, S. The effect of curing conditions on the properties of geopolymeric

materials derived from fly ash. International RILEM Symposium on Concrete Science and Engineering: A Tribute to Arnon Bentur, 2004. RILEM Publications SARL.

SO, H.-S., YI, J.-B., KHULGADAI, J. & SO, S.-Y. 2014. Properties of strength and pore structure of reactive powder concrete exposed to high temperature. *ACI Mater. J,* 111**,** 335-346.

SONG, J. & LIU, S. 2016. Properties of reactive powder concrete and its application in highway bridge. *Advances in Materials Science and Engineering,* 2016.

STANDARD, A. 2010. General purpose and blended cements. *Standard, Standard Australia.*

STANDARD, A. 2014a. Methods of testing concrete. *Method 9: Compressive strength tests— Concrete, mortar and grout specimens.*

STANDARD, A. 2014b. Methods of testing concrete *Method 5: Determination of mass per unit volume of freshly mixed concrete.*

STANDARD, A. N. Z. 2016a. Supplementary cementitious materials. *Part 3: Amorphous silica.*

STANDARD, A. N. Z. 2016b. Supplementary cementitious materials. *Part 1: Fly ash.*

SU, H., XU, J. & REN, W. 2016. Mechanical properties of geopolymer concrete exposed to dynamic compression under elevated temperatures. *Ceramics International,* 42**,** 3888-3898.

SU, L., WANG, Y.-F., MEI, S.-Q. & LI, P.-F. 2017. Experimental investigation on the fundamental behavior of concrete creep. *Construction and Building Materials,* 152**,** 250-258.

SWANEPOEL, J. & STRYDOM, C. 2002. Utilisation of fly ash in a geopolymeric material. *Applied Geochemistry,* 17**,** 1143-1148.

TEAM, E. 2007. Reactive Powder Concrete.

TEMUUJIN, J., MINJIGMAA, A., LEE, M., CHEN-TAN, N. & VAN RIESSEN, A. 2011. Characterisation of class F fly ash geopolymer pastes immersed in acid and alkaline solutions. *Cement and Concrete Composites,* 33**,** 1086-1091.

TIAN, K. P., JU, Y., LIU, H. B., LIU, J. H., WANG, L., LIU, P. & ZHAO, X. Effects of silica fume addition on the spalling phenomena of reactive powder concrete. Applied Mechanics and Materials, 2012. Trans Tech Publ, 1090-1095.

TING, E. & PATNAIKUNI, I. Influence of mix ingredients on the compressive strength of very high strength concrete. 17th Conference on OUR WORLD IN CONCRETE STRUCTURES, 1992. 25-27.

TOPCCEDIL, I. B. & UYGUNOĞLU, T. 2010. Influence of mineral additive type on slump-flow and yield stress of self-consolidating mortar. *Scientific Research and Essays,* 5**,** 1492-1500.

VAN JAARSVELD, J. & VAN DEVENTER, J. 1999. Effect of the alkali metal activator on the properties of fly ash-based geopolymers. *Industrial & Engineering Chemistry Research,* 38**,** 3932-3941.

VIJAI, K., KUMUTHA, R. & VISHNURAM, B. 2010. Effect of types of curing on strength of geopolymer concrete. *International Journal of Physical Sciences,* 5**,** 1419-1423.

WALLAH, S. 2010. Creep behaviour of fly ash-based geopolymer concrete. *Civil Engineering Dimension,* 12**,** 73-78.

WALLAH, S., HARDJITO, D., SUMAJOUW, D. & RANGAN, B. Sulfate and acid resistance of fly ash-based geopolymer concrete. Australian Structural Engineering Conference 2005, 2005. Engineers Australia, 733.

WALLAH, S. & RANGAN, B. V. 2006. Low-calcium fly ash-based geopolymer concrete: long-term properties. *Res. Report-GC2, Curtin University, Australia. pp***,** 76-80.

WANG, C., YANG, C., LIU, F., WAN, C. & PU, X. 2012. Preparation of ultra-high performance concrete with common technology and materials. *Cement and concrete composites,* 34**,** 538-544.

WARDHONO, A. 2014. The durability of fly ash geopolymer and alkali-activated slag concretes.

WASHER, G., FUCHS, P. & GRAYBEAL, B. Elastic properties of reactive powder concrete. International Symposium on Non-Destructive Testing in Civil Engineering (NDT-CE 2003), Germany, 2003.

WATSON, R. T., ZINYOWERA, M. C. & MOSS, R. H. 1996. *Climate change 1995. Impacts, adaptations and mitigation of climate change: scientific-technical analyses*.

WATTIMENA, O. K., ANTONI & HARDJITO, D. A review on the effect of fly ash characteristics and their variations on the synthesis of fly ash based geopolymer. AIP Conference Proceedings, 2017. AIP Publishing, 020041.

WIJAYA, A. L. & EKAPUTRI, J. J. Factors influencing strength and setting time of fly ash based-geopolymer paste. MATEC Web of Conferences, 2017. EDP Sciences, 01010.

WILLAM, K., RHEE, I. & XI, Y. 2005. Thermal degradation of heterogeneous concrete materials. *Journal of materials in civil engineering,* 17**,** 276-285.

WILLIAMSON, R. B. & RASHED, A. I. 1984. High strength concrete and mortars in high temperature environments. *MRS Online Proceedings Library Archive,* 42.

XU, H. & VAN DEVENTER, J. 2000. The geopolymerisation of alumino-silicate minerals. *International journal of mineral processing,* 59**,** 247-266.

YANG, S., MILLARD, S., SOUTSOS, M., BARNETT, S. & LE, T. T. 2009. Influence of aggregate and curing regime on the mechanical properties of ultra-high performance fibre reinforced concrete (UHPFRC). *Construction and Building Materials,* 23**,** 2291-2298.

YAO, X., ZHANG, Z., ZHU, H. & CHEN, Y. 2009. Geopolymerization process of alkali–metakaolinite characterized by isothermal calorimetry. *Thermochimica Acta,* 493**,** 49-54.

YAZıCı, H., DENIZ, E. & BARADAN, B. 2013. The effect of autoclave pressure, temperature and duration time on mechanical properties of reactive powder concrete. *Construction and Building Materials,* 42**,** 53-63.

YAZıCı, H., YARDıMCı, M. Y., AYDıN, S. & KARABULUT, A. Ş. 2009. Mechanical properties of reactive powder concrete containing mineral admixtures under different curing regimes. *Construction and building materials,* 23**,** 1223-1231.

YAZıCı, H., YIĞITER, H., KARABULUT, A. Ş. & BARADAN, B. 2008. Utilization of fly ash and ground granulated blast furnace slag as an alternative silica source in reactive powder concrete. *Fuel,* 87**,** 2401-2407.

YU, J., YU, K. & LU, Z. 2012a. Residual fracture properties of concrete subjected to elevated temperatures. *Materials and structures,* 45**,** 1155-1165.

YU, J. T., YU, K. Q. & LU, Z. D. Residual Fracture Toughness of Concrete Subject to Elevated Temperatures. Key Engineering Materials, 2012b. Trans Tech Publ, 743-746.

YUNSHENG, Z., WEI, S., SIFENG, L., CHUJIE, J. & JIANZHONG, L. 2008a. Preparation of C200 green reactive powder concrete and its static–dynamic behaviors. *Cement and Concrete Composites,* 30**,** 831-838.

YUNSHENG, Z., WEI, S., ZONGJIN, L., XIANGMING, Z. & CHUNGKONG, C. 2008b. Impact properties of geopolymer based extrudates incorporated with fly ash and PVA short fiber. *Construction and Building Materials,* 22**,** 370-383.

ZDEB, T. 2017. An analysis of the steam curing and autoclaving process parameters for reactive powder concretes. *Construction and Building Materials,* 131**,** 758-766.

ZHANG, B. 2011. Effects of moisture evaporation (weight loss) on fracture properties of high performance concrete subjected to high temperatures. *Fire Safety Journal,* 46**,** 543-549.

ZHANG, H. Y., KODUR, V., QI, S. L., CAO, L. & WU, B. 2014. Development of metakaolin–fly ash based geopolymers for fire resistance applications. *Construction and Building Materials,* 55**,** 38-45.

ZHAO, R. & SANJAYAN, J. G. 2011. Geopolymer and Portland cement concretes in simulated fire. *Magazine of Concrete research,* 63**,** 163-173.

ZHENG, W., LI, H. & WANG, Y. 2012a. Compressive behaviour of hybrid fiber-reinforced reactive powder concrete after high temperature. *Materials & Design,* 41**,** 403-409.

ZHENG, W., LI, H. & WANG, Y. 2012b. Compressive stress–strain relationship of steel fiber-reinforced reactive powder concrete after exposure to elevated temperatures. *Construction and Building Materials,* 35**,** 931-940.

ZHENG, W., LUO, B. & WANG, Y. 2013. Compressive and tensile properties of reactive powder concrete with steel fibres at elevated temperatures. *Construction and Building Materials,* 41**,** 844-851.

ZHUKOV, V. 1976. Reasons for explosive deterioration of concrete during fire. *Russian Concrete and Reinforced Concrete*.

ZULKIFLY, K., YONG, H., ABDULLAH, M., MING, L., PANIAS, D. & SAKKAS, K. Review of Geopolymer Behaviour in Thermal Environment. IOP Conference Series: Materials Science and Engineering, 2017. IOP Publishing, 012085.